Preservation of Astrocytic Coupling Prevents Epileptogenesis

Dissertation

zur

Erlangung des Doktorgrades (Dr. rer. nat.)

der

Mathematisch-Naturwissenschaftlichen Fakultät

der

Rheinischen Friedrich-Wilhelms-Universität Bonn

vorgelegt von

Julia Müller

aus

Potsdam

Bonn 2018

Angefertigt mit Genehmigung der Mathematisch-Naturwissenschaftlichen Fakultät der Rheinischen Friedrich-Wilhelms-Universität Bonn

1. Gutachter	**Prof. Dr. Christian Steinhäuser**
	Institut für Zelluläre Neurowissenschaften
	Universität Bonn
2. Gutachter	**Prof. Dr. Christa Müller**
	Pharmazeutisches Institut
	Universität Bonn
Tag der Promotion:	14. September
Erscheinungsjahr:	2018

Auch wenn's grad nicht so gut läuft,
wie gewohnt
Egal, es wird gut,
sowieso.
- Mark Forster

Danksagung

Zunächst möchte ich mich bei meinem Vorgesetzten Prof. Dr. Christian Steinhäuser bedanken, der mir die Möglichkeit gab an diesem großartigen Projekt arbeiten zu dürfen. Ich möchte mich für die exzellente Betreuung und die wissenschaftliche Freiheit bedanken, die ich sehr zu schätzen weiß. Außerdem haben mich die fruchtbaren Diskussionen und die Unterstützung stets voran gebracht als Wissenschaftlerin.

Ich möchte mich bei Prof. Dr. Müller für die Übernahme des Koreferats bedanken und für die investierte Zeit und Mühe bei der Überprüfung dieser Arbeit. Ebenso bedanke ich mich bei Prof. Dr. Gieselmann und Prof. Dr. Witke für die Bereitschaft, als fachnaher und fachfremder Gutachter Teil meiner Promotionskommission zu sein.

Insbesondere möchte ich mich bei Dr. Bedner für seine wertvolle wissenschaftliche Beratung, exzellente Unterstützung und für seine hervorragende Betreuung bedanken im XPro1595 Projekt, sowie für die Ermutigungen und dieselbe Begeisterung hinsichtlich der Durchführung des GABA Projektes.

Ich möchte mich bei PD Dr. Seifert für die Durchführung von RT-PCRs und Genotypisierungen des Cytokin- und GABA Projektes bedanken, sowie für die Organisation der Mauszucht.
PD Dr. Ronald Jabs danke ich für die wertvolle methodische und technische Unterstützung bei allen Arten von Fragen und Problemen, insbesondere hinsichtlich der Elektrophysiologie.

Mein besonderer Dank gilt Aline Timmermann für die hervorragende Durchführung der Messungen im GABA Projekt und der hoffentlich sehr zeitnahen gemeinsamen Publikation. Auch danken möchte ich Camille Philippot und Dilaware Khan für endlose Stunden Astrozytenzählung und Lukas Henning für den Erfahrungsaustausch, wissenschaftliche Diskussionen und Zusammenarbeit in den Epilepsieprojekten.

Thomas Erdmann und Dr. Silke Künzel danke ich für ihre großartige Hilfe bei Bestellungen und der Administration.

Allen Kollegen des Instituts danke ich für die sehr angenehme Arbeitsatmosphäre, die Zusammenarbeit, Hilfe und eine schöne gemeinsame Zeit: Alberto, Aline, Antonia, Björn, Camille, Cátia, Daniel, Dmitry, Ines, Lukas, Magda, Michel, Kirsten, Steffi A. (jetzt H.), Steffi G., Stefan H., Tushar, Zhou.

Mein tiefster Dank gilt meiner ganzen Familie, die mich in meinem Leben immer unterstützt und ermutigt hat. Besonders bedanke ich mich bei Sebastian für seine mentale Unterstützung, Geduld und Ermutigungen im Laufe der Jahre.

Contents

Abbreviations

ACSF	artifical cerebrospinal fluid
AD	Alzheimer's disease
AED	antiepileptic drug
AHS	Ammon's horn sclerosis
AMPAR	alpha-amino-3-hydroxy-5-methyl-4-isoxazolepropionic acid receptor
Anakinra	human interleukin-1 receptor antagonist protein
ATP	adenosine triphosphate
ATROSAB	antagonistic tumor necrosis factor receptor one-specific antibody
BBB	blood brain barrier
BCA	bicinchonin acid assay
biocytin	N-biotinyl-L-lysine
CA	cornu ammonis
cAMP	cyclic adenosine monophosphate
caspase	cysteine-aspartic acid protease
CD	cluster of differentiation
C_m	membrane capacitance
CNS	central nervous system
COX	cyclooxygenase
CSF	cerebral spinal fluid
Cx	connexin
DG	dentate gyrus
dH_2O	destilled water
dKO	double knockout
dnTNF	dominant-negative TNF derivative
dpi	days post injection
EC	entorhinal cortex
e.g.	for example
eGFP	enhanced green fluorescent protein
ELISA	enzyme-linked immunosorbent assay
Fig.	figure
FVB	Friend leukemia virus B
G	relative centrifugal force
GABA	gamma-aminobutyric acid
GCD	granule cell dispersion

GFAP	glial fibrillary acidic protein
GJ	gap junction
GJC	gap junction coupling
GLAST	glutamate aspartate transporter
GLT-1	glutamate transporter 1
HD	Huntington's disease
hGFAP	human glial fibrillary acidic protein
HMGB1	high mobility group box 1
hpi	hours post injection
hrs	hours
HS	hippocampal sclerosis
I	current
ICE	interleukin-1 converting enzyme
IL-1β	interleukin-1 beta
IL-1R1	interleukin-1 receptor type 1
IL-1Ra	interleukin-1 receptor antagonist protein
ILAE	International League Against Epilepsy
IKK	inhibitor of kappa B kinase
i.p.	intraperitoneal
IP_3	inositol-1,4,5-triphosphate
KA	kainic acid
kDa	kilo Dalton
Kir	inward-rectifier potassium channels
KO	knock-out
LLOD	lower limit of detection
MAPK	mitogen-activated protein kinase
mGluR	metabotropic glutamate receptor
MP	membrane potential
mpi	months post injection
MS	multiple sclerosis
MTLE	mesial temporal lobe epilepsy
n	number of samples
NaCl	sodium chloride
NaDOC	sodium deoxycholate
n.d.	not detectable
NeuN	neuronal nuclei antigen
NFκB	nuclear factor kappa B
NG2	neuron-glial antigen 2
NGS	normal goat serum
NK	natural killer cells
NMDAR	N-methyl-D-aspartate receptor
no.	number

p	postnatal day
P2YR1	purinergic G protein-coupled receptor 1
p53	tumor suppressor protein with 53 kDa weight
PBS	phosphate buffered saline
PD	Parkinson's disease
PFA	paraformaldehyde
PNS	peripheral nervous system
pyr.	pyramidale
RA	rheumatoid arthritis
rad.	radiatum
rcf	relative centrifugal force
RIPA	radio immunoprecipation assay
RIPK	receptor-interacting serine/threonine-protein kinase
R_m	membrane resistance
ROS	radical oxygen species
rpm	rotation per minute
R_s	series resistance
RT	room temperature
S100β	S100 calcium binding protein beta
S262	serine 262
SCI	spinal cord innjury
SD	standard deviation
SDS	sodium dodecyl sulfate
SE	status epilepticus
solTNFα	soluble tumor necrosis factor alpha
SR101	sulforhodamine 101
SRS	spontaneous recurrent seizures
str.	stratum
TACE	TNF alpha converting enzyme
TLE	temporal lobe epilepsy
TLR	toll like receptor
tmTNFα	transmembrane tumor necrosis factor alpha
TNF-α	tumor necrosis factor alpha
TNFR	tumor necrosis factor receptor
tPA	tissue-type plasminogen activator
T_{regs}	T regulatory cells
TROS	TNF receptor one silencer
U	voltage
vs.	versus
WT	wildtype
w/v	weight per volume
XPro1595	dominant negative inhibitor of soluble TNF alpha

1 Introduction

The nervous system consists of the central nervous system (CNS) and the peripheral nervous system (PNS). The CNS is composed of the spinal cord and brain, whereas the remaining neuronal tissue of the body belongs to the PNS. The skull protects the brain, which is covered by three meninges: The dura mater is the outer meninx protecting the inner arachnoidea and pia mater, both forming the subarachnoid space containing the cerebrospinal fluid (CSF). The CSF regulates the intracranial pressure and maintains the glymphatic clearance as well as the immunological protection within the ventricals in the inner part of the brain. Anatomically, the brain can be structured into the telen-, dien- and mesencephalon, cerebellum, pons and medulla oblongata. The telencephalon, consists of two cerebral hemispheres, which can be divided into four lobes: i) frontal, ii) parietal, iii) occipital and iv) temporal lobe containing the hippocampus. As this study focuses on the hippocampus, it will be explained in further details below.
In the brain diverse cell types have been found with different functions. Neurons form a complex network, in which they receive, process and transmit information. They communicate through chemical signals via synapses. The majority of brain cells are glial cells, which make up 90% in human and 65% in mouse brain (Allen and Barres, 2009). They surround and ensheat neurons for mainting their proper function. Therefore, glia cells support neurotransmission, maintain ionic balance in the extracellular space and have an active role in information processing (Allen and Barres, 2009). Nowadays, glia cells are recognised for their importance in the brain (Barres, 2008; Jäkel and Dimou, 2017). They are subdivided into microglia, astrocytes, oligodendrocytes, NG2 and ependymal cells.
The following study focuses on the role of microglia and astrocytes in the healthy and diseased brain.

1.1 Hippocampus

The hippocampus is located in the medial temporal lobe of the brain and belongs to the limbic system. Each hemisphere contains a hippocampus. The name originates from its shape, which is formed like a seahorse. It is divided into the *dentate gyrus* (DG) and *cornu ammonis* (CA1-4). The CA consists of densely packed pyramidal neurons, which somas' are forming the *stratum pyramidale* (*str. pyr.*), whereas their axons extent into the *subiculum* towards entorhinal cortex (EC) and the dendrites project into the

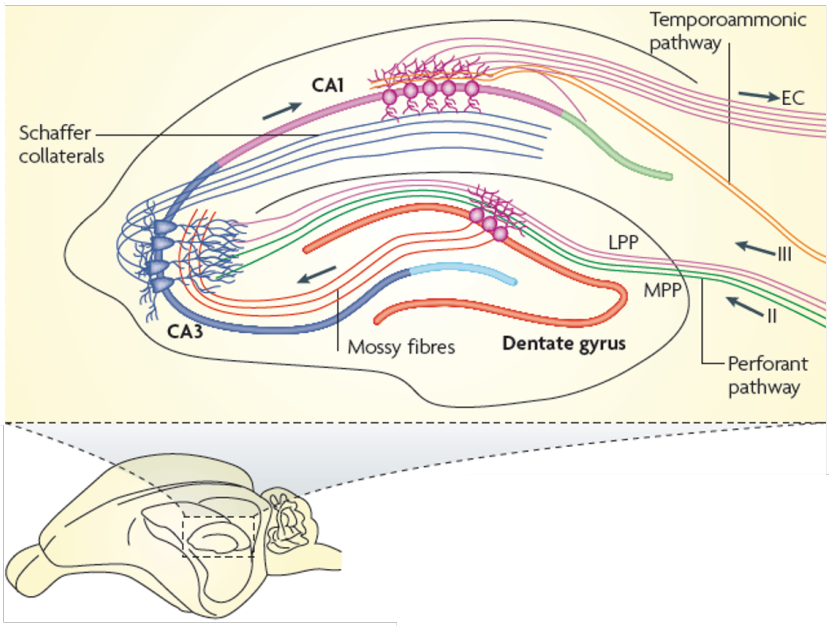

Figure 1.1 Neuronal trisynaptic circuit in the hippocampus: The hippocampus receives input from the entorhinal cortex (EC) via the perforant path to the dentate gyrus. The dentate granule cells project on CA3 neurons, which transmit information via the Schaffer collaterals to CA1 pyramidal neurons. Their axons signal into the subiculum towards the EC. The small image illustrates the localization of the hippocampus in the rodent brain. LPP, lateral perforant pathway; MPP, medial perforant pathway. *Source: modified from Deng et al. (2010)*

layer called *stratum radiatum* (*str. rad.*). Between the *str. rad.* and DG is the *stratum lacunosum moleculare*. The DG contains the granule cells, which form a V-shape layer. The inner layer is called hilus and includes the subgranular zone, which is one of the neurogenic niches in the adult brain with the ability to continuously develop neural stem cells (Seri et al., 2001).

The hippocampus has been well studied for its information transmission from the DG, CA3 to CA1, which together form a trisynaptic circuit. The DG receives input from the EC and projects by unmyelinated axons called mossy fibers to CA3 pyramidal neurons. They (Schaffer collaterals) project on dendrites of CA1 pyramidal neurons in the *str. rad.*, whose axons signal back to the EC (Fig. 1.1) (Deng et al., 2010; Ramón y Cajal, 1909). Due to its neuronal signalling circuit, the hippocampus plays an important role in learning and memory consolidation. Long-term potentiation and long-term depression are widely used to study synaptic transmission and plasticity, which is correlated with memory function (Bliss and Gardner-Medwin, 1973; Hebb, 1949).

1.1.1 Microglia

Microglia are part of the immune system, born in the yolk sac and enter the brain from circulating blood (Allen and Barres, 2009). They are involved in synaptic remodelling during development and the resident immune cells of the CNS, which scan the brain for infection or damage (Kreutzberg, 1996; Schafer et al., 2013; Heneka et al., 2015). Resting microglia have a small cell body with fine and ramified processes. They patrol the CNS and within minutes reorganise their processes and appear to probe the neuronal microenvironment (Nimmerjahn et al., 2005; Fetler and Amigorena, 2005; Garden and Möller, 2006).
In pathophysiological conditions it is still debated whether microglial cells are harmful or rather helpful (Allen and Barres, 2009; Wang et al., 2015). During the development of a disease, microglia shift from a neuroprotective to a classically activated phenotype (Wang et al., 2015). Neuronal damage (ATP), bacterial products (LPS), pathological proteins (amyloid beta) and cytokines (TNF-α) can activate microglial cells, which undergo phenotypical transformation into an amoeboid form due to long-term changes of gene expression (Kreutzberg, 1996; Garden and Möller, 2006) (Fig. 1.2). This classical activation phenotype is also called "M1" (Boche et al., 2013). They display a large number of receptors on their surface initiating or modulating further immune responses (Hanisch, 2002). The "M2" phenotype promotes tissue remodelling and angiogenesis by releasing antiinflammatory molecules, such as IL-10, IL-4, IL-13 and TGF-β (Wang et al., 2015). Activated microglial cells are the first ones that respond to injury, pathogens or other pathophysiological triggers by increasing their cytokine expression and releasing proinflammatory mediators, such as IL-1β and TNF-α to effect neighbouring cells (Wang et al., 2015). It was shown in a transgenic TNFR dKO mouse model with ischemic brain injury that TNF-α activated exclusively microglial cells, which in turn produced neurotoxic substances (Bruce et al., 1996). Therefore, microglia can trigger synergistic cytokine release with activated astroytes (Pascual et al., 2012). Finally, microglia transform into active phagocytes, cleaning up dead cells and debris (Kettenmann et al., 2013).

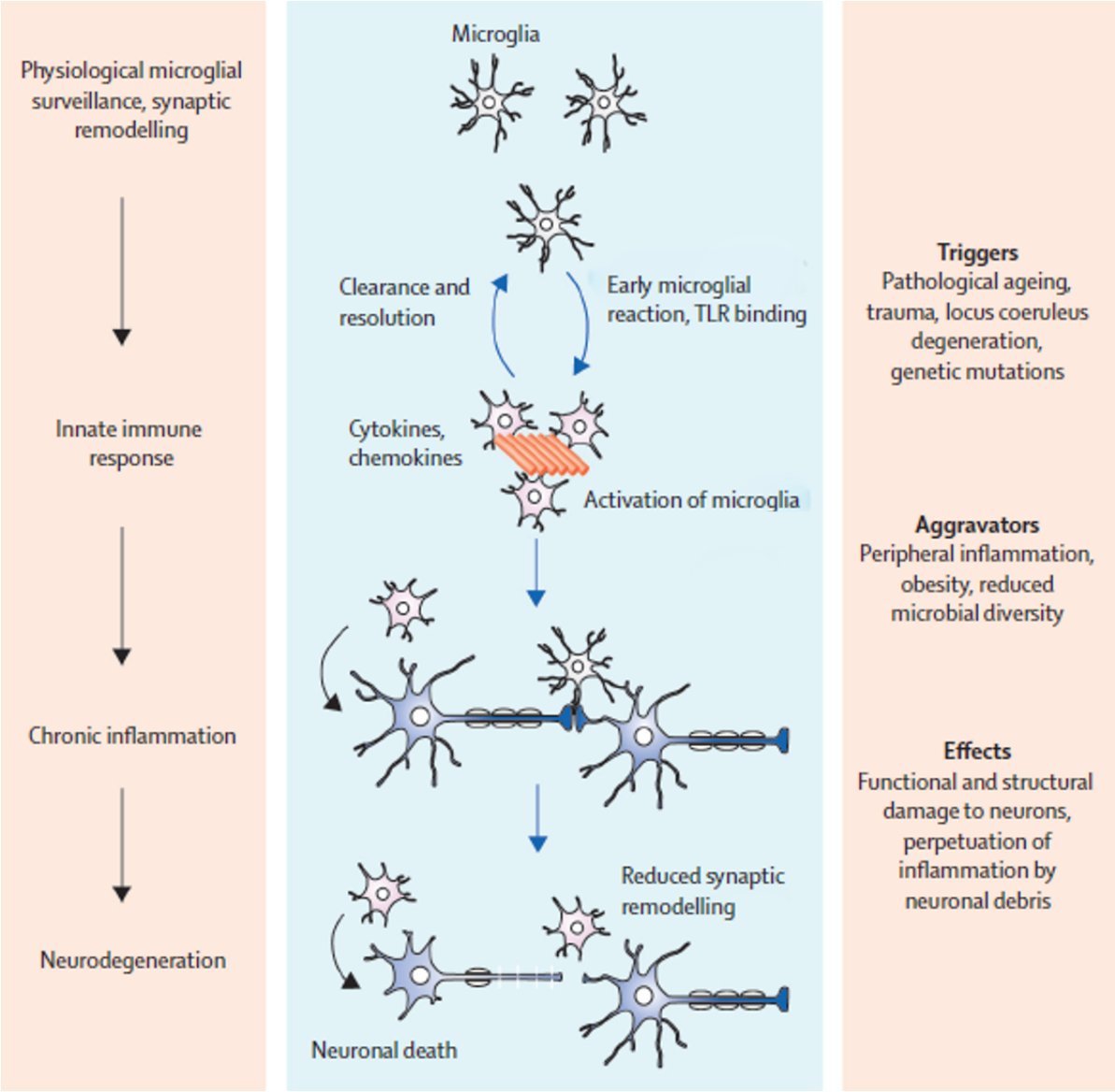

Figure 1.2 Pathomechanistic sequelae of microglia activation: Physiological function of microglia includes the tissue surveillance and synaptic remodelling. Certain triggers, like persistent exposure to proinflammatory cytokines cause an immune activation, which finally results in chronic neuroinflammation. Microglia retract their processes causing functional and structural changes that result in neuronal degeneration. TLR=Toll-like receptor. *Source: modified from Heneka et al. (2015)*

1.1.2 Astrocytes

Astrocytes are the most abundant cells in the mammalian brain and the name originates from their star-like morphology (Kettenmann and Ransom, 2013; Gonzalez-Perez et al., 2015). There are two main types: i) protoplasmic and ii) fibrous astrocytes (Ramón y Cajal, 1909). Protoplasmic astrocytes are found in the grey matter and exhibit a spongiform morphology due to fine radially spread processes. The fibrous astrocytes are present in the white matter and display longer processes, which provide structural support for axons. Both types can be identified by the glial fibrillary acidic protein (GFAP), which is used as a typical astrocyte marker in immunohistochemistry (Nolte et al., 2001). Protoplasmic astrocytes have fine branched processes, which are in close proximity to synapses. Therefore, they contribute to metabolic and homoeostatic balance in the brain. Moreover, they contribute to functional integrity of the blood-brain-barrier (BBB) (Wilhelmsson et al., 2006). Astrocyte endfeet enwrap the walls of blood vessels tightly (Abbott, 2002). That gives them the chance to actively regulate the diameter of vasculature and to control the blood flow in the brain (Haydon and Carmignoto, 2006; Wang and Bordey, 2008). They are able to take up ions, metabolites and water from the blood. Vice versa this connection is used for the release of toxic substances, clearance of ions and metabolites. Therefore, astrocytes are important for maintaining the homoeostasis in the brain. To due so, they express many transporters and channels in their endfeet such as glucose transporters, aquaporins and potassium channels (Wang and Bordey, 2008).
Astrocytes occupy their own domains, meaning that they contact the neighbouring astrocyte in a non-overlapping manner (Pekny et al., 2014; Bushong et al., 2002). They only overlap each other by 10% of their distal processes (Halassa et al., 2007).
Astrocytes coordinate the transport of glucose from blood vessels to neurons, by converting glucose into lactate by glycolysis, which neurons demand for their energy supply, e.g. for generating action potentials (Howarth, 2014; Rouach et al., 2008). This metabolite conversion is known as astrocyte-neuron lactate shuttle and provides a constant energy supply (Giaume et al., 2010). Furthermore, during neuronal firing ions and neurotransmitters are spilled over. Those are taken up by astrocytes maintaining the homoeostasis in the brain (see chapter 1.4.2).
Through gap junction coupling (GJC) astrocytes communicate intercellularly by distributing molecules with less than 1-1.2 kDa weight and 1.5 nm diameter through their network (Giaume et al., 2010). Studies investigating in the permeability of gap junction channels have shown, that the exchange of molecules depends on their weight, structure and charge, as well as on their specific interactions within the channel pore, such as electrostatic binding forces (Giaume et al., 2010). Via GJC an equal distribution of ions (K^+, Na^+), second messenger molecules (IP_3, cAMP), water, metabolites (glucose, lactate) and transmitters is maintained (Wallraff, 2006; Giaume et al., 2010; Bedner et al., 2006; Niermann et al., 2001; Rouach et al., 2008). Gap junctions are formed by connexins (Cx), which are transmembrane proteins. They form homo- or heterohexamers, called

connexons, displaying different biophysical properties such as conductance, selectivity, gating properties and sensitivity to transjunctional voltage. Two connexons from adjacent cells form a gap junction channel. Such can be between neurons and between glial cells in the CNS (Nakase et al., 2003). The two major connexins expressed in astrocytes are Cx43 and 30. Their expression differs within various regions in the brain (Gosejacob et al., 2011; Griemsmann et al., 2015). A study has shown that the degree of intercellular coupling is higher in the CA1 region than in the CA3 (D'Ambrosio et al., 1998). Coupling between hippocampal astrocytes is predominantly (78%) mediated by Cx43 (Gosejacob et al., 2011).
Astrocytes control the extracelllar ion concentration by their ability to take up K^+ via their inward-rectifying K^+ channels (Kir) and two-pore domain TREK-1/TWIK channels, which are highly present in the astrocytic membrane mediating the passive conductance (Wallraff, 2006; Seifert et al., 2009; Hwang et al., 2014). $Kir_{4.1}$ channels are responsible for the clearance of excess extracellular K^+ spillover during high neuronal activity. Furthermore, the K^+ uptake occurs by the $Na^+/K^+/Cl^-$ cotransporters and Na^+/K^+-ATP pumps (Kofuji and Newman, 2010; D'Ambrosio et al., 2002). As astrocytes are coupled, it allows them to distribute the uptaken K^+ from sites displaying high extracellur concentrations and redistribute it throuh their network to sites with low extracellular concentrations. This mechanism works due to the difference in resting membrane and equilibrium K^+ potential resulting in a driving force of K^+ influx in astrocytes (Orkand, 1986). This role in spatial K^+ buffering is essential to keep the balance of K^+ in the brain (Orkand, 1986; Kofuji and Newman, 2010). Studies have demonstrated that in transgenic double knockout mice for Cx43/Cx30, the potassium buffering was impaired and caused spontaneous epileptiform events and a reduced threshold for the generation of epileptic activity (Seifert et al., 2010; Wallraff, 2006).
Furthermore, astrocytes actively take part in the formation of synapses and in modulating synaptic function through bidirectional communication (Bernardinelli et al., 2014). In the "tripartite synapse" astrocyte contribute to synaptic activity by releasing neuron-activating molecules such as glutamate or γ-aminobutyric acid (GABA), and thereby either enhancing or inhibiting the neuronal activity (Araque et al., 2014; Newman, 2003). Glutamate release is dependent on the increase of intracellular Ca^{2+} levels (Edwards and Gibson, 2010). The uptake of glutamate occurs via the excitatory amino acid transporters GLAST and GLT-1, which prevents an accumulation of the neurotransmitter in the synaptic cleft, resulting in neuronal hyperactivity (Seifert et al., 2010; Chaudhry et al., 1995). If extracellular glutamate binds to astrocytic metabotropic glutamate receptors (mGluR3/5) the intracelluar astrocytic Ca^{2+} level rises and calcium waves mediated by inositol-1,4,5-triphosphate (IP_3) propagate through GJC (Giaume and Venance, 1998; Hatton and Parpura, 2004; Steinhäuser and Seifert, 2012). Another way of calcium wave propagation, which is thought to be the major determinant mechanism, is via ATP-mediated P2YR1 activation on neighbouring astrocytes (Tian et al., 2006). Astrocytic ATP is stored in lysosomes, which are released by calcium-dependent exocytosis (Zhang et al., 2007; Li et al., 2008). Blocking of these lysosomes prevented the astrocytic release

of ATP and the spread of calcium waves (Bowser and Khakh, 2007). Thus, astrocytic calcium signalling is able to synchronise the neuronal network activity, resulting in the release of gliotransmitters and modulation of synaptic transmission (Sasaki et al., 2014; Malarkey and Parpura, 2008).
Nowadays, the physiological importance of astrocytes on the neuronal survival, synaptic transmission and plasticity, as well as controlling the homoeostasis in the brain is highly acknowleged in research. Therefore, an increasing number of studies try to understand the role which astrocytes play in neurodegenerative diseases, like epilepsy.

1.2 Epilepsy

Epilepsy is a neurological disorder affecting approximately 65 Million people worldwide. The brain shows unpredictable occurence of seizures, which are characterised by abnormal, excessive or synchronised neuronal activity (Fisher et al., 2005; Goldberg and Coulter, 2013).
Patients suffer from a decreased quality of their life: the daily routine is restricted by sudden appearance of seizures, which limits the ability to carry out everyday tasks if no successful therapy is possible. The International Leage Against Epilepsy (ILAE) works on standardising classification of epilepsies and reports a refined version with new terminology and concepts yearly. In their last report from 2017 they classified epileptic seizures based on their site of origin into focal (subdivided into aware or non-aware seizures, and further "subgrouped as those with motor and nonmotor signs and symptoms at the onset"), generalised (arises and involves the entire brain and is divided into motor and nonmotor (absence) seizures) or unknown onset (with additional features including motor, nonmotor or tnoic-clonic spasm and "a seizure type of unknown onset may later become classified as either of focal or generalized onset) (Fisher et al., 2017). Of clinical relevance is also a classification of seizures according to their cause (genetic, structural/metabolic or unknown) (Shorvon, 2011; Panayiotopoulos, 2012).
Epileptic patients receive at first hand medical treatment with antiepileptic drugs (AEDs), which mainly target neuronal mechanisms, such as inhibiting voltage-gated sodium channels (e.g. Phenytoin, Carbamazepine) and/or the calcium channels (e.g. Valproic acid, Felbamate) or increasing the GABAergic neuromodulation (e.g. Phenobarbital) and reducing the glutamatergic systems (e.g. Topiramate) additionally. Some AEDs act through unknown mechanisms or their functionality is not yet fully understood (Levetiracetam, Valproate). Still AEDs have the disadvantage to have an impact on the CNS in general, leading to cognitive impairment or mood alterations. Beside that, one third of the patients with treatment still have seizures or even become pharmacoresistant. For these intractable patients, a resection of the epileptogenic area can help to live seizure-free after the operation. Specilists in epilepsy centres need to evaluate the risks of postoperative neurological deficits or infections (Georgiadis et al., 2013; Rogawski and Löscher, 2004; White et al., 2007).

1.2.1 MTLE-HS

In 2010 the ILAE published a classification based on the strucural origins of human epilepsy neuropathology (Berg et al., 2010). The most common form of epilepsy-related structural causes is hippocampal sclerosis (HS) or Ammon's horn sclerosis (AHS), which is characterised by the loss of neurons in the *str. pyr.*, granule cell dispersion (GCD), astrogliosis, microvascular proliferation and mossy fiber sprouting (Blümcke et al., 1999; Thom, 2014). It was shown that most of the epileptic seizures originate in the hippocampus, which is part of the medial temporal lobe (De Lanerolle et al., 2003). Temporal lobe epilepsy (TLE) is "characterised by recurrent seizure activity originating within the temporal lobe" (Hubbard and Binder, 2016). TLE is the most common form of epilepsy in adults and seizures are medically intractable in about 75% of patients with mesial TLE (Schmidt and Löscher, 2005) MTLE-HS is classified by the ILAE into type 1 the "classical HS" displaying severe loss of neurons and gliosis in CA1 and CA4 area and "atypical HS" showing a predominant neuronal cell loss with gliosis in either CA1 (type 2) or CA4 (type 3) (Thom, 2014; Hubbard and Binder, 2016) (Fig. 1.3).

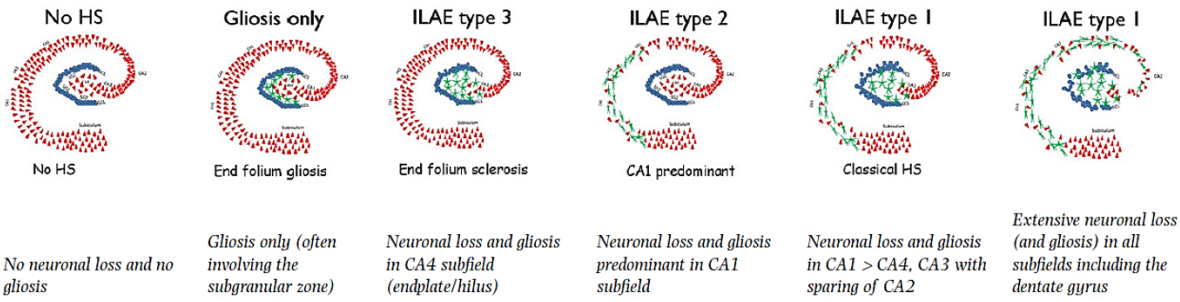

Figure 1.3 Classification scheme of hippocampal sclerosis in epilepsy: In the pictures, pyramidal neurons of hippocampal subfields and subiculum are shown in red, granule cells in blue and astrocytosis in green. *Source: modified from Thom (2014)*

The neuronal loss results from seizure activity and is accompanied with loss of glutamatergic neurotransmission or/and excessive changes in Na^+ and Ca^{2+} homoeostasis. Neurons become stressed, resulting in the production and release of free-radical oxygen species (ROS) accumulating in the cells and causing necrosis (Henshall, 2007; Dericioglu et al., 2013). Additionally, osmolytic stress activates molecular cell pathways for apoptosis, a form of p53-driven controlled cell death (Hanahan and Weinberg, 2000). Moreover, the GCD is typically seen in context of hippocampal neuronal loss and it was suggested by Thom (2014) that this is an aquired process rather than a pre-existing abnormality as it was found in epilepsies with early onset, like febrile seizures occuring in

infants in long lasting forms of epilepsy (Blümcke et al., 2009). There are two theories, explaining the occurrence of dispersed neurons: either they are newly generated following atypical neurogenesis (Fahrner et al., 2007; Engel et al., 2011) or occur by abnormal migration of mature neurons, so called 'somatic translocation' (Murphy and Danzer, 2011). This describes the shift of the cell body into an apical dendrite and was reported in animal models and resected tissue from epileptic patients with HS, which displayed a wider branching of dendrites (Murphy and Danzer, 2011; Freiman et al., 2011). Finally, the reduction or loss of neurons in HS has been associated with impairment of memory performance in TLE, indicating its importance for epileptic patients (Coras et al., 2010; Karádi et al., 2012).
Astrogliosis or reactive gliosis refers to hypertrophic glial cells, which are present in slerotic but also non-sclerotic human tissue (Das et al., 2012; Binder and Steinhäuser, 2006). Animal models have shown that astrocytes typically display thickened and long processes in the latent phase and early chronic stage of epileptogenesis. Those hypertrophic astrocytes are prominently exhibited in immunohistochemical staining against GFAP. Beside an upregulation of GFAP high vimentin immunoreactivity is a second pronounced marker of sclerotic hippocampus (Das et al., 2012). In the late chronic phase (9 months after *status epilepticus*) rather diffuse GFAP staining pattern was found and cell structures difficult to detect (Bedner et al., 2015). Similarities were found in hippocampal sclerosis from epileptic patients, which also displayed pronounced diffuse GFAP-immunoreactivity or rather long astrocytic fibrils (Hinterkeuser et al., 2000). Moreover, co-staining of individual cells with S100β was necessary to clearly identify glial cells in the hippocampus of AHS specimen (Bedner et al., 2015; Hinterkeuser et al., 2000). Furthermore, several other glial specific proteins are altered in their expression and used as 'hallmarks of HS' (Pekny and Nilsson, 2005; Wilhelmsson, 2004).

1.2.2 Animal models of epilepsy

This chapter shall give a brief overview of animal models of epilepsy. As different types of epilepsy appear, several animal models are established to study specifically the underlying mechanism or approaching the distinct type of epilepsy. This project aimed to investigate TLE in a kainate-induced mouse model.
A perfect model would need to mimick the human situation very closely: i) age of onset, ii) the seizure phenotype and EEG characteristics and iii) comorbidities and long-term consequences (Raol and Brooks-Kayal, 2012). Depending on the intention of investigation, several animal models have been developed following a variety of goals: i) discovery and characterisation of new AEDs, ii) understanding the relevant processes for the seizure onset and epileptogenesis and iii) discovery of antiepileptogenic treatments in chronic models of epilepsy (Hubbard and Binder, 2016; Löscher and Brandt, 2010; Löscher, 2011). Animal models, which have the purpose to study the development of epilepsy should depict typical characteristics of epileptogenesis, that includes the initial

precipitating insult (e.g. SE, traumatic brain injury, febrile seizures), the seizures-free latent phase and the subsequent period of spontaneous recurrent seizures (SRS) activity. For induced TLE models the chemoconvulsants kainic acid (KA) or pilocarpine are applied either systemically into the body or locally into the brain. Both models are used for understanding the processes in human TLE with HS (Kandratavicius et al., 2014). In systemically injected models, the animals show bilateral neuronal damage, which even exceed the limbic structures while human sclerosis in TLE patients is usually confined to one hippocampus (Jefferys et al., 2016). Despite that, the mortality rate is very high and difficult to bring in line with the directive 2010/63/EU on the protection of animals used for scientific purposes and national government regulations nowadays. Therefore, models with an unilateral local injection have been developed. The three most commonly models use KA injections into the amygdala, hippocampus and cortex (Mouri et al., 2008; Li et al., 2012; Araki et al., 2002; Gröticke et al., 2008; Bedner et al., 2015). All recapitulate the characteristics of HS, such as neurodegeneration, astrogliosis and mossy fiber sprouting in the ipsilateral KA-injected side and develop chronic epilepsy with SRS, serving well as models for the human MTLE-HS (Jefferys et al., 2016; Lévesque and Avoli, 2013). All models have an artificial trigger, but the aim is that already in the early phase after epilepsy induction, comparable similarities exist to epileptic patients and that animal models predict a similar outcome in the chronic phase, closely mimicking the human pathophysiological situation.
Animal models are still essential to understand the time course of epileptogenesis and for developing new AEDs as the resected tissue from neurosurgical operation are exclusively from chronic pharmacoresistant patients and the research lacks 'control of human tissue' to fully understand the process of the neurological disorder.

1.3 Inflammation

Basically inflammation describes a complex condition of the body to fight foreign pathogens. The immune response consists of two types: i) the innate and ii) the adaptive response. The innate is a fast, non-specific response with the aim to prevent an initial infection by activating natural killer (NK) cells and the complement cascade that progresses into an adaptive immune response. This response requires more time as B-lymphocytes need to be activated. They memorise permanently the pathogen or produce antibodies tagging the pathogen and activate T-lymphocytes that induce cell death or help to activate other immune cells. Neuroinflammation in the brain is mainly a local response by activated microglial cells, which are the innate immune cells in the brain, and astrocytes. Both cell types are able to release proinflammatory cytokines (small proteins balancing the adaptive and innate response) like interleukin-1β (IL-1β) and tumor necrosis factor alpha (TNF-α) (Clark et al., 2010; Liddelow et al., 2017; Liddelow and Barres, 2017).

1.3.1 IL-1β

The superfamily of interleukins belongs to the cytokines, which are released from macrophages, lymphocytes and NK cells as a response to a stimulus and bind to their target receptors on a diversity of cells. IL-1β acts as a mediator in a variety of inflammatory responses and has its impact on several cascades of (patho-)physiological events. The immature pro-IL-1β needs to be cleaved in its active form by the interleukin-1 converting enzyme (ICE), an cysteine-aspartic protease (caspase) and binds to its receptor one (IL-1R1) (Thornberry et al., 1992). IL-1β has a naturally produced antagonist (IL-1Ra), which binds to the same receptor (IL-1R1) without inducing the down-stream signalling cascade of nuclear factor-κ-B (NFκB)- or mitogen-activated protein kinase (MAPK) pathway, resulting in gene transcriptional changes in the cell nucleus.
In the brain interleukins are expressed at very low or even undetectable concentrations under physiological conditions. Their expression is often upregulated in pathophysiological cases by a variety of stimuli. The proinflammatory cytokine TNF-α as well as hypoxia and cellular injury are able to induce an IL-1β mRNA increase within minutes and an upregulation of its protein within hours (Allan et al., 2005). An early increase is often seen in innate immune cells, like monocytes and the macrophage lineage including microglial cells, wherease a subsequent expression occurs in astrocytes and invading immune cells, which contribute to neuronal damage (Boutin et al., 2003; Ching et al., 2005). Therefore, decreasing IL-1β signalling is from great therapeutical interest. A clinically approved IL-1β receptor antagonist called Anakinra (Sobi) is a drug used to treat rheumatoid arthritis (RA) (Fleischmann et al., 2006).

1.3.2 TNF-α

Tumor necrosis factor α was initially found to be a potent cytokine produced from immune cells to cause necrosis in tumour cell lines. Several years later the large TNF ligand family was discovered and TNF-α is nowadays controversially discussed as a pleiotropic cytokine for its role in normal physiology, in pathophysiology like inflammation and/or autoimmune disease (Tracey and Cerami, 1994; Chu, 2013).
TNF is mainly produced by macrophages, but also synthesised by other cell types in the CNS, such as lymphocytes, some populations of neurons, microglia and astrocytes (Lieberman et al., 1989; Clark et al., 2010; Figiel, 2008). TNF-α exists in two biologically active forms, a transmembrane bound (tmTNF) and a soluble form (solTNF). The latter is produced by cleavage of the tmTNF form through the TNF-α converting enzyme (TACE) (Chu, 2013; Kriegler et al., 1988; Black et al., 1997). The TNF receptor (TNFR) family has two members, TNFR1 (p55) and TNFR2 (p75). TNFR1 is expressed in most tissues while TNFR2 is rather found on immune cells like lymphocytes, endoepithelial cells and microglia (Wajant et al., 2003; Chu, 2013; McCoy and Tansey, 2008). The two TNF ligands can bind to both TNFRs, but TNFR1 is rather activated by the soluble form, whereas TNFR2 signalling is induced by the transmembrane form

(Wajant et al., 2003; Grell et al., 1995). Interestingly, only the TNFR1 contains a death domain, which gets activated after the ligand has bound to its receptor, leading to a conformation change and internalisation of the receptor (Sedger and McDermott, 2014; Palladino et al., 2003).
This change induces various downstream signalling factors, like caspase-8 and -3, which initiate apoptosis. Or necroptosis is induced via activating receptor-interacting serine/ threonine-protein kinases (RIPK1 and RIPK3). Alternatively, the activation of IKKβ-NFκB pathway and MAPK-pathway occurs leading to gene transcriptional changes in the nucleus (Fig. 1.4) (Smolen and Steiner, 2003). Several DNA binding sites for the NFκB have been detected in TNF$-\alpha$ genes located on chromosomes 7 and 17. Therefore, the TNF-α expression seems to be dependent on the NFκB-pathway and allows the cytokine to induce its own regulation (Chu, 2013; Philip and Epstein, 1986). Especially in the brain, TNF-α signalling is not only inducing injury-mediated microglia and astrocyte activation, it also has an impact on the synaptic plasticity scaling (Tansey and Wyss-Coray, 2008; Beattie et al., 2002). TNF-α plays a pivotal role depending on its concentration: at high levels it causes septic shocks, progresses autoimmune diseases like RA, leukemia or Crohn's disease and is a hallmark of neurodegenerative conditions, e.g. Alzheimer's disease (AD), Parkinson's disease (PD), multiple sclerosis (MS), whereas low TNF-α concentrations may cause cachexia (Wajant et al., 2003; Chu, 2013; McCoy and Tansey, 2008). It is considered to be one of the major proinflammatory mediators, with the capacity to induce cell death via apoptosis or necrosis, and a promising target for therapeutical approaches.
TNF-α signalling can be inhibited via its i) receptors (Etanercept, Lenercept), ii) ligands (Infliximab, XPro1595), iii) converting enzymes like TACE (GW333, Apratastat) or iv) other pathways, such as inactivating the downstream signalling cascade of p38 MAPK-pathway (VX-702, RWJ67657) (Fig. 1.5) (Palladino et al., 2003; McCoy and Tansey, 2008; Kontermann et al., 2009). As the ligands can bind to both TNFRs, inducing via TNFR1 cell death but via TNFR2 cell survival, it is important that next-generation therapeutics target specifically the solTNF-α/TNFR1 signalling pathway and spares the tmTNF/TNFR2 cascade (Probert, 2015; Marchetti et al., 2004). Therefore, two new inhibitor strategies have been developed within the last 10 years: i) exclusive inhibition of the solTNF-α form, e.g. through XPro1595, XENP345 and ii) selective binding to a TNFR1-domain, e.g. with DMS5540, TROS (Fischer et al., 2015). Selective solTNF-α inhibitors have a dominant-negative structure (dnTNF), which allows them to form inactive heterotrimers without inducing the TNFR1 signalling cascade, thus leaving tmTNF unaffected (Fischer et al., 2015). One example of a dnTNF inhibitor is the afore mentioned XPro1595 (Xencor) (Steed et al., 2003), which inhibits the downstream signalling via NFκB pathway (Wajant and Scheurich, 2011; Fischer et al., 2015). XPro1595 has been used so far in animal models of neurodegenerative diseases investigating the role of solTNFα in spinal cord injury (SCI) (Novrup et al., 2014), AD (MacPherson et al., 2017), PD (Barnum et al., 2014), HD (Hsiao et al., 2014), MS (Karamita et al., 2017) and limbic epilepsy (Patel et al., 2017) (chapter 6.4).

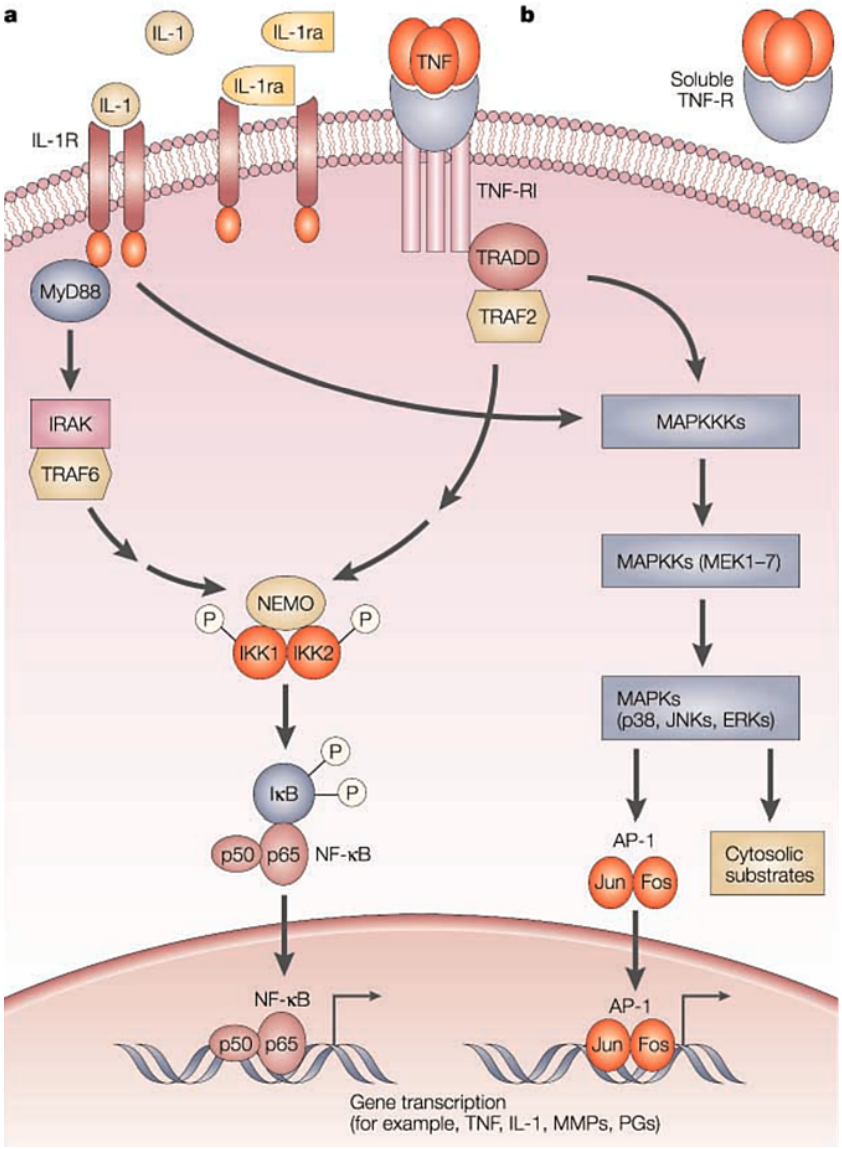

Figure 1.4 Simplified overview of TNF-α and IL-1β signalling pathway: Two major pathways, the NFκB (left) and the MAPK pathway (right) are activated by the proinflammatory cytokines TNF-α and IL-1β. **(a)** The ligation of receptors with proinflammatory cytokines activates the IκB kinase (IKK) complex, which phosphorylates the NFκB proteins (IκB), leading to their degradation. Thereby, NFκB enters the nucleus and activates several genes coding for molecules, such as cytokines, chemokines, cyclooxygenase-2, antiapoptotic and stress proteins. **(b)** After receptor ligation activates upstream kinases of MAPKs pathway, the transcription factor AP-1 induces activation of genes coding for various cytokines, including TNF-α and IL-1β themselves, and other molecules. Proinflammatory cytokines mostly induce the JNK and p38 MAPK cascades. AP-1, activator protein-1; IRAK, IL-1 receptor-associated kinase; MyD88, myeloid differentiation protein 88; NEMO, NFκB essential modulator; TRADD, TNF receptor-associated death domain protein; TRAF, TNF receptor-associated factor. *Source: modified from Smolen and Steiner (2003)*

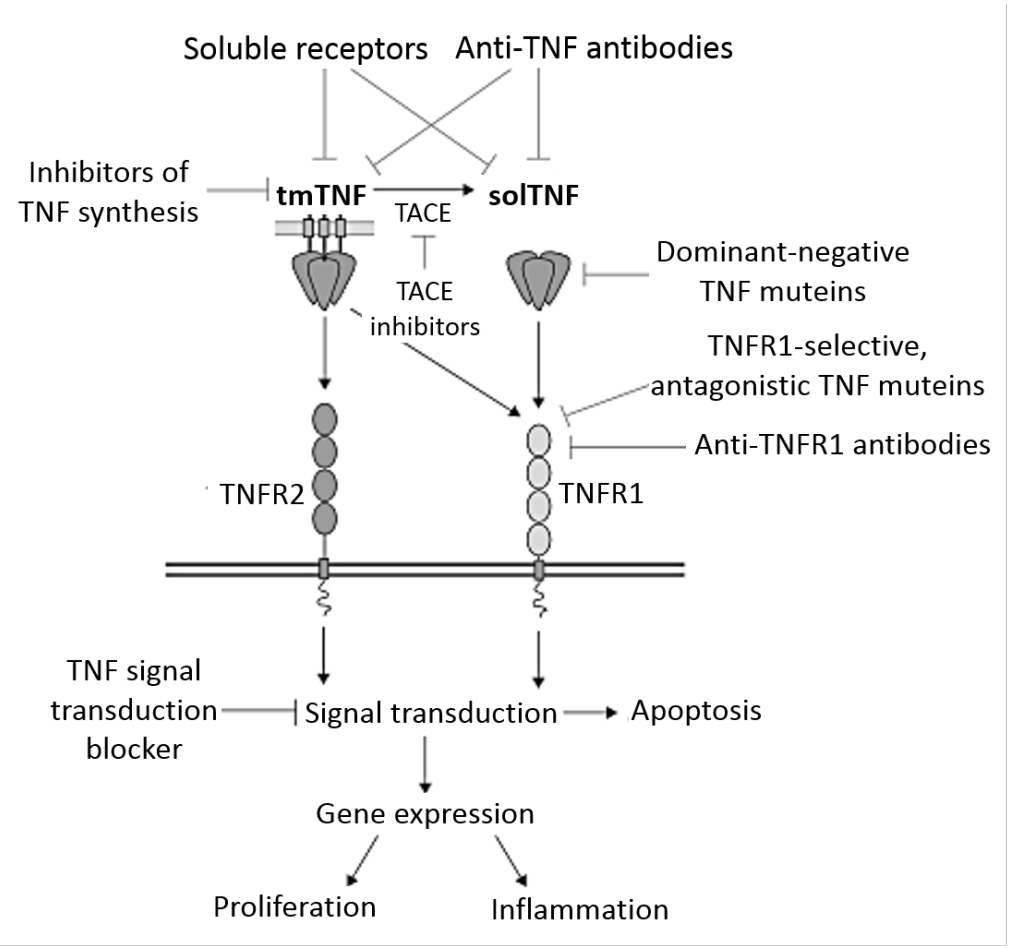

Figure 1.5 Strategies to interfere with TNFR action: Anti-TNF antibodies (Infliximab, Adalimumab, Certolizumab pegol) and soluble TNFRs (Etanercept, Lenercept) act on both TNF-α forms. Current solTNF-α/TNFR1 targeting agents under development are selective solTNF-α inhibitors (TNF muteins) (XPro1595, XENP345) and selective anti-TNFR1 antibodies (DMS5540, TROS, ATROSAB, R1antTNF). Abbr. tmTNF, transmembrane TNF; solTNF, soluble TNF; TACE, TNF-α converting enzyme *Source: modified from Kontermann et al. (2009) and Fischer et al. (2015)*

1.4 Inflammation in TLE

Until today, the molecular mechanisms underlying TLE are still not fully understood. Several morphological and functional changes occur within the disease progression in neuronal and glial cells.
Most prominent are the alterations in astrocytes and microglia, which transform into an activated pathological state, called gliosis. Gliosis is found in human epileptic brain (McKhann et al., 2000). Tissue, resected from TLE patients, showed massive gliosis, characterised by hyperthrophic astrocytes. Several studies found alterations in receptor expression (mGluR5, P2YR1, IL-1R) and transporter functionality (GLT-1), dysfunction in BBB, impaired K^+ and water homoeostasis, altered Ca^{2+} transients, release of gliotransmitters and cytokines (Fig. 1.6).
Furthermore, microgliosis has been found in patients with recurrent seizures as well as in the hippocampus in experimental models of epilepsy (Beach et al., 1995; Drage et al., 2002; Van Vliet et al., 2012). Studies showed that activated microglia were present in patients with intractable MTLE-HS (Beach et al., 1995; Zattoni et al., 2011) and in close proximity of regions with neuronal loss (Borges et al., 2006). Therefore, some authors suggest that microgliosis faciliates neuronal malfunction (Beach et al., 1995; Taniwaki et al., 1996). The author Mirrione et al., observed that KA-induced excitotoxicity caused neuronal tissue-type plasminogen activator (tPA) release (Mirrione et al., 2007). TPA activates microglial cells, which in turn are able to release tPA and provoke further neuronal injury (Siao et al., 2003). Thus, microglial cells facilitate seizure recruitment and the chronic maintenance of convulsions (Buckmaster et al., 2002; Winokur et al., 2004).
It is well known, that activated microglia also express GLT-1 and contribute 10% to glutamate uptake, while astrocytic GLT-1 is downregulated (Nakajima et al., 2001; Shaked et al., 2005; Persson et al., 2006). As microglia are the main innate immune cells in the brain, their proinflammatory role is "postulated to be the etiologic driver of epileptogenesis" (Zhao et al., 2018; Abraham et al., 2012; Aronica et al., 2017; Colonna and Butovsky, 2017).
The impact of inflammation on the development of epilepsy is undeniable. In human and experimental febrile seizure and TLE, increased levels of cytokines were found. A study by French et al. reported that around 40% of MTLE-HS patients experienced febrile seizures in their childhood (French et al., 1993). Therefore, inflammation seems to play an important role as a trigger in the development of TLE, more than just being a consequence. (Choy et al., 2014; Vezzani et al., 2008; Khan et al., 2016).

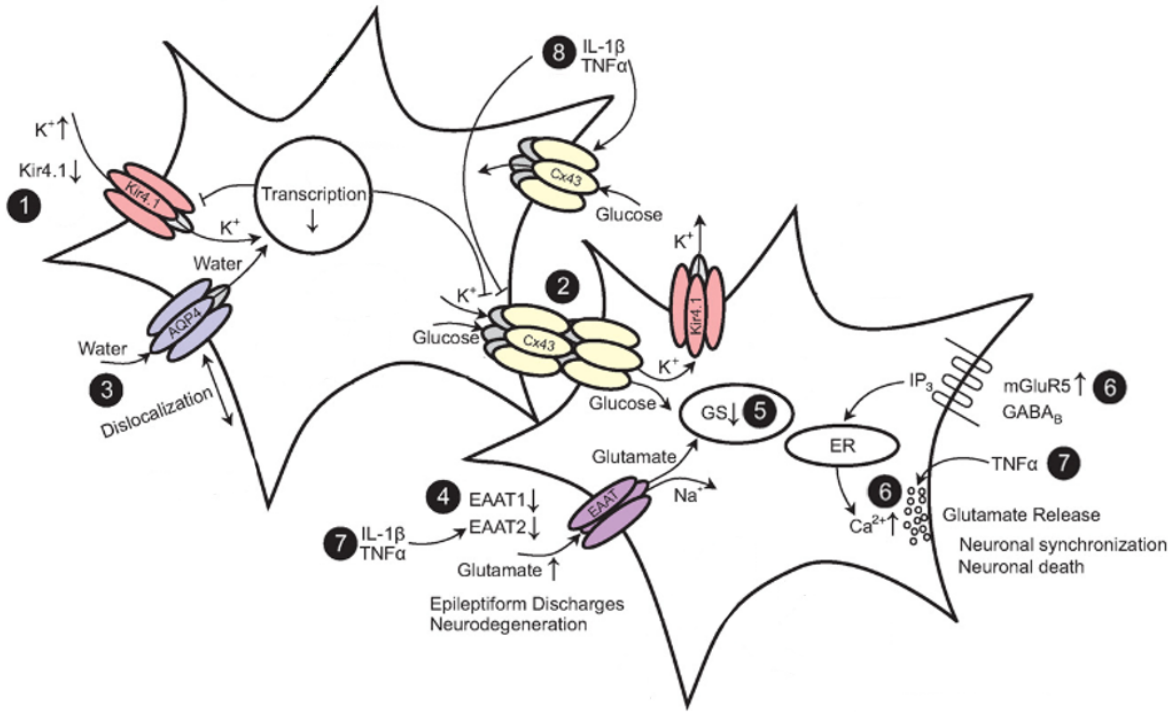

Figure 1.6 Dysfunction of astrocytes in epilepsy: **(1)** Extracellular elevated K^+ due to seizure activity is taken up by $Kir_{4.1}$ channels, which are downregulated in human and experimental epilepsy. **(2)** Gap junctional coupling mediates the redistribution of ions and metabolites. Transgenic knockout animals displayed an impaired K^+ buffering. **(3)** Dislocation of water aquaporin4 channels leads to impaired potassium buffering and astrocyte cell swelling. **(4)** Via glutamate transporters (EAAT1 and EAAT2) astrocytes take up glutamate. In human epileptic hippocampus both transporters were found to be reduced, leading to decreased threshold for seizure induction. **(5)** The glutamine synthethase (GS) converts glutamate into glutamine. Hippocampus tissue from epilepsy patients releaved a loss of GS, causing increased extracellular glutamate levels. A downregulation of GS was also found in experimental epilepsy in the chronic period. **(6)** Extracellular glutamate binds to metabotrobic glutamate receptors resulting in intracellular release of Ca^{2+} and calcium wave propagation within the coupled astrocytes, resulting in astrocytic glutamate release and neuronal synchronisation. In human and experimental epilepsy mGluR5 levels have been found to be upregulated. **(7)** Pro-inflammatory cytokines IL-1β and TNF-α inhibit glutamate uptake and lead to astrocytic glutamate release, contributing to neuronal hyperexcitability. TNF-α released from astrocytes during epileptogenesis might boost neuroexcitotoxicity and neuronal death. **(8)** IL-1β and TNF-α decrease Cx43-mediated GJC, due to phosphorylation of Cx43 C-terminus. *Source: modified from Seifert et al. (2010)*

1.4.1 Proinflammatory cytokines IL-1β and TNF-α in human and experimental TLE

Several studies have investigated the role of inflammation in epileptogenesis. Especially the results from experimental models differ slightly, which might be due to the study design: "different ages of mice used in the studies, the diverse times chosen to observe the results and the distinct doses" and ways of inducing epilepsy (Lu et al., 2008).
Hence, the following chapter will mainly focus on alterations of the proinflammatory cytokines IL-1β and TNF-α and their signalling in human and KA-induced experimental models of TLE.
Data obtained from neurosurgically resected specimen from patients with intractable TLE, show various neuroinflammatory changes: activated astrocytes and microglial cells exhibit increased proinflammatory cytokine levels, such as IL-1β and TNF-α (Bordey and Sontheimer, 1998; Hufnagel et al., 2003; Ravizza et al., 2008; Balosso et al., 2013; Ashhab et al., 2013). Moreover, parenchymal and perivascular astrocytes display an upregulation of the TNFR1 signalling pathway (Yamamoto et al., 2006; Balosso et al., 2013) and a study by Crespel et al. (2002) describes NFκB expression in reactive astrocytes, but not in microglial cells, in patients with febrile seizures in early childhood (Crespel et al., 2002). Additionally, a compromised BBB was found to be contributing to seizure activity (Dedeurwaerdere et al., 2012; Weinberg et al., 2013).
Several studies investigated the question how TNF-α and its receptors contribute to the development of seizure activity. The TNF-α/TNFR1 signalling pathway is suggested to have a proconvulsive role, whereas the TNF-α/TNFR2 signalling rather mediates anticonvulsive effects (Balosso et al., 2005; Weinberg et al., 2013). These results are from studies on transgenic TNFR-KO animals with KA-induced SE and overexpression of TNF-α via injection or viral transfection in wildtype and KA-injected rodents. Furthermore, the same studies show that the TNFR1 expression is first upregulated in pyramidal neurons (1 day post SE) and subsequently in astrocytes (1-2 days post SE). Neuronal TNFR2 expression was decreased and not detectable in astrocytes. An upregulation of TNFR1 in astrocytes in mice with intranasal application of KA showed an induction of astrogliosis (Lu et al., 2008). Another study by Probert et al. (1997) found that overexpression of TNF-α in naive animals induced astrogliosis. Moreover, these authors found that these reactive astrocytes were able to produce TNF-α, which was shown to alter the BBB. Overexpression of TNF-α also mediated microgliosis in naive and KA-injected animals (Probert et al., 1997; Zhu et al., 2010). Activated microglia have been shown to express TNF-α 24 hrs after SE induction (Vinet et al., 2016; Zheng et al., 2009). The TNF-α production and release by activated glia cell has been shown to induce neuronal injury (Rizzi et al., 2003). Damaged neurons also contribute to the overexpression of TNF-α, which results in seizures and early mortality (Balosso et al., 2013; Probert et al., 1997).
Primary hippocampal damage within the first day after SE induction is a directly KA-induced neuronal death. Whereas, the neuronal cell death, which is observed after that

time point, is indirectly mediated by the hyperactivity and its induced activation of enzymatic and nuclear mechanisms (Doble, 1999). The SE-induced neuronal death beyond the acute phase was also seen after intraamygaloid injection of KA in rats, which was caspase-3 mediated (Zhu et al., 2010). Caspase-3 activation occurs via the TNFR1 death domain signalling pathway resulting in apoptosis. Another study in microglia specific IKK-KO mice found that the KA-induced neuronal death was decreased, suggesting that dead neurons release microglia activational factors, such as high mobility group box-1 (HMGB1) (Cho et al., 2008; Dedeurwaerdere et al., 2012). Indeed, Cho et al. (2008) observed less activated microglial cells and astrocytes in the transgenic animals, indicating that the activation of microglia precedes that of astrocytes. The IKK-NFκB pathway is also activated by the IL-1β/IL-1R1 signalling. IL-1β is produced by astrocytes during the acute and chronic phase after SE induction, while in microglial cells IL-1β production was only present in the acute phase (Rizzi et al., 2003; Vezzani et al., 2002; Ravizza et al., 2008). IL-1R1 expression was found to be upregulated in hippocampal neurons and astrocytes in the acute phase, and decreased in astrocytes in the chronic phase after SE induction (Vezzani et al., 2002; Ravizza et al., 2008). In microglial cells IL-1R1 was not expressed (Vezzani et al., 2002; Ravizza et al., 2008). Overexpression of IL-1β is able to induce TNF-α production in astrocytes and microglial cells in naive animals via the IKK-NFκB pathway (Vezzani et al., 2002; O'Neill and Bowie, 2007) (Fig. 1.4).
Microglia are the "upstream partners" of astrocytes and are the first cells releasing inflammatory mediators, like TNF-α, triggering the activation of astrocytes (Lund et al., 2006; Pascual et al., 2012; Wang et al., 2015). Activated astrocytes synergise with microglia to release TNF-α (Garden and Möller, 2006; Bezzi et al., 2001), which attenuates together with IL-1β the glutamate uptake by astrocytes (Ye and Sontheimer, 1996; Hu et al., 2000). Furthermore, glial release of TNF-α induces Ca^{2+} increase via binding to P2YR1 and elevated extracellular glutamate levels (Vezzani et al., 2011; Santello et al., 2011). High extracellular glutamate levels contribute to seizure generation by hyperactivation of AMPAR and NMDAR on the postsynaptic neuron (Beattie et al., 2002; Stellwagen and Malenka, 2006; Viviani et al., 2003). A third observation found in *in situ, in vitro and in vivo* studies is that both proinflammatory cytokines inhibit the astrocytic GJC, which is known to result in extracellular accumulation of K^+ and glutamate (Même et al., 2006; Bedner et al., 2015).
In summary, different proinflammatory cytokines have been shown to exert various effects, depending on the type of receptor expression in the brain tissue and the inflammatory trigger. Still, most studies favour proconvulsive role of TNF-α and IL-1β in the development of TLE.

1.4.2 Role of astroglial coupling in TLE

The role of astroglial GJC in the development of TLE is still debated, as it has anti- as well as proconvulsive effects on epileptogenesis.

The astrocytic GJC has an anticonvulsive role in clearing neurotoxic substances, such as high levels of K^+ and glutamate.
During neuronal activity extracellular K^+ concentration increases. To keep the K^+ balance in the brain, astrocytes take it up through the $Kir_{4.1}$ channels and distribute it via their GJC (spatial buffering). Therefore, the astrocytic GJC preserves the potassium homoeostasis even during neuronal hyperactivity, which occurs during seizure activity (Wallraff, 2006). Furthermore, glutamate released into the synaptic cleft during neuronal activity is taken up by astrocytes mainly via GLT-1 and transport it within the network to astrocytes displaying lower glutamate concentration.
A study from Pannasch et al. (2011) using the transgenic mice devoid of the astrocytic proteins Cx43 and Cx30, in which the astrocytic GJC is completely lost, found decreased glutamate clearance causing alterations in synaptic transmission. Such a disturbance can cause enhanced neuronal susceptibility to hypersynchronisation resulting in neuroexcitotoxicity, which is typically seen in epilepsy (Meldrum, 1994; Coulter and Steinhauser, 2015).
Other studies in transgenic dKO mice for Cx43 and Cx30 revealed the importance of astrocytic GJC for the K^+ clearance. The mouse line $Cx30^{-/-}$; $Cx43^{fl/fl}$hGFAP-Cre lacks both connexins and therefore lacks astrocytic GJC. In these mice the spatial buffering exhibited epileptiform events (Wallraff, 2006). A recent study from Bedner et al. (2015) investigated the role of astrocytic K^+ spatial buffering in the SE-induced KA model of TLE *in vivo*. Four hours post KA injection, the GJC was already found to be reduced by 50% and the K^+ clearance was impaired.
In conclusion, the astrocytic GJC manages the redistribution of K^+ and glutamate accumulation from sites of high neuronal activity to avoid their accumulation in the extracellular space and the consequential seizure activity (Pannasch et al., 2011; Bedner et al., 2015). As the reduction in the astrocytic coupling appeared even before neuronal death at an early time point, Bedner et al. (2015) suggested that the astrocytic uncoupling causes the development of TLE.
Other studies claim a proconvulsive role of astrocytic GJC in epilepsy. Through the astrocytic GJC glucose and lactacte can be transported to supply neurons, which demand energy for generating epileptiform activity (Rouach et al., 2008; Giaume et al., 2010).
The delivery of metabolites for neurons via the GJC is more efficient than free extracellular diffusion of glucose, and covers a longer distance (Rouach et al., 2008). Moreover, there is some evidence that glutamate binds to astrocytic mGluR1/5 and contributes to calcium wave propagation within the coupled astrocytes (Ding et al., 2007; Seifert et al., 2010). That causes glutamate release from astrocytes contributing to the modulation of synaptic transmission and to non-synaptic neuronal synchronisation

(Ding et al., 2007). It was shown that high levels of glutamate are not only able to induce seizures, but also cause neuronal loss in epilepsy (Meldrum, 1994; Chapman, 1998). Whether the astrocytic GJC plays an anti- or proconvulsive role depends on the specific experimental condition.
In conclusion, a reduction of GJC leads to neuronal hyperactivity as K^+ and glutamate cannot be redistributed via the network. Neurons need subsequent delivery of metabolites for ongoing activity, which is hardly affordable in cases of reduced GJC. Furthermore reduced propagation of calcium waves are possible in cases of decreased GJC, and therefore neuronal synchronised firing would not occur.
An increase of GJC contributes to an equal distribution of K^+ and glutamate, preventing neuronal hyperexcitability. Still via calcium waves glutamate release is triggering neuronal firing, which is sustained by metabolic supply via the increased astrocytic GJC. Taken together, the increase or decrease of GJC in the astrocytic network plays an important role in the neuronal supply and maintainance of homoeostasis in the brain.

Studies, investigating the changes of Cx43 expression levels of mRNA or protein revealed controversial results. Often an increase of expression was found in animal models of experimental epilepsy (Takahashi et al., 2010; Szente et al., 2002). Also in cell culture elevated Cx43 protein levels were seen after KA-induced SE (Samoilova et al., 2003), suggesting that an upregulation of Cx43 compensates the elevated K^+ levels during epileptiform activity (Seifert et al., 2010). In contrast, in *in vivo* models of epilepsy no significant changes of the mRNA levels of Cx43 were found in epileptic hippocampus (Khurgel and Ivy, 1996; Söhl et al., 2000; Samoilova et al., 2003). Other studies found a downregulation of Cx43 mRNA (Elisevich et al., 1997; Elisevich et al., 1998) and protein level and GJC in a mouse model of tuberous sclerosis (Xu et al., 2009).
These controversial results may derive from the differences of the used animal models of epilepsy, such as study design, the examined time point and choice of animals.
Study results from human epileptic tissue are contentious. Hippocampal tissue resected from patients with MTLE displayed an increase of Cx43 protein level (Fonseca et al., 2002; Collignon et al., 2006). In line with that are the studies of Naus et al., Aronica et al. and Desphande et al., which found elevated levels of Cx43 in pharmacoresistant (tumour-associated) epilepsy patients (Naus et al., 1991; Aronica et al., 2001; Deshpande et al., 2017).
Furthermore, Steinhäuser et al. suggested that alterations of mRNA and protein levels of Cx43 do not give direct information of the functional GJC of astrocytes in TLE (Steinhäuser et al., 2012). The function of gap junctions are regulated by posttranslational modifications like kinase-induced phosphorylation, which influences the assembly of connexons, open probability and their location and GJ gating properties.
Therefore, our group has investigated recently the subcellular localisation of Cx43 in tissue obtained from MTLE-HS patients and experimental TLE (Deshpande et al., 2017). This study revealed a redistribution of Cx43 protein towards perivascular endfeet in HS. Furthermore, the authors suggest that rather increased phosphorylation at serine 255

at the C-terminus of Cx43 might contribute to the astrocytic uncoupling in MTLE-HS, than reduced connexin expression.
To identify the mechanism causing the SE-induced early loss of astrocytic GJC, which has been shown to crucially contribute to the cause of TLE, Deshpande et al. (2018) investigated the Cx43 expressional changes and phosphorylation status in KA-induced epilepsy mouse model (Deshpande et al., 2018). Four hours after SE induction, the authors found an increase of phosphorylation at the serine 262 (S262) position of the C-terminus of Cx43, but no changes in the Cx43 expression. S262 is phosphorylated by MAPKs, resulting in decreased open probability and a rapid internalisation of Cx43 GJ channels (Lampe et al., 1998; Thevenin et al., 2013). As lately, Bedner et al. (2015) found a significant reduction of astrocytic GJC also 4 hrs after KA-induced SE and showed that proinflammatory cytokines, like IL-1β and TNF-α, significantly decreased the astrocytic GJC in control tissue, Deshpande et al. (2018) inhibited the solTNF-α by applying the antagonist XPro1595. In this study, the authors found no astrocytic uncoupling *in situ* and demonstrated that by the inhibition of solTNF-α the phosphorylation of S262 was prevented. These results assume that the release of proinflammatory cytokines contributes to astrocytic GJC alteration in the early development of TLE.

2 Aim of the Study

About one third of epilepsy patients do not adequately respond to available antiepileptic drugs, which merely suppress seizures without curing the underlying disorder. Consequentially, new strategies for the development of disease-modifying or antiepileptogenic drugs are urgently needed. There is indeed growing evidence that brain inflammation is not only a consequence but often a causal event in epilepsy (Vezzani et al., 2011). The present study aimed at understanding the contribution of inflammation-induced astrocyte malfunction in the development of TLE. This gave me the intention to focus on the following questions:

(i) Are proinflammatory cytokine levels altered and do they have an impact on astrocytic gap junction coupling within the development of TLE?
Astrocytic gap junction coupling is reduced by 50% four hours after SE and completely lost after three months (Bedner et al., 2015). As cytokines mediate this alteration (Même et al., 2006; Bedner et al., 2015), that part of the study aimed at characterising the cytokine expression levels within the first day after SE. To better understand the contribution of gap junction coupling in the progression of TLE, it was a goal to further characterise the coupling strength in the latent and chronic phase.

(ii) Does inhibition of soluble TNF-α rescue astrocytic gap junction coupling?
The application of XPro1595 *in situ*, a specific inhibitor of soluble TNF-α, restored the proinflammatory cytokine-mediated astrocytic uncoupling in acute brain slices in wildtype animals (Desphande et al., 2018). The aim of this part of the study was to assess whether XPro1595 administrations before and after SE influences seizure-induced astrocytic uncoupling in the intracortical model of TLE. The results would provide an important basis to understand the function of solTNF-α/TNFR1 signalling in epilepsy.

(iii) Does inhibition of soluble TNF-α suppress the development of chronic seizures and hippocampal sclerosis?
The application of antiinflammatory drugs has been shown to decrease seizure activity (Ravizza and Vezzani, 2006; Libbey et al., 2011). The present study focused on the specific inhibition of solTNF-α/TNFR1 casacade as it is reported to have a proconvulsive role in the development of epilepsy (Balosso et al., 2005; Weinberg et al., 2013). The goal was to examine if XPro1595 attenuates the histopathological changes and reduces epileptic seizure activity, if applied before SE, in the acute phase or after the first spontaneous generalised convulsive seizure.

3 Materials

3.1 Chemicals

Compound	Company
Anakinra	Swedish Orphan Biovitrum (Sobi), Stockholm, Sweden
Antisedan®	Orion Pharma, Espoo, Finland
Aquapolymount	Polysciences, Warrington, USA
Bepanthen®	Bayer, Leverkusen, Germany
Baytril 2.5%	Bayer, Leverkusen, Germany
Betaisodona®	Mundipharma GmbH, Limburg, Germany
Biocytin	Sigma-Aldrich, München, Germany
$CaCl_2.6H_2O$	AppliChem GmbH, Darmstadt, Germany
Carbogen	Linde, Pullach, Germany
Cepetor	CP-Pharma, Burgdorf, Germany
Ethanol 99%	AppliChem GmbH, Darmstadt, Germany
Glucose	AppliChem GmbH, Darmstadt, Germany
Hoechst 33342	Molecular Probes, Eugene, USA
Isofluran	Piramal Healthcare, Morpeth, UK
Kainic acid	Tocris, Bristol, UK
Ketamin® 10%	WDT, Garbsen, Germany
Lipopolysachharide	Sigma-Aldrich, München, Germany
$MgSO_4.7H_2O$	AppliChem GmbH, Darmstadt, Germany
Na-Azide	Sigma-Aldrich, München, Germany
NaCl	AppliChem GmbH, Darmstadt, Germany
NaDOC	AppliChem GmbH, Darmstadt, Germany
NaH_2POH_4	AppliChem GmbH, Darmstadt, Germany
$NaHCO_3$	AppliChem GmbH, Darmstadt, Germany
NP-40	AppliChem GmbH, Darmstadt, Germany
Pala clear	Paladur, Hanau, Germany
Paraformaldehyde	AppliChem GmbH, Darmstadt, Germany
Rimadyl®	Pfizer, New York, USA
SDS	AppliChem GmbH, Darmstadt, Germany
Sodium pyruvate	AppliChem GmbH, Darmstadt, Germany
SR101	Sigma-Aldrich, München, Germany
Streptavidin-Cy3	Sigma-Aldrich, München, Germany

Sucrose	AppliChem GmbH, Darmstadt, Germany
Surgical PGA and Polyester	Smi, St. Vith, Belgium
Tris	AppliChem GmbH, Darmstadt, Germany
TritonX-100	Sigma-Aldrich, München, Germany
Tween-20	AppliChem GmbH, Darmstadt, Germany
XPro1595	Xencor, Monrovia, USA
Xylazine hydrochloride	Sigma-Aldrich, München, Germany

3.2 Software

Programme name	**Company**
Dataquest A.R.T 4.00 Gold/Platinum	DSI, St. Paul, USA
Igor Pro	Wave Metrics, Portland, USA
ImageJ	NIH, Maryland, USA
Imaris 8.0	Bitplane, Belfast, UK
LAS AF	Leica Microsystems, Wetzlar, Germany
SeeTec Office 5	SeeTec, Philippsburg, Germany
Tida	Heka, Lambrecht, Germany

3.3 Devices and equipment

Device	**Company**
Axioskop	Zeiss, Jena, Germany
centrifuges	Eppendorf, Wesseling, Germany
DMZ Zeitz-Puller	Zeitz, Martinsried, Germany
EPC-9	Heka, Lambrecht, Germany
fluorescence lamp	HBO100 Zeiss, Jena, Germany
heating plate	FMI, Beerbach, Germany
Leica SP8 LSM	Leica Microsystems, Wetzlar, Germany
Infinite M200Pro	Tecan, Männedorf, Switzerland
IR camera Axis 221	Axis Communications AB, Lund, Schweden
IPC pump	Ismatec, Wertheim, Germany
micromanipulator MHW-3	Narishige, Tokyo, Japan
microsyringe	Hamilton, Bonaduz, Switzerland
PCO (camera setup)	CCD Imaging, Kehlheim, Germany
perfusor	Braun, Melsungen, Germany
pH meter	Mettler Toledo, Giessen, Germany
Precellys24	Bertin Technologies, Montigny-le-Bretonneux, France
QuickPlex SQ120	MSD, Maryland, USA

radio receiving plate	DSI, St. Paul, USA
stereotactic frame	TSE Systems GmbH, Bad Homburg, Germany
syringe pump SP220IZ	WPI, Sarasota, USA
table top small centrifuge	VWR, Darmstadt, Germany
Vibratome VT1200S	Leica, Nussloch, Germany
vortexer	VWR, Darmstadt, Germany
V-Plex Kit 15048D	MSD, Maryland, USA
weight balance	Sartorius group, Göttingen, Germany

3.4 Antibodies

Primary Antibodies

Epitope	Species	Type	Dilution	Company
GFAP	mouse	mc	1:500	Abcam
GFAP	rabbit	pc	1:500	Dako
NeuN	mouse	mc	1:300	Chemicon
S100b	mouse	mc	1:500	Sigma
S100b	rabbit	pc	1:500	Abcam
TNFR1	rabbit	pc	1:1000	Abcam

Secondary Antibodies

Antibody	Species	Dilution	Company
anti-mouse-A488	goat	1:500	Molecular Probes
anti-rabbit-A488	goat	1:500	Molecular Probes
anti-mouse-A647	goat	1:500	Molecular Probes
anti-rabbit-A647	goat	1:500	Molecular Probes

Streptavidine Conjugates

Streptavidin-Cy3 1:300

3.5 Solutions and buffers

3.5.1 Solutions for electrophysiology

Preparation solution

NaCl	87	mM
KCl	2.5	mM
NaH_2PO_4	1.25	mM
$NaHCO_3$	25	mM
$MgSO_4.7H_2O$	7	mM
$CaCl_2.6H_2O$	0.5	mM
Glucose	25	mM
Sucrose	75	mM

pH 7.35-7.4 at 24°C adjusted with carbogen (95% CO_2 and 5% O_2.)
Osmolarity 320-330 mosmol

Artificial cerebrospinal fluid (ACSF)

NaH_2PO_4	1.25	mM
NaCl	126	mM
KCl	3	mM
$MgSO_4.7H_2O$	2	mM
$CaCl_2.6H_2O$	2	mM
Glucose	10	mM
$NaHCO_3$	26	mM

pH 7.35-7.4 at 24°C adjusted with carbogen (95% CO_2 and 5% O_2.)
Osmolarity 305-315 mosmol

Intracellular K-gluconate solution

K-gluconate	130	mM
$MgCl_2.6H_2O$	1	mM
Na_2-ATP	3	mM
EGTA	10	mM
HEPES	20	mM

pH 7.2 at 4°C, Osmolarity 280-285 mosmol
supplemented with 0.5% biocytin

3.5.2 Solutions and buffers for immunohistochemistry

Phosphate buffered saline (PBS 10x)

NaCl	1.5	mM
Na_2HPO_4	83	mM
NaH_2PO_4	17	mM

dissolved in dH_2O, pH 7.4

PBS with sodium azide

NaN_3	0.01%	(w/v)	dissolved in 1x PBS

Paraformaldehyde solution

Paraformaldehyde 4% (w/v) dissolved in PBS and dH_2O, pH 7.4

Blocking solution

NGS	10%	(v/v)
TritonX-100	0.5-2%	(v/v)

diluted in 1x PBS, pH 7.4

1st antibody solution

NGS	2-5%	(v/v)
TritonX-100	0.1-1%	(v/v)

diluted in 1x PBS, pH 7.4

2nd antibody solution

NGS	2%	(v/v)
TritonX-100	0.1%	(v/v)

diluted in 1x PBS, pH 7.4

Hoechst nuclei staining solution

Hoechst	0.5%	(v/v)

diluted in dH_2O

3.5.3 Solutions and buffers for ELISA

Phosphate buffered saline (10x)

NaCl	8000	mg/l
KCl	200	mg/l
Na_2HPO_4	1150	mg/l
KH_2PO_4	200	mg/l
$MgCl_26H_2O$	100	mg/l
$CaCl_2$	100	mg/l

dissolved in dH_2O, pH 7.4

Homogeneity solution Complete Protease Inhibitor, Roche 1 tablet
dissolved in 25 ml dH_2O

RIPA solution (2x)

Tris	50	mM
NaCl	150	mM
NP-40	2	%
NaDOC	1	%
SDS	0.2	%

dissolved in dH_2O

3.6 Animals

Animals used in this project were handled on the directive 2010/63/EU on the protection of animals used for scientific purposes and national government regulations. All experiments were designed and realised to minimise the number of animals due to the "Three Rs" presented in the directive 2010/63/EU. The animals were facilitated in the "Haus für Experimentelle Therapie" (HET) under standard housing conditions with a 12 / 12 hrs dark-light cycle. Employed keepers ensured the availability of food and drinking water during the whole time. For the project male transgenic mice with either FVB (Friend leukemia virus B) or C57BL/6 background were used.

3.6.1 hGFAP-eGFP mice

This transgenic mouse line with FVB background has an endogenous green flourescent protein (eGFP) expressed under the human glial fibrillary acidic promotor (hGFAP). A fragment of the hGFAP promotor was injected into a multiple cloning site into FVB/N oocytes (Nolte et al., 2001). In those animals mainly astrocytes are labbeled in green in the whole brain, including the hippocampus (Nolte et al., 2001). Additionally eGFP expression is found in NG2 cells (Wallraff et al., 2004). Male mice aged p90 to p120 were used for whole-cell patch-clamp recordings, stainings and molecular approaches like ELISA.

3.6.2 TNFR1 KO mice

The TNFR1 knockout animals or homozygous p55 lacking mice were originally ordered from Jackson Laboratory, ordering number 003242 known as *Tnfrsf1a* $^{tm1/mx}$ and were a gift from Zeinab Abdullah. They are C57BL/6 inbred. This transgenic mouse line is useful for investigating the role of TNFR1 signalling in different biological responses, such as TNFR1 contribution in neuroinflammatory-induced diseases. Mice aged p90 to p120 were used for whole-cell patch-clamp experiments, stainings and molecular approaches.

4 Methods

4.1 Electrophysiology

4.1.1 Preparation of acute brain slices

For the preparation of acute brain slices animals were deeply anaesthetised with isoflurane and decapitated. After the quick removal of the brain, coronal brain sections of 200 μm were cut for whole-cell patch-clamp experiments at a vibratome (VT1200S, Leica) with the speed of 0.08-0.12 mm/s and an amplitude of 1-1.2 mm. During cutting, the brain was placed in ice-cold preparation solution, which was constantly gased with carbogen (95% oxygen and 5% carbogen). To distinguish between the left (non-epileptic hemisphere) and right (ipsilateral) a little cut was made at the bottom on the left hemisphere. Sections only around the KA injection spot were used for the recordings. After cutting 5 slices, they were placed into 35°C warm and carbogenised sucrose to let them recover for 20 min. To better visualise the hippocampal astrocytes in adult mice brain, all sections were stained with 1 μM sulforhodamin 101 (SR101) in carbogenised ACSF at 35°C for additional 20 min (modified protocol from Schnell et al. (2012)). Finally, the sections were placed into a beaker with ACSF at room temperature (RT) for patch-clamp recordings. The compounds of all solutions are described in chapter 3.5.1.

4.1.2 Electrophysiological setup

Whole-cell patch-clamp recordings of astrocytes were obtained at an electrophysiological setup placed in a Faraday cage and balanced on a vibration isolated table (Newport) to sustain stationary recordings. Brain sections were cut into half and one of them placed in a bath chamber, which is perfused with carbogenised ACSF continously by a peristaltic pump (speed 1 ml/min). To keep the tissue at its place, it was placed under a U-shaped platinum wire with nylon strings glued on it. Patch-clamp electrodes made of borosilicate glass (1.5 mm diameter) were pulled with a DMZ Zeitz Puller and had an opening resistance between 3-5 MΩ filled with 0.5% biocytin intracellular solution (chapter 3.5.1). In the glass pipettes a teflon-coated silver wire with a chloride tip was inserted. To maintain a closed circuit a reference electrode with a silver-silver chloride pellet was placed in the bath solution and connected with the head stage of the amplifier. For moving the patch pipette a hydraulically controlled micromanipulator (MHW-3, Narishige) was used.

To visualise the section an upright microscope (Axioskop, Zeiss) was used with a magnification of 60x immersion objective and camera (PCO, CCD Imaging). To identify astrocytes the wave length of 605 nm was applied by a fluorescence lamp (HBO100, Zeiss). For recording the current of cells a patch-clamp amplifier (EPC-9, HEKA) was used. With a software programme (TIDA, HEKA) the currents could be measured.

4.1.3 Whole-cell patch-clamp recording of astrocytes

The patch-clamp technique was developed around 1980 by Erwin Neher and Bert Sakmann (Neher and Sakmann, 1976). This technique allows to record currents of multiple channels simultaneously, over the entire cell membrane.
Thereby, a patch pipette filled with internal solution was placed in the bath chamber. Additionally, overpressure was applied to keep the pipette tip opened during approaching the cell. Only fluorescenct cells at the wavelength of λmax = 605 nm and showing the typical whole-cell current pattern for an astrocyte were selected for patch-clamp recordings (Fig. 4.1a). After reaching the target cell the overpressure was taken away and the cell was simultaneously clamped at -80 mV. For a stable recording over 20 min, a tight cell-attached mode is essential. Therefore, low underpressure was applied to obtain a close contact between the pipette tip and cell membrane until a high resistance at 1 GΩ (Gigaseal) was achieved. After sealing a short underpressure suck was done to open the cell membrane and to gain access.
Before accessing the cell, a fast artefact compensation (C_{FAST}) using a 30 kHZ and 10 kHz filter was applied to decline the artefact current generated by immersion of the patch pipette and batch solution. After opening the cell the artefact data was filtered with 10 kHz and 3 kHz, a measure for the access quality. For analysing the input and series resistance the Igor Pro tool written by PD Dr. Ronald Jabs was used. This calculates the series resistance based on the mathematical equation $R_s = \Delta U / I(t_0)$ and $R_m = \Delta U / I(t_1) - R_2$ for the membrane resistance (Fig. 4.1b).
All cells were electrophysically identified by their whole-cell current pattern meaning that over 50 ms 10 mV steps were applied towards depolarisation (+20 mV) and followed by hyperpolarisation (-160 mV) (Fig. 4.1a). Depending on the presence of various channels in the membrane, every cell shows a typical current cell pattern. For astrocytes mainly the Kir channels determine its appearance.
As the biocytin internal solution contains K-gluconate, the liquid junction potential of -12 mV was compensated during the measurements by adjusting the holding potential.
From KA-injected animals only the slice with a clear injection mark was taken and additionally, two previous slices and two following of the injection mark. In total a maximum of 5 slices were considered being suitable for patching astrocytic gap junction coupling (GJC). After 20 min filling of a patched astrocyte with biocytin, the slices were fixed in 4 % PFA for 24 hrs and stored in 1x PBS, pH 7.4 at 4°C until immunohistochemistry was performed.

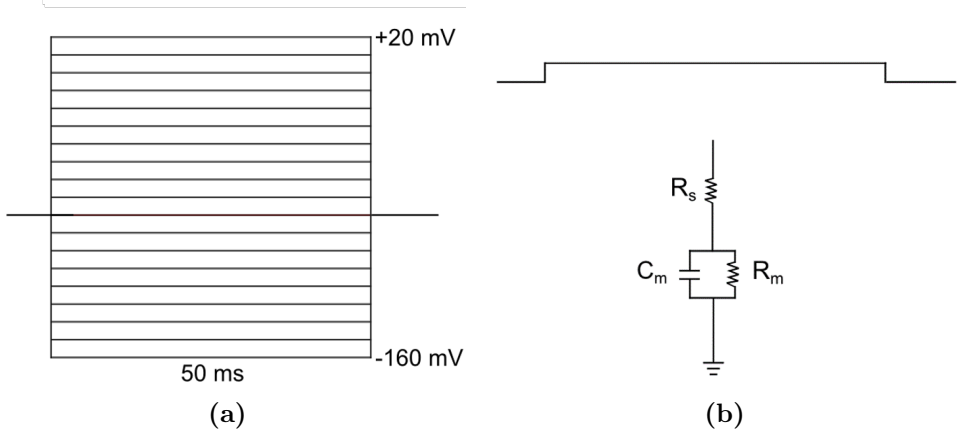

Figure 4.1 Electrophysiological whole-cell patch-clamp analysis. (a) Applying de- and hyperpolarising voltage steps, between -160 mV to +20 mV for 50 ms, allows to identify the cell type, as every cell has its cell-type specific pattern. **(b)** The upper image shows an example for a 10 mV current steps (upper line) of 50 ms duration. The picture below depicts a circuit diagramme of the whole-cell mode. The series resistance (R_s) originates at the pipette tip and the resistance of the membrane (R_m) depends on the cell membrane properties, characterised inter alia by different types of ion channels and their density. The capacity (C_m) depends on the membrane surface area.

4.1.4 Analysis of astrocytic gap junction coupling

For the quantification of astrocytic GJC all cells filled with biocytin were counted by using the software Fiji, plugin Cell counter by Kurt De Vos. Only cells achieving the following patch-clamp criteria were included in the analysis: i) at the beginning of recording the cell had a membrane potential (MP) below -60 mV, ii) after 10 min the MP is within a difference of 10 mV compared to the initial MP value, iii) during the first 10 min the R_s was below 10 mV and the R_m not higher than 20 mV.
Cells were counted manually and identified, beside their biocytin fluorescence, by astrocytic markers for GFAP and S100β for their morphology. All images were counted twice, once by myself and secondly by another experimentally blinded colleague, either Camille Philippot, Dilaware Khan or Lukas Henning.
Evaluating the astrocytic GJC (number of biocytin-positive cells) only the ipsi- and contralateral hippocampi were compared with each other, which were obtained from the same brain slice.

4.2 Immunohistochemistry

4.2.1 Tissue preparation

Adult animals were deeply anaesthesised by intraperitoneal (i.p.) injection with 100-120 μl consisting of 80 mg/kg ketamine hydrochloride (WDT) and 1.2 mg/kg xylazine hydrochloride (Sigma-Aldrich). After testing the hind paw reflexes the transcardial perfusion was applied with 30 ml 1x PBS (4°C) followed by 30 ml 4% PFA (4°C). The brain was removed and an additional fixation with 4 % PFA overnight was performed. The storage of the tissue was maintained in 1x PBS at 4°C until the sectioning was done.

4.2.2 Staining

For stainings slices of either patch-clamp performed experiments with 200 μm thickness for bioyctin labelling or slices from 4 % PFA-perfused animals were used, which were cut into 40 μm thickness at a vibratom. Each slice was transferred into a well of a 24-well plate and able to freely move during the whole staining procedure. To avoid unspecific binding of antibodies, all slices were incubated in blocking solution for 2 hrs at RT, containing 1x PBS 0.5-2% TritonX-100 for cell membrane permeabilisation and 10 % normal goat serum (NGS). First antibodies were diluted in 1x PBS, 0.1-1 % TritonX-100 and 2-5 % NGS and the slices were incubated overnight shaking at 4°C. On the following day every slice was washed three times with 1x PBS for 10 min each, followed by incubation with its secondary antibody solution for 2 hrs at room temperature. After washing them again three times with 1x PBS for 10 min the nuclei staining with Hoechst (1:200 diluted in dH_2O) was performed for 10 min at RT. A final washing step was performed and all slices mounted with Aquapolymount on objective slides and covered with cover slips. Before confocal imaging was performed the slides were stored at 4°C overnight to allow the best fixation.

4.2.3 Confocal microscopy

All immunofluorescent stainings were imaged at a laser scanning microscope (SP8, Leica) either in standard or photon counting detection mode (8 bit). Image resolution was 1024 x 1024 pixels taken at a speed of 400 Hz. For the detection of Hoechst a photomultiplier tube was used, whereas for all other stainings hybrid detectors were aquired. For the immersion objectives 40x and 63x a motor correction was performed to improve the resolution, depth of penetration and signal strength. Biocytin filled astrocytes were imaged using a 20x objective with the zoom factor 1.2. All z-stacks were taken in 2 μm thick planes.

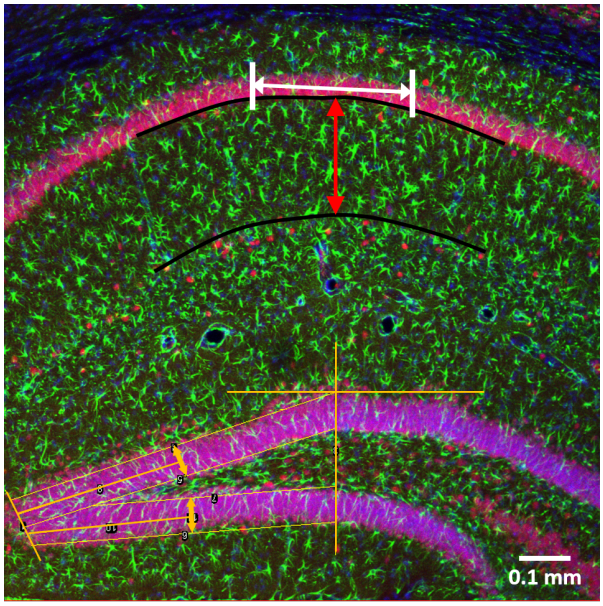

Figure 4.2 Analysis of morphological alterations after SE. The thickness of *str. rad.* was measured above the highest point of the granule cell layer (red arrow). The number of neurons in the *str. pyr.* was counted above the peak of the DG (white arrow). The GCD was always measured at half of the distance of the hilus (orange arrows).

4.2.4 Data analysis

The immunohistochemical stainings were quantified either with software Fiji/ImageJ or Imaris8.0. The analysis of astrocytic GJC was performed like described in chapter 4.1.4. Sections from epileptic animals were analysed for severity of sclerosis by evaluating the GCD of the DG, the thickness of the *str. rad.* (using Fiji) and the loss of neurons in the *str. pyr.* (using Imaris8.0). In the the DG the thickness of the granule cells were measured as indicated in Fig. 4.2. Therefore, half of the distance between the tip to the "highest" point of the hilus was used as the criteria determining the thickness. An orthogonal line giving the thickness was drawn at the upper and lower granule cell "band" (orange arrows). Both values were meaned.
The shrinkage of *str. rad.* was measured directly above the "highest" bow of the hilus to the *str. pyr.* as shown in Fig. 4.2, red arrow. For determining the number of neurons in the *str. pyr.* the cell type specific marker NeuN (labels neurons) was analysed with the software Imaris8.0. The number of neurons was counted in a box of 360x120x40 μm, which was placed directly above the hilus (Fig. 4.2, white arrow) in the NeuN fluorescence channel. With the Imaris spot tool, parameters were evolved for the counting of NeuN soma. These counting parameters were kept the them in all images.

4.3 Unilateral kainate mouse model and seizure activity recording

4.3.1 Intracortical kainate injection

Kainic acid or kainate (KA) is a natural acid found in marine seaweed and produced industrially known as (2S,3S,4S)-carboxy-4-(1-methylethenyl)-3-pyrrolidineacetic acid (IUPAC name). It is a selective agonist at kainate receptors and potent excitant neurotoxin. One injection of KA i.p. or into the brain is able to induce epileptic seizures, as it was shown in several KA-induced mouse models of epilepsy (Araki et al., 2002; Li et al., 2008; Mouri et al., 2008; Riban et al., 2002; Bedner et al., 2015). In this project we used an unilateral intracortical KA mouse model of temporal lobe epilepsy (TLE) (Bedner et al., 2015). It was developed from an intrahippocampal KA model, which is commonly used in research (Riban et al., 2002; Gröticke et al., 2008; Bouilleret et al., 1999). The difference between these two models is that the intracortical application is using a blunt cannula, which is slightly "pushing" onto the hippocampus without damaging it (like it is the case in the intrahippocampal model) (Fig. 4.3a). Furthermore, a progredient development of generalised spontaneous seizure activity is observed in these animals, as well as morphological alterations like hippocampal sclerosis, which is typical in MTLE. Sclerosis is characterised by the loss of pyramidal neurons in the CA1 and the CA3, shrinkage of the *str. rad.* and GCD in the DG.
Moreover, the intracortical model, published in Bedner et al. (2015), has several advantages compared with other commonly used epilepsy models of systemic KA or pilocarpin injection: i) it shows very low mortality rate less than 5%, ii) the onset of seizure activity is limited to the hippocampus, iii) its unilateral application allows the use of the non-injected contralateral side as a control from the injected animal. The unilateral KA injection was only performed with deeply anaesthesised animals, which were fixed stereotactically in a microinjection unit (TSE Systems GmbH). Using a 0.5 μl microsyringe (Hamilton) 70 nl consisting of 20 mM KA dissolved in 0.9% sterile NaCl was injected into the animals' right cortex slightly above the dorsal hippocampus with the coordinates 1.9 mm posterior from bregma, 1.5 mm from the *sutura sagittalis* (midline) and 1.7 mm from the skull surface. The cannula was kept for 2 min into its position to limit the flow back along the cannula track. After removing the animals from the microinjection unit they either got a transmitter implantated or the skin was immediately clamped, desinfected and the anaesthesia was stopped with Atipamezol (300 mg/kg) i.p. injection.

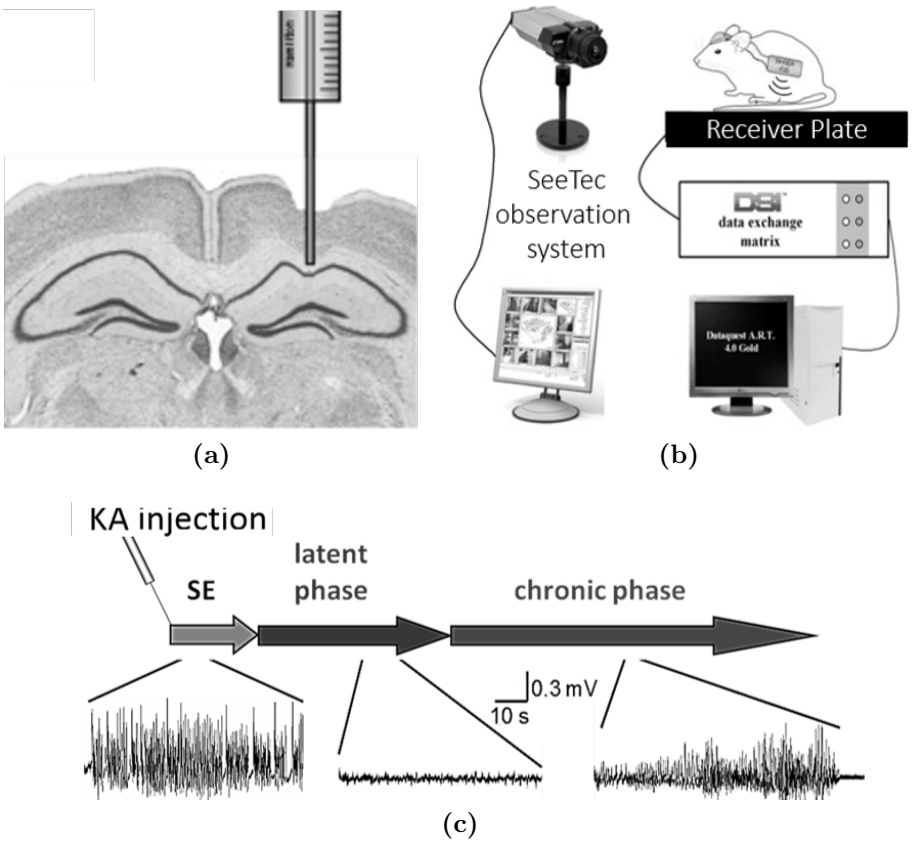

Figure 4.3 KA-induced mouse model of TLE. (a) The intracortical KA injection is applied into a single hemisphere, this side is termed ipsilateral. The non-injected side serves as control and is named contralateral. **(b)** Seizure activity can be tracked by SeeTec observation system and allows the animals to move freely in their cages. **(c)** Progression of seizure activity displays three phases, *status epilepticus* (SE) is followed by the latent and chronic phase. *Source: modified from Bedner et al. (2015)*

4.3.2 Transmitter implantation for EEG recording and video monitoring

Electrographic seizures in mice were recorded with a wireless/ telemetric system from DSI allowing the animals to move freely around in their cages. Therefore, all transmitters TA10EA-F20 were cleaned in glutaraldehyd overnight before implanting them into the animals. Adult animals were deeply anaesthesised with 40 mg/kg ketamine hydrochloride (WDT) and 0.3 mg/kg medetomidine (Cepetor, cp-pharma) i.p. injection. After testing the hind paw reflexes, the fur was removed at the abdominal region and a small skin incision was made. A tiny subcutanously passage allowed to move the transmitter wires from the abdominal incision to the skull. The wires were placed into two holes slightly posterior of the KA injection coordinates into the cortex and covered with dental cement (Paladur). Finally, the skin was sutured and the anaesthesia stopped (see above). Additionally, the animals were injected with 4 mg/kg carprofen i.p. to reduce their pain. Due to the operation all animals got aftertreatment by monitoring their body temperature rectally on a heating plate (TKM-0904, FMI). When their body temperature was at 36.5°C and the animals started to move, they were gently placed back in their cages. To reduce the risk of infection 0.25% enfrofloxacin was given via drinking water for at least one week after the surgery.
The signal from each transmitter was captured by a radio receiving plate (RPC-1, DSI) on which the individual animals were placed. With the software Dataquest A.R.T 4.00 Gold/Platinum from DSI the signal was processed from digital output of the exchange matrix into an analog output (Fig. 4.3b).
With two infrared cameras 8 animals could be video monitored simultaneously for additional approval of seizure severity. The data was displayed and stored with the network-based programme from SeeTec Office 5 on a computer.

4.3.3 Data analysis

All telemetric EEG data was analysed manually following certain criteria. Potential seizures could be confirmed by typical behaviour through video monitoring (see below). For analysing the SE, only ictal events lasting more than 20 s followed by postictal depression were added showing up within the first 12 hrs after KA injection. To determine the duration of SE, it was defined as the time from the onset until no seizure activity was recorded for at least 1 h. The duration of the latent period in which hardly any seizures are present and the onset of chronic phase were correlated beside EEG with convulsive behaviour of stage III-V defined by Racine's classification (Racine, 1972). For analysing electrographic seizures in the chronic phase, high-frequency spiking activity (up to 60 Hz) with gradually increasing amplitudes lasting about 60 s were taken into account. Typically the seizure activity ended by an abrupt roll out of EEG called postictal depression. Most chronic seizures were present with tonic-clonic or exclusive clonic convulsions.

4.4 Immunoprecipitation

4.4.1 Tissue preparation

ELISA of cytokines TNF-α and IL-1β was performed using FVB hGFAP-eGFP mice. Adult animals were deeply anaesthesised with 100-120 μl consisting of 80 mg/kg ketamine hydrochloride (WDT) and 1.2 mg/kg xylazine hydrochloride (Sigma) (i.p.). After testing the hind paw reflexes, the thorax was opened and the blood sample was taken from the heart with a multivette600 (Sarstedt). The blood was allowed to coagulate for 13-15 min and centrifuged at RT with 10.000 G for 5 min before the supernatant was transferred into a 1.5 ml tube and centrifuged for 10 minutes at 1.000 G. Finally, the serum was immediately frozen in liquid nitrogen and stored at -80°C until it was used for immunoprecipitation. Afterwards the transcardial perfusion was applied with 20 ml 1x PBS at 4°C. Both dorsal hippocampi were removed quickly and frozen in liquid nitrogen and stored at -80°C until the tissue was used for immunoprecipitation.
To clarify the cytokine profile during KA-induced SE, animals from different time points were investigated: 1 hpi, 4 hpi and 1 day post injection. As negative controls, we injected NaCl into the ipsilateral side of animals having the same age and breeding background. They were decapitated at the same time points after injection. Additionally, samples from LPS [10 mg/kg] i.p. injected animals were prepared 3 days after the injection. These animals served as a positive control as the dose of 10 mg/kg is sufficient to cause sepsis.

4.4.2 Tissue lysis

Frozen hippocampi were homogenised with a solution containing protease inhibitors (chapter 3.5.3). Per 1 μg of tissue the 6.5x amount of solution was used and 10-20 beads added. Using the device Precellys24 (Bertin technologies) the tissue was smoothly homogenised 2x 20 s at 5.000 rpm. After a short centriguation 2x RIPA buffer was pipetted into each sample (same volume as used as for homogeneity solution) and incubated on ice for at least 30 min. The lysate was centrifuged for 15 min with 20.000 rcf at 4°C.
Total protein concentration was assayed with bicinchoninic acid (BCA) using 3 μl of each sample. Probes were always pipetted in duplicates. Results with a variation of 5% were discarded.

4.4.3 ELISA

Cytokine level detection was performed using a multispot enzym-linked immunosorbent assay (ELISA) system kit K15048D from Mesoscale within one month after freezin them in liquid nitrogen. To measure cytokine levels 50 μg of total protein from hippocampus sample per well was used. For serum samples 2-fold dilution was used. With this method, cytokine levels are specifically measured within small volume sample according

to the sandwich immunoassay, meaning that detection antibodies conjugated with electrochemiluminescent labels (MSD Sulfo-Tag) bind to the cytokine, which is also bound by the capture antibody. That one finally emits light when voltage is applied to the plate electrodes and allows a quantitative measure of the each cytokine in the sample, which is proportional to its amount.
Lysates were mixed with diluent 41 as recommended in the kit's manual and incubated for 2 hrs at 600 rpm at RT. After 3x washing step with 1x PBS containing 0.05% Tween-20, the sulfo-tagged antibody was mixed with diluent 45 (see manual) and incubated at 600 rpm at RT for another 2 hrs followed by 3x washing. Finally Read Buffer T was loaded and cytokine levels measured by using the device QuickPlex SQ120 (MSD). ELISA was supervised by Dr. Frederic Brosseron and financially supported in the co-operation with Prof. Dr. Michael T. Heneka.

4.4.4 Data analysis

For the analysis, results which are higher than the median lower limit of detection (LLOD), like indicated in the Mesoscale manual, were used. Data points lower LLOD are named as not detectable (n.d.) and excluded from the statistical analysis.

4.5 Statistics

All statistical analysis was performed with Origin (OriginLab, version 9, US), JMP (SAS Institutes, version 10-11, US) and online available tools from astatsa.com.
Data is displayed as mean ± SD and were statistically tested for their normal distribution with Shapiro-Wilk. For comparing two groups either a parametric test (Students' *t*-test) or non-parametric test (Mann-Whitney-U test) was used. If a non-parametric test was applied it will be indicated in the text and figures. More than two groups were statistically tested by analysis of variance (ANOVA) with *post-hoc* Tukey HSD. Differences between means were considered as being significant at $p \leq .05$ (*t-test or # ANOVA).
Statistical analysis for significant changes in the seizure activity was obtained within one condition by comparing the seizures from a time point of interest with the previous time point of seizure data set. If two or more conditions were compared with each other, like in chapter 5.6.1, the seizure activity was compared between the conditions for the same time point.

5 Results

5.1 Acute and chronic SE-induced changes in TLE

The unilateral intracortical kainate (KA) mouse model (Fig. 5.1a) fits best for understanding the development of human MTLE-HS. Beside the very low mortality in this model the changes observed on the ipsilateral hippocampus are exclusively due to the KA-induced hyperactivity and not resulting from damaged tissue by the injection syringe. Furthermore, published data have shown that the model mimicks very closely the chronic human disorder (Bedner et al., 2015). Therefore, we assume it serves also as an experimental model of TLE to study the mechanisms underlying the pathogenesis. Animals, which were injected exclusively with KA and did not receive further administration of other substances, are named as "KA-only" animals in this work.
The following time points were investigated in this study: 4 hrs, 1 day, 3-5 days, 14 days, 28 days, 2 months and 3 months post KA injection.

5.1.1 EEG recording

All hGFAP-eGFP animals injected with KA-only developed *status epilepticus* (SE), which was characterised by repetitive seizure activity without regaining consciousness inbetween (Lowenstein et al., 1999) (Fig. 5.1b). The SE started immediately after KA injection and lasted on average 4.4 $\pm$ 2.4 hrs (n = 69) (Bedner et al., 2015).
After SE, a latent phase of 3 $\pm$ 2.4 days (n = 4) with no seizure activity was observed. After that period animals developed secondaryly generalised spontaneous seizures lasting 20 - 80 s (Bedner et al., 2015). The seizure activity during the first 4 weeks after SE is shown in Fig. 5.1c. Comparing the seizure frequency between the first, second and third months revealed no significant increase (first vs. second month p=0.535, first vs. third month p=0.481, second vs. third month p=0.899).
Video-monitoring analysis revealed that spontaneous electrographic seizures were always accompanied by behavioural tonic-clonic convulsions.

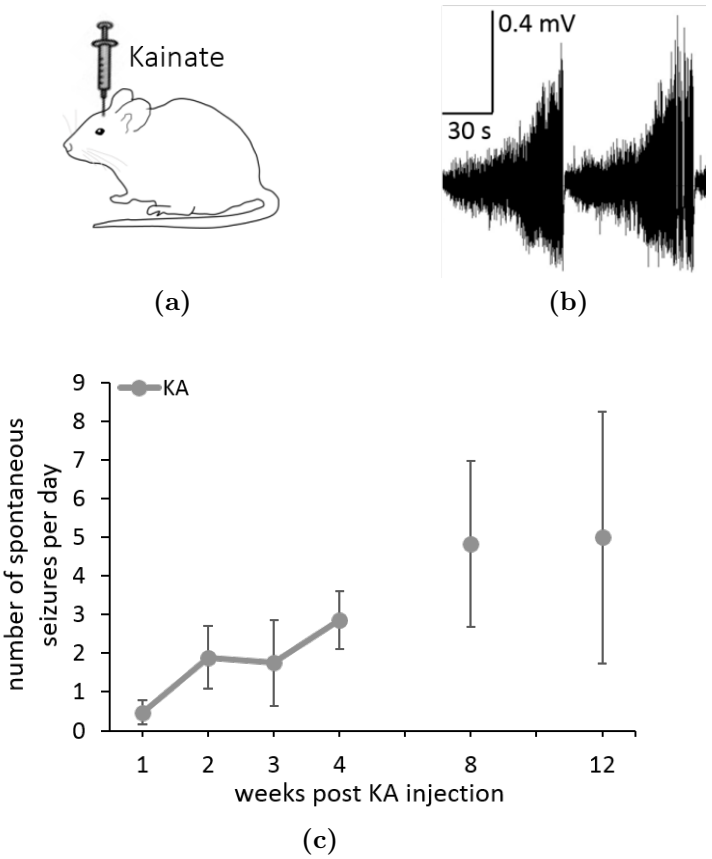

Figure 5.1 Seizure activity in hGFAP-eGFP mice after unilateral intracortical KA injection. (a) A single KA injection was applied unilaterally into the cortex. **(b)** All KA-only animals (n = 4) developed SE, which is in agreement with previously published data by Bedner et al. (2015). **(c)** After SE the seizure frequency rapidly increased within 3 months.

5.1.2 Morphological changes

Several morphological changes like GCD in the DG, the loss of pyramidal neurons in the CA1 region and shrinkage of the *str. rad.* are well known from epileptic tissue resected from patients with pharmacoresistant TLE-HS (Blümcke et al., 1999; Thom, 2014). These hallmarks of sclerosis can be found also in the unilateral intracortical KA mouse model and therefore, this model serves very well for investigating the morphological changes occurring during the development of MTLE (Bedner et al., 2015).
For each parameter 3 slices per animal and 3 animals in total were stained with cell type specific markers. For the analysis of cell dispersion the neuronal marker NeuN was used (like described in chapter 4.2.4) in KA-only animals. Three months after SE induction the granule cell layer was significantly dispersed on the ipsilateral side (p=0.001*) (see table 5.7, Fig. 5.16 B_2, yellow arrow). Additionally, the number of pyramidal neurons was quantified by NeuN staining at the same time point (see chapter 4.2.4). On the ipsilateral side a significant reduction by 87% was detected (p=0.001*) (see table 5.8, Fig. 5.16 B_2, white arrow). Three months post SE induction also the width of the *str. rad.* was significantly shrunken on the ipsilateral hippocampus (p=0.001*) (see table 5.9, Fig. 5.16 B_2, red box).

5.1.3 Changes of the astrocytic coupling in TLE

Astrocytes in the hippocampus are connected with each other via gap junction channels composed of Cx43 and Cx30 (D'Ambrosio et al., 1998). They form a very homogenous network in the *str. rad.* of the CA1 region (Mishima and Hirase, 2010). The tracer spread assay is a reliable approach to compare the astrocytic coupling strength. Biocytin was chosen as a tracer, because it is well known to be small enough to efficiently diffuse via GJ into the network (Rouach et al., 2008). It is easily applied via the intracellular pipette solution into the patched cell.
In Fig. 5.2a,b two example images of biocytin tracer spread in hGFAP-eGFP mice are shown, patched 4 hrs after KA injection. All patched cells were electrophysiologically characterised (described in chapter 4.1.3) and displayed astrocyte typical large passive current patterns. SR101 was used to visualise astrocytes (Schnell et al., 2012). Only astrocytes on the contralateral side, but not on the ipsilateral, showed fluorescence. To understand how impairment of astrocytic coupling contributes to the development of TLE, different time points after KA injection were analysed. As already published in Bedner et al. (2015) astrocytic coupling was significantly reduced ipsilaterally 4 hrs after KA injection and completely vanished 3 months post injection. Further time points were investigated to study the coupling strength within the progression of TLE (see table 5.1 and Fig. 5.2c).
After 28 days the astrocytic coupling was significantly reduced by 67% on the ipsilateral hippocampus (p=0.004*). Animals, which were patched at the time points 4 hrs, 3 days, 5 days and 9 days post KA injection had received additional NaCl i.p. injection, as those

were used as control condition for XPro1595 administration. Assuming that the NaCl injection had no influence on the astrcytic GJC, all data gained from KA-only injected animals with and without additional NaCl injection are displayed in the Fig. 5.2c.

Table 5.1 Astrocytic gap junction coupling in KA-only animals

time point after KA injection	**no. of biocytin$^+$ cells on** contralateral side	ipsilateral side	**statistical** t-test	**no. of slices** (no. of animals)
4 hpi	126 ± 16	63 ± 7	p=0.001*	11 (4)
3 dpi	174 ± 11	91 ± 21	p=0.003*	12 (3)
5 dpi	217 ± 79	158 ± 56	p=0.108	8 (2)
9 dpi	210 ± 39	172 ± 9	p=0.173	12 (3)
14 dpi	125 ± 41	98 ± 56	p=0.510	27 (8)
28 dpi	115 ± 41	38 ± 15	p=0.004*	20 (8)

In conclusion, the unilateral intracortical KA injection leads to seizure activity and morphological changes closely mimicking human TLE. The astrocytic GJC was significantly reduced within the first 3 days post SE promoting seizure activity. The astrocytic coupling strength recovery during the onset of chronic seizure might have a positive impact on reducing seizures. In the late chronic phase the seizures' frequency increase was accompanied by a complete loss of astrocytic coupling (Bedner et al., 2015).

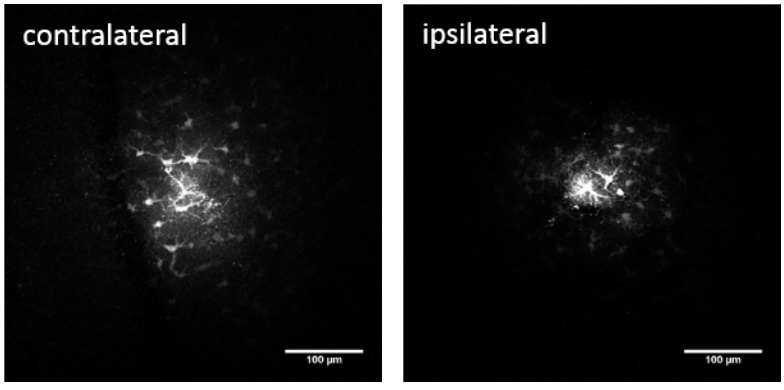

(a)

(b)

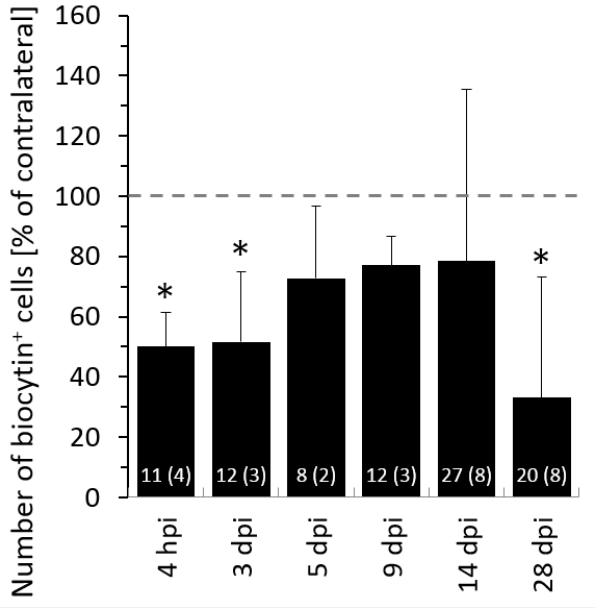

(c)

Figure 5.2 Astrocytic coupling after SE-induced seizures. (a,b) A hippocampal astrocyte was filled with biocytin, which diffuses through GJC into neighbouring astrocytes. The representative examples show significantly reduced GJC 4 hrs post SE induction only on the ipsilateral hippocampus. **(c)** Mean values of astrocytic GJC over time in dorsal hippocampal slices after SE induction. Number in bars indicate the number of slices and in brackets the number of investigated animals is displayed. A significant reduction in coupling was found within 3 days after SE. This effect is missing in the late latent and early chronic phase 14 days post KA injection. Progression of epileptogenesis leads to the loss of astrocytic coupling in the late chronic phase. Asterisk indicates significant difference from contralateral hippocampus.

5.2 Acute SE-induced changes in IL-1β and TNF-α

Cytokine changes are often reported to occur in epilepsy. Not only Ravizza et al. (2008) and Ashhab et al. (2013) found significant changes in TNF-α and IL-1β in human epileptic tissue, but also in several animal models of epilepsy cytokines play an important role (Ravizza et al., 2008; Ashhab et al., 2013; Vezzani et al., 1999; Vezzani et al., 2002; Penkowa et al., 2005).
It was shown in Bedner et al. (2015) that cytokines signficantly reduce the astrocytic coupling strength, while incubating WT slices in IL-1β and TNF-α for several hours. To proof that the reduction of astrocytic coupling is caused by TNF-α, its antagonist XPro1595 (Xencor) was additionally applied in the incubation solution. Indeed, Alexander Dupper could demonstrate that the inhibition of TNF-α by co-incubation with XPro1595 prevented uncoupling *in situ* (Dupper, 2014).
Therefore, IL-1β and TNF-α play an important role in the loss of astrocytic coupling and the application of their antagonists is preventive in acute brain slices. Hence, it is worth to study these cytokines and their role in pathophysiological conditions, like TLE *in vivo*.

5.2.1 ELISA analysis of cytokine levels in the dorsal hippocampus

IL-1β and TNF-α play a pivotal role in inflammatory processes and act differently depending on their concentration, activation of molecular signalling cascades and the related disease.
In previous papers varying results of cytokine levels were published (Vezzani et al., 2002; Penkowa et al., 2005; Patel et al., 2017). This discrepancy emerges from the use of diverse animal models. The measurement of IL-1β and TNF-α in our intracortical KA-induced mouse model by ELISA was necessary to assess the molecular mechanisms behind the effect of XPro1595. We have chosen the time points 1 hr, 4 hrs and 1 day post KA injection. As controls we used sham-injected animals to evaluate the influence of the injection procedure itself. For each condition and time point 4 animals were used. The samples were prepared like described in chapter 4.4.2. To study local cytokine changes samples from dorsal hippocampi were taken.
In sham-injected animals, at all time points IL-1β levels were too low to be detected on the contralateral side and therefore stated as not detectable (n.d.)(see table 5.2). On the ipsilateral hippocampus after 1 hr the cytokine was not detectable. KA-only animals displayed significantly increased IL-1β on the ipsilateral hippocampus 4 hrs after SE induction. No IL-1β was detected ipsilaterally at the very early time point 1 hr post KA injection.
No difference was found between the sham and KA-only mice after 4 hrs (p=0.762), implying that the upregulation of IL-1β in both conditions was mainly due to the needle placement in the cortex itself. Surprisingly, elevated IL-1β levels were detected on the contralateral hippocampus in KA-only injected animals, but not in sham mice,

Table 5.2 Changes in IL-1β concentration after different time points of injection

time point after SE induction	**condition**	**IL-1β concentration in pg/ml** contralateral side	ipsilateral side	**statistical** t-test	**no.** of animals
1 hpi	sham	not detectable	not detectable		4
	KA	not detectable	not detectable		4
4 hpi	sham	not detectable	2.7 ± 0.85		4
	KA	1.76 ± 0.55	3.26 ± 0.85	p=0.029*	4
1 dpi	sham	not detectable	0.18 ± 0.06		4
	KA	0.53 ± 0.39	0.64 ± 0.25	p=0.899	4

suggesting that KA-induced seizures lead to an upregulation of IL-1β levels in the non-injected side (Fig. 5.3).

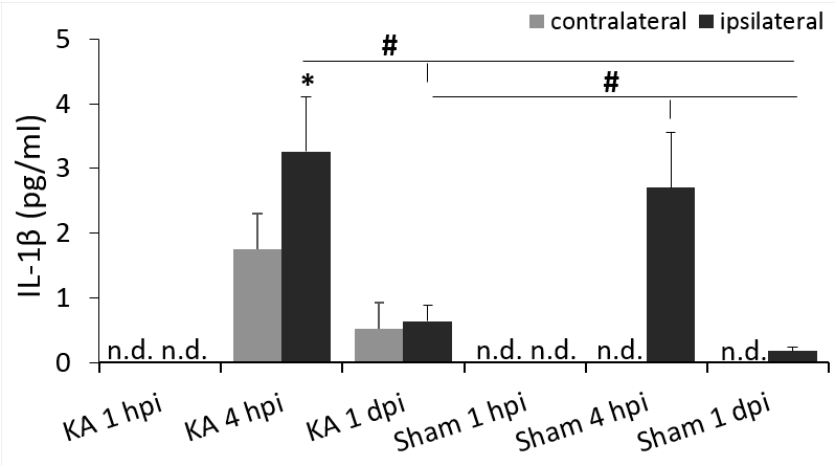

Figure 5.3 IL-1β levels in KA-injected animals. IL-1β levels were elevated in KA-only and sham animals on ipsilateral hippocampus 4 hrs after injection, indicating that the injection *per se* caused a IL-1β release. That was significantly decreased 24 hrs post injection. Asterisk indicates significant difference from contralateral hippocampus. Diamonds point out significant difference from another treated group.

In KA-injected animals TNF-α significantly increased 4 and 24 hrs post-injection (table 5.3). Remarkably, TNF-α could not be detected on the ipsilateral side 1 hr post SE induction, and on the contralateral hippocampus TNF-α was measured slightly above detection level. As shown in Fig. 5.4 in sham-injected animals no significant difference of TNF-α levels were detected in both hippocampi.
Regarding the observation that the injection causes an upregulation of the cytokine *per se*, the difference of TNF-α levels is significantly 21-fold higher in KA-only mice (p=0.008*).

Table 5.3 Changes in TNF-α concentration after different time points of injection

time point after SE induction	**condition**	**TNF-α concentration in pg/ml** contralateral side	ipsilateral side	**statistical** t-test	**no.** of animals
1 hpi	sham	not detectable	1.0 ± 0.46		4
	KA	not detectable	0.34 ± 0.18		4
4 hpi	sham	0.23 ± 0.06	3.19 ± 1.44	p=0.899	4
	KA	1.63 ± 0.38	23.85 ± 10.62	p=0.001*	4
1 dpi	sham	not detectable	0.37 ± 0.07		4
	KA	2.14 ± 1.24	5.1 ± 0.96	p=0.009*	4

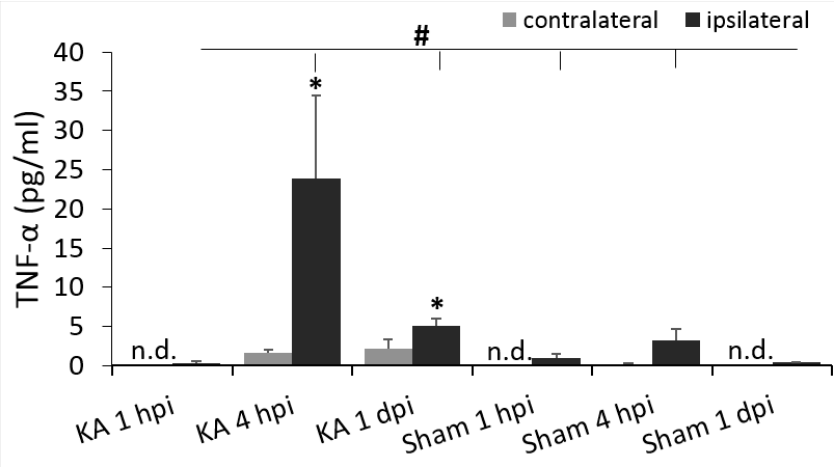

Figure 5.4 TNF-α levels in KA-injected animals. Four hours after sham injection increased levels were detected on the ipsilateral hippocampus, indicating an activation by the injection *per se*, which is significantly diminished after 24 hrs. In KA-only injected animals, TNF-α levels were significantly elevated on the ipsilateral side 4 and 24 hrs post injection. Asterisks indicate significant difference from contralateral hippocampus. Diamonds point out significant difference from another treated group.

In summary, the comparison of cytokine levels indicate that TNF-α was significantly higher on both sides in KA-injected animals than IL-1β levels. Elevated cytokine levels resulted from KA-induced SE and not from the injection needle.

5.2.2 ELISA analysis of cytokine levels in the serum

Serum was collected from the same animals, which were used for the ELISA analysis in the dorsal hippocampus. We investigated their changes in the serum. Therefore, the samples were prepared like described in chapter 4.4.1 and assessed by ELISA (chapter 4.4.3). TNF-α levels were higher than IL-1β in the blood but no significant differences between the different time points or treatments were observed (Fig. 5.5). As a positive control we used animals injected i.p. with 10 mg/kg LPS, which is a commonly used model for sepsis (Fink, 2014; Buras et al., 2005).

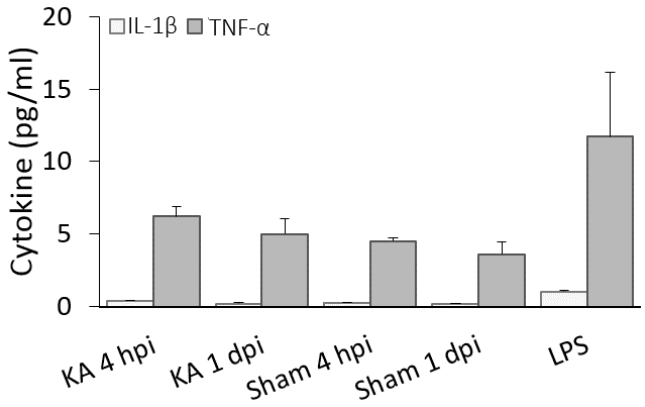

Figure 5.5 Serum levels of TNF-α and IL-1β in KA-injected animals. TNF-α serum levels were elevated compared with IL-1β levels at all time points and in all conditions. LPS i.p. injection served as a positive control.

5.2.3 Incubation with antagonists for proinflammatory cytokines

To clarify which influence TNF-α and IL-1β have in the development of TLE in our KA model we incubated acute brain slices *in situ* from 1 day post KA-injected animals with the solTNF-α antagonist XPro1595 [10 μg/ml] and IL-1β receptor antagonist Anakinra [10 ng/ml]. As the time of incubation with antagonists might have an impact on the astrocytic GJC, two groups were set up: GJC in slices being incubated below 3 hrs or above. We found no significant effect between the two groups with different incubation times (contralateral p=0.454, ipsilateral p=0.178). Moreover, no significant difference between the contralateral and ipsilateral hippocampus was seen (149 $\pm$ 23.3 vs. 122 $\pm$ 43.3 biocytin positive cells, p=0.299, n=17 slices from 4 animals) (Fig. 5.6).
In conclusion, these experiments demonstrate that the inhibition of solTNF-α and IL-1β restored the astrocytic gap junction coupling in TLE animals 1 day post KA injection.

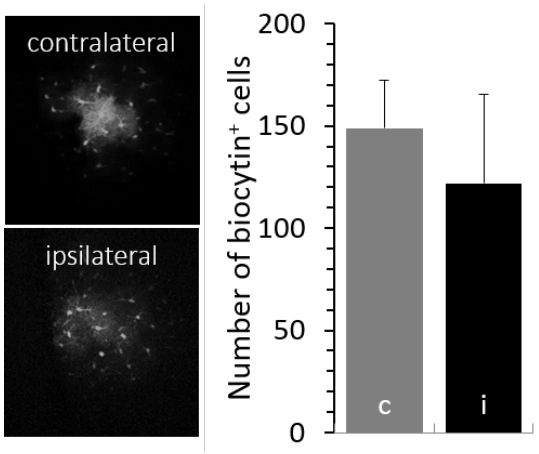

Figure 5.6 Astrocytic coupling is restored by *in situ* incubation with TNF-α and IL-1β antagonists. One day after KA injection, acute brain slices were incubated with cytokine antagonists Anakinra and XPro1595. No difference in the extent of tracer diffusion could be detected between the contra (c)- and ipsilateral (i) hippocampus.

5.3 Comparison of KA-only versus XPro Prev

XPro1595 was administered three times i.p. in 3-days interval before KA injection, as indicated in Fig. 5.7a. This condition is termed as "XPro Prev" animals in this work. We measured the seizure activity, investigated morphological changes and the astrocytic coupling up to 3 months post KA injection.

5.3.1 EEG recording

All animals were injected with XPro1595 before KA administration and developed SE, which qualitatively did not differ from animals without XPro1595 treatment (Fig. 5.7a, b). Intriguingly, the animals did not develop secondary generalised spontaneous seizures. The spontaneous seizure activity is depicted in table 5.6. In accordance with the EEG data, no behavioural tonic-clonic seizures could be detected by video-monitoring in XPro Prev treated KA-injected animals. Recordings were terminated 3 months post SE induction and animals were either used for patch-clamp analysis or were perfused for morphological analysis.
Accordingly, the treatment with XPro1595 had an impact on the development of epilepsy. The seizure activity of XPro Prev was recorded over 3 months after the KA injection and was compared with KA-only animals. After the first week no significant changes between the conditions were observed (p=0.376). From the second week on, the seizure frequency was significantly reduced in XPro Prev treated animals compared with KA-only animals (2nd week p=0.001#, 3rd week p=0.019#). Notably, after 1, 2 and 3 months, XPro Prev treated animals continued to show no generalised spontaneous seizure (Fig. 5.7c).

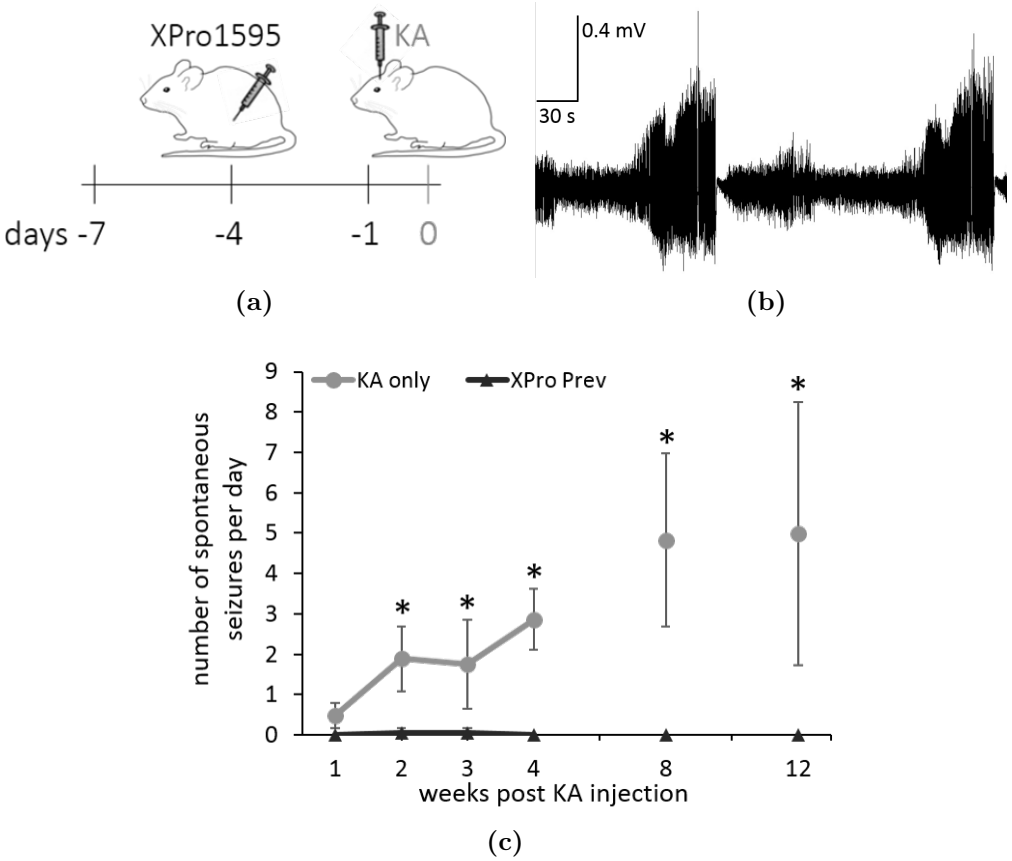

Figure 5.7 Seizure activity in XPro Prev animals. **(a)** To investigate effects of solTNF-α in experimental epilepsy XPro1595 was given three times i.p. in 3-days interval before KA injection to ensure sufficient levels of the inhibitor. **(b)** All XPro Prev animals (n = 6) developed SE, which is in agreement with the observations from KA-only animals. Qualitatively XPro injection had no effect on the seizure activity during SE. **(c)** After SE the seizure activity was completely inhibited in XPro Prev animals indicating that inactivation of solTNF-α can prevent the development of seizure activity. Asterisks indicate significant difference from another treated group.

5.3.2 Morphological changes

Three months post KA-only injection animals without further treatment showed a significant loss of pyramidal neurons, shrinkage of the *str. rad.* and a pronounced GCD in the DG. To clarify if pre-application of the solTNF-α blocker XPro1595 is able to alter these typical morphological changes in epilepsy, 3 slices per animal and in total 3 animals were stained with cell type specific markers.
For the analysis of cell dispersion the neuronal marker NeuN was used in the DG (like described in chapter 4.2.4) in XPro Prev animals. Three months post SE the granule cell layer was found not to be dispersed on the ipsilateral side (p=0.899) (see table 5.7, Fig. 5.16 C_2, yellow arrow). In KA-only animals the neurons on the ipsilateral side were significantly dispersed compared with the width of granule cell layer in XPro Prev (p=0.001#). That indicated that inhibiting solTNF-α had an impact on the development of GCD.
Additionally, the number of pyramidal neurons was quantified by NeuN staining at the same time point (see chapter 4.2.4). On the ipsilateral hippocampus a significant reduction of 44% was detected (p=0.002*) (see table 5.8, Fig. 5.16 C_2, white arrow). Most importantly, in XPro Prev animals the extent of neuronal loss was significantly less compared with KA-only ipsilateral side (p=0.004#), showing that inhibiting solTNF-α before SE induction is able to signficantly prevent neuronal death (Fig. 5.14).
Three months post SE the width of *str. rad.* was not shrunken (p=0.899) (Fig. 5.16 C_2, red box). In KA-only injected animals the ipsilateral side was significantly shrunken compared with the corresponding contralateral, moreover the ipsilateral hippocampus was significantly thinner than in sham injected animals (p=0.001#) (table 5.9). Pretreatment with XPro1595 even prevented a significant shrinkage of *str. rad.* comparing it with KA-only ipsilateral hippocampus (p=0.001#). Neither alterations between contra- and ipsilateral hippocampi (p=0.899) nor the ipsilateral sides of XPro Prev and sham-injected mice displayed a significant difference (p=0.595) (Fig. 5.15).
In conclusion, the administration of XPro1595 before KA injection attenuated the pyramidal neuronal loss, prevented GCD and shrinkage of the *str. rad.*. That indicates that solTNF-α supports neuronal survival and attenuates astrogliosis in the KA-induced mouse model of TLE.

5.3.3 Loss of the astrocytic coupling is prevented by XPro1595

The animals were injected with XPro1595 before KA injection and decapitated at different time points to determine how the astrocytic coupling strength changes. The astrocytic coupling strength was measured at several time points to study the progression of TLE (Fig. 5.8c). For the acute phase, 4 hrs after SE induction was chosen, for the latent phase 3 and 5 days and for the chronic phase 3 months (table 5.4). No significant difference was observed between the contralateral and ipsilateral number of biocytin positive cells at any time point, indicating that XPro1595 application before

inducing SE has an impact on the astrocytic GJC.
To proof that the observed coupling is an effect of XPro1595, we injected NaCl i.p. before KA administration, instead of XPro1595. Assuming that the additional injection of NaCl into the abdomen has no impact on the astrocytic GJC in the hippocampus, the results from those animals are shown in the same figure together with KA-only injected animals (without additional NaCl administration) (Fig. 5.2c). Therefore, a comparison of astrocytic coupling strength between KA-only injected and XPro Prev administered animals was done at the following time points: 4 hpi, 3 dpi and 3 mpi.
At the early phase, the SE-induced uncoupling in KA-only animals displayed 50% reduction in astrocytic GJC, whereas XPro Prev animals showed no significant impairement in coupling (p=0.478) (see table 5.4). This also applies to the 3 dpi time point; in KA-only injected animals the ipsilateral astrocytic coupling was significantly reduced by 48% (p=0.003*). In XPro Prev treated animals no significant alteration was detected (p=0.309), demonstrating that XPro Prev treatment indeed prevented SE-induced uncoupling. During the chronic phase at 3 mpi, XPro1595 application also prevented the reduction of astrocytic GJC (p=0.681), whereas in KA-only animals complete loss of astrocytic coupling was detected on the ipsilateral hippocampus (see Bedner et al., 2015).

Table 5.4 Astrocytic gap junction coupling in XPro Prev treatment

time point after KA injection	**no. of biocytin$^+$ cells on** contralateral side	ipsilateral side	**statistical** t-test	**no. of slices** (no. of animals)
4 hpi	116 ± 17	103 ± 36	p=0.478	15 (5)
3 dpi	171 ± 24	195 ± 26	p=0.309	11 (3)
5 dpi	253 ± 73	207 ± 14	p=0.340	14 (3)
3 mpi	145 ± 17	154 ± 29	p=0.681	13 (3)

In conclusion, the application of XPro1595 before KA injection prevented SE-induced astrocytic GJ uncoupling and attenuated the development of sclerosis. Furthermore, it blocked almost completely the development of chronic seizures.
Those results indicate that the application of a solTNF-α inhibitor can prevent the development of epilepsy.

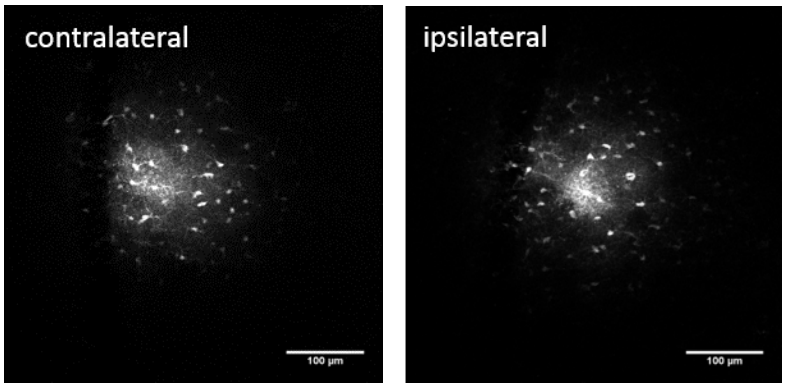

(a)

(b)

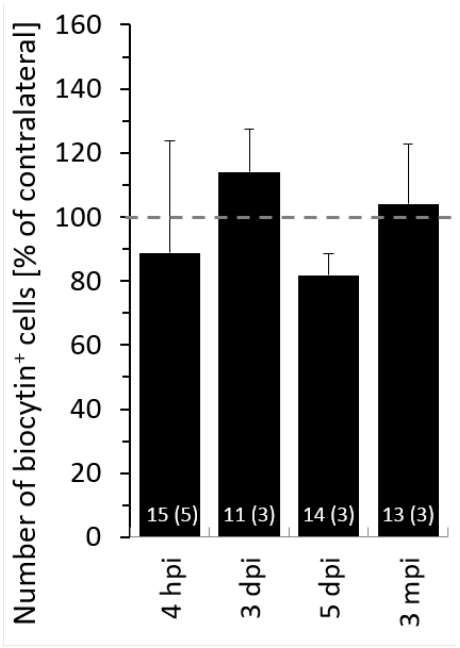

(c)

Figure 5.8 Loss of astrocytic coupling is prevented in XPro Prev animals. (a,b) Hippocampal astrocytes were filled with biocytin. The representative examples display no significantly reduced GJC in XPro Prev treatment prior to KA injection. **(c)** Mean values of astrocytic GJC over time in dorsal hippocampal slices after SE induction. Number in bars indicate the number of slices and in brackets the number of investigated animals is displayed. No significant impairment of astrocytic coupling was found at any time point.

5.4 Comparison of KA-only versus XPro Resc

Knowing that XPro1595 prevents KA-induced SE prompted us to ask whether the application of solTNF-α inhibitor can attenuate the progression of TLE. Therefore, we injected XPro1595 three times with the same concentration in 3-days interval after the KA injection, trying to rescue the TLE related characteristics. This condition is termed as "XPro Resc" animals in this work. We recorded the seizure activity, investigated morphological changes and astrocytic GJC up to 3 months post KA injection.

5.4.1 EEG recording

All animals within the XPro Rescue group (n = 14) were injected first with KA and 4 hrs later with XPro1595. In 3-days interval, all animals received two further XPro1595 i.p. injections on day 3 and 6 after SE induction (Fig. 5.9a). All animals developed SE, which started immediately after KA injection and qualitatively did not differ from animals without XPro1595 treatment (Fig. 5.9b). The SE was followed by a latent period of 4.4 $\pm$ 3.2 days. The recorded spontaneous seizure activity up to 3 months after SE induction is displayed in Fig. 5.9c and in table 5.6.
For seizure activity monitoring within the first month post SE, we recorded 14 animals. For the later time points 2 months post SE we studied 5 animals and 4 animals up to 3 months post injection. Video-monitoring analysis revealed that spontaneous electrographic seizures were always accompanied by behavioural tonic-clonic seizures. Recordings were terminated 3 months post SE induction and animals were either used for patch-clamp analysis or were perfused for morphological analysis.
The development of seizure frequency within the first month after SE induction did not significantly improved in XPro Prev animals, comparing the seizure activity weekly with each other (first vs. second week p=0.200, first vs. third week p=0.220, second vs. third week p=0.899). Interestingly, XPro Resc animals displayed a significant reduction in the seizure frequency compared with KA-only animals in the 2nd and 3rd month post SE (from 1st to 2nd month p=0.001#; from 2nd to 3rd month p=0.010#).
Thus, the treatment with XPro1595 after SE induction significantly reduced the seizure frequency in the long-term.

5.4.2 Morphological changes

Three months post SE, KA-only animals showed significant loss of pyramidal neurons, shrinkage of the *str. rad.* and pronounced GCD. To clarify if application of the solTNF-α blocker XPro1595 is able to prevent or dampen these typical morphological changes, 3 slices per animal and in total 3 animals were stained with cell type specific markers.
For the analysis of cell dispersion the neuronal marker NeuN was used in the DG (like described in chapter 4.2.4) in XPro Resc animals. Three months post SE the granule cell layer was found not to be dispersed on the ipsilateral side (p=0.167) (see table

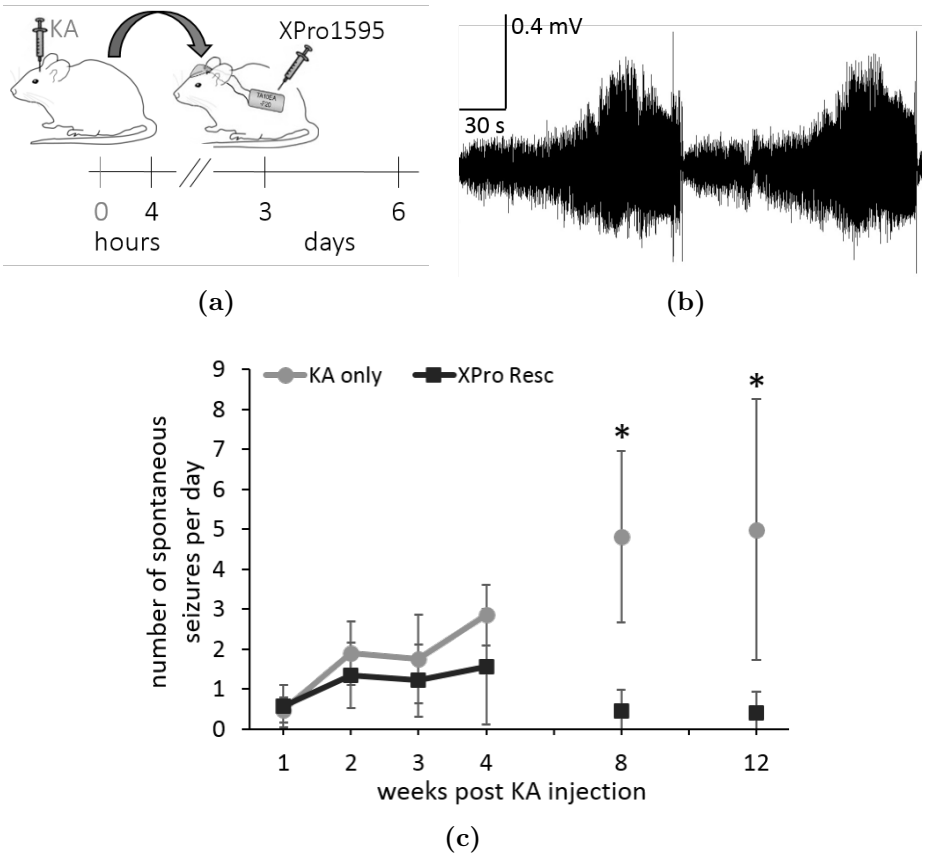

Figure 5.9 Seizure activity in KA-injected animals with or without post-treatment of XPro1595. **(a)** To assess the impact of solTNF-α, XPro1595 was given three times after KA at 3-days interval. The first i.p. injection was administered 4 hrs after KA injection, followed by two more XPro1595 injections 3 and 6 days after SE induction. **(b)** During the first 4 hrs all animals developed SE, which was qualitatively similar to KA-only animals. XPro1595 injection itself is not inhibiting the SE caused by KA injection. **(c)** After the latent period, secondary generalised spontaneous seizures are present in XPro Resc animals, which are however, significantly reduced within the 2nd month. Asterisks indicate significant difference from another treated group.

5.7, Fig. 5.16 D_2, yellow arrow). In KA-only animals the neurons on ipsilateral side were significantly dispersed compared with the width of granule cell layer in XPro Resc (p=0.001#) (Fig. 5.13). That indicated that inhibiting solTNF-α had an impact on the development of GCD.
Additionally, the number of pyramidal neurons was quantified by NeuN staining at the same time point (see chapter 4.2.4). On the ipsilateral hippocampus a significant reduction of 58% was detected (p=0.001*) (see table 5.8, Fig. 5.16 D_2, white arrow). XPro Resc animals showed a significant loss of neurons on the ipsilateral side compared with sham mice (p=0.005#). Notably, it was less prominent in XPro Resc treated animals than in KA-only (p=0.005#) (Fig. 5.14). The result indicated that inhibiting solTNF-α 4 hrs post injection prevented neuronal cell loss.
Three months post SE induction the width of the *str. rad.* was significantly shrunken on the ipsilateral hippocampus compared with its contralateral side (p=0.001*) (see table 5.9, Fig. 5.16 D_2, red box). Furthermore, the ipsilateral side of XPro Resc found to be significantly changed from sham (p=0.001#). Remarkably, the *str. rad.* of XPro Resc mice was significantly less shrunken than in KA-only animals (p=0.001#) (Fig. 5.15), showing that XPro1595 post-injection is able to attenuate the shrinkage.
In conclusion, the administration of XPro1595 4 hrs, 3 and 6 days after KA injection attenuated the neuronal loss in CA1 and GCD and shrinkage of the *str. rad.* in KA-induced mouse model of TLE. These results show that by subsequent XPro1595 application the development of epilepsy could be stopped.

5.4.3 Loss of astrocytic coupling is rescued by XPro1595

The animals were injected with XPro1595 after the KA injection and decapitated at different time points to determine how astrocytic coupling strength changes (Fig. 5.10). The time points 3, 5 and 9 days after SE induction were chosen. For the chronic phase of epilepsy two time points at 28 days and 3 months after KA injection were investigated (table 5.5). No significant difference was observed between the contralateral and ipsilateral number of biocytin positive cells at any of the investigated time points, indicating that XPro1595 application after SE has an restoring influence on the astrocytic GJC.
In conclusion, the application of XPro1595 post SE induction rescues SE-induced astrocytic GJ uncoupling and attenuates the development of sclerosis. Furthermore, it decreased the frequency of chronic spontaneous seizures. These results indicate that the inhibition of solTNF-α attenuates the development of TLE.

Table 5.5 Astrocytic gap junction coupling in XPro Resc treatment

time point after KA injection	**no. of biocytin$^+$ cells on** contralateral side	ipsilateral side	**statistical** t-test	**no. of slices** (no. of animals)
3 dpi	164 ± 21	171 ± 12	p=0.651	11 (3)
5 dpi	213 ± 41	213 ± 23	p=1.000	14 (3)
9 dpi	167 ± 26	134 ± 31	p=0.093	10 (4)
28 dpi	243 ± 19	219 ± 5	p=0.094	8 (3)
3 mpi	171 ± 41	224 ± 31	p=0.083	14 (4)

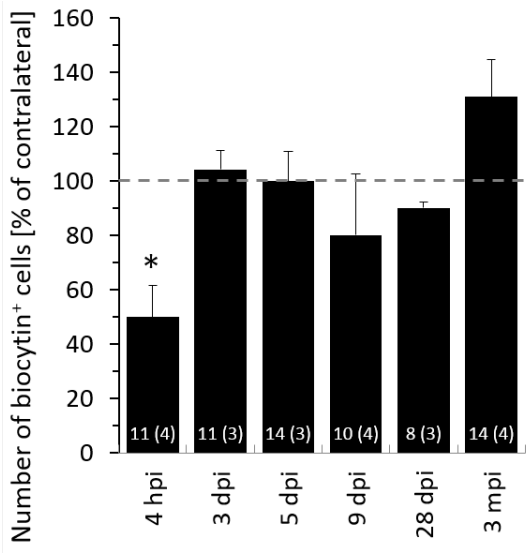

Figure 5.10 Astrocytic coupling is restored in XPro Resc animals. The hippocampal astrocytic GJC was visualised with the tracer spread assay and analysed. Mean values of astrocytic GJC over time in dorsal hippocampal slices after SE induction are displayed. Number in bars indicate the number of slices and in brackets the number of investigated animals is displayed. No significant reduction in the astrocytic coupling was present at any time point. Asterisk indicates significant difference from contralateral hippocampus.

5.5 Comparison of KA-only versus XPro Chronic

XPro1595 is able to prevent and rescue the reduction of astrocytic coupling and consequentially able to lower or even inhibit spontaneous seizure activity. Therefore, its potential as therapeutical medication was studied. All animals received the first XPro1595 injection after their first generalised spontaneous seizure was identified in the EEG. That happened mostly 4-6 days post SE induction. Two further XPro injections followed at 3-days interval to keep the application pattern (Fig. 5.11a). This condition is termed as "XPro Chronic" animals in this work. We recorded the seizure activity and investigated morphological changes up to 3 months post KA injection.

5.5.1 EEG recording

XPro Chronic treated animals were injected with XPro1595 i.p. after detecting their first generalised spontaneous seizure after the latent period. All animals (n = 5) developed SE, which started immediately after KA injection and qualitatively did not differ from animals without XPro1595 treatment (Fig. 5.11b). The SE was followed by a latent phase of 3.2 ± 1.64 days. The recorded spontaneous seizure activity is displayed in Fig. 5.11c and in table 5.6.
Video-monitoring analysis revealed that spontaneous electrographic seizures were accompanied by behavioural tonic-clonic seizures. Recordings were terminated 3 months post SE induction and the animals were perfused for morphological analysis.
Comparing the seizure frequency within the first month after SE induction, neither a significant improvement was observed nor a significant difference with KA-only mice without XPro1595 (1st week p=0.661, 2nd week p=0.137, 3rd week p=0.343, 4th week p=0.062). In the 2nd and 3rd month after SE induction, XPro Chronic mice displayed a significant reduction in seizure frequency compared with KA-only mice (2nd month p=0.001#; 3rd month p=0.021#).
Thus, the treatment with XPro1595 after the first generalised spontaneous seizure and two further XPro1595 injections, significantly reduced the seizure frequency in the long-term. Therefore, XPro1595 might be considered for therapeutical approach as it decreased seizure acitivity, which is a clinical parameter and read out for the efficiency of a therapeutical drug.

5.5.2 Morphological changes

To elucidate, if application of the solTNF-α blocker XPro1595 after the first generalised spontaneous seizure followed by two more XPro1595 injections, are still able to attenuate the development of hippocampal sclerosis, 3 slices per animal and in total 3 animals were stained with cell type specific markers.
For the analysis of cell dispersion the neuronal marker NeuN was used in the DG (like described in chapter 4.2.4) in XPro Chronic animals. Three months post SE induction

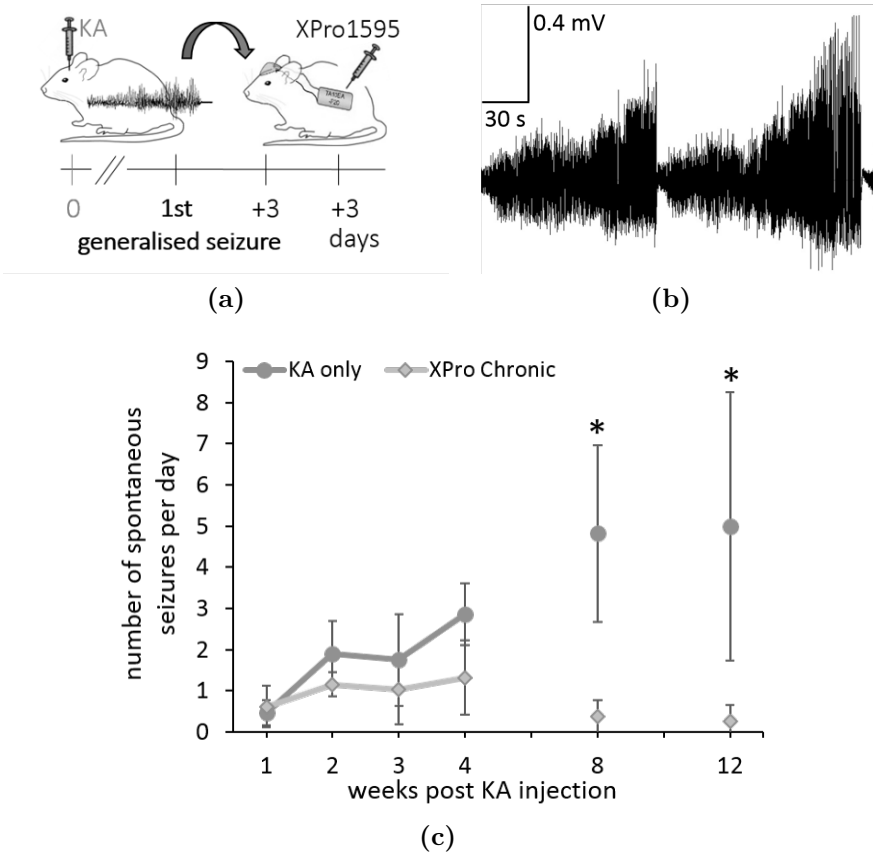

Figure 5.11 Animals treated with XPro1595 after occurance of the first generalised spontaneous seizure. **(a)** To study the therapeutical potential of XPro1595, it was injected after animals had developed their first generalised spontaneous seizure, followed by two further XPro1595 injections in 3-days interval. **(b)** All XPro Chronic animals (n = 5) developed SE, which is in agreement with the observation from control animals. **(c)** Animals treated with XPro1595 after occurance of the first spontaneous seizure, the frequency was not altered within the first month, but was significantly reduced in long-term. Asterisks indicate significant difference from another treated group.

the granule cell layer was found not to be dispersed on the ipsilateral side (p=0.899) (see table 5.7, Fig. 5.16 E_2, yellow arrow). In KA-only animals the neurons on the ipsilateral side were significantly dispersed compared with the width of granule cell layer in XPro Chronic (p=0.001#) (Fig. 5.13). That indicated that inhibiting solTNF-α had an impact on the development of GCD.
Additionally, the number of pyramidal neurons was quantified by NeuN staining at the same time point (see chapter 4.2.4). On the ipsilateral hippocampus a significant reduction of 54% was detected (p=0.002*) (see table 5.8, Fig. 5.16 E_2, white arrow). XPro Chronic conditions showed a significant loss of neurons on the ipsilateral side compared with sham mice (p=0.001#). Giving XPro1595 after the first spontaneous generalised seizure the loss of neurons is not significantly different from KA-only mice on ipsilateral side (p=0.051) (Fig. 5.14).
Three months after SE induction the width of the *str. rad.* was significantly shrunken on the ipsilateral hippocampus compared with its contralateral side (p=0.001*) (see table 5.9, Fig. 5.16 E_2, red box). Furthermore, the ipsilateral side of XPro Chronic animals found to be significantly different from sham (p=0.001#). Remarkably, the *str. rad.* of XPro Chronic mice was significantly less shrunken than in KA-only animals (p=0.001#) (Fig. 5.15), showing that XPro1595 post-injection is able to attenuate the shrinkage even after the first spontaneous generalised seizure occured.
In conclusion, the application of XPro1595 after the first generalised spontaneous seizure and two further XPro1595 injections, attenuated the development of sclerosis. Furthermore, it decreased the frequency of generalised spontaneous seizures. These results indicate that the inhibition of solTNF-α attenuates the development of TLE at a clinically relevant time point.

5.6 XPro1595 treatments - Comparison with each other

5.6.1 Spontaneous seizure activity

The treatment with XPro1595 had an impact on the development of TLE. The seizure activity was recorded up to 3 months post KA injection and was compared with KA-only animals. The data of KA-only and all XPro1595 treated animals is displayed in Fig. 5.12 and in table 5.6.
Within the first month neither significant changes between the conditions XPro Prev and XPro Chronic were observed (1st week p=0.088; 2nd week p=0.103; 3rd week p=0.255; 4th week p=0.324) nor between XPro Resc and XPro Chronic (1st week p=0.899; 2nd week p=0.493; 3rd week p=0.616; 4th week p=0.685). Only between XPro Prev and XPro Resc a significant change in spontaneous seizure activity was observed within the first 4 weeks (1st week p=0.041#; 2nd week p=0.002#; 3rd week p=0.016#; 4th week p=0.033#). No differences between XPro treatments existed in the long-term (2nd month Prev vs. Resc p=0.899, Prev vs. Chronic p=0.899, Resc vs. Chronic p=0.899; 3rd

month Prev vs. Resc p=0.899, Prev vs. Chronic p=0.899, Resc vs. Chronic p=0.899), showing that XPro1595 is able to efficiently decrease seizure activity in the chronic phase of epilepsy, even administered post-treatment.

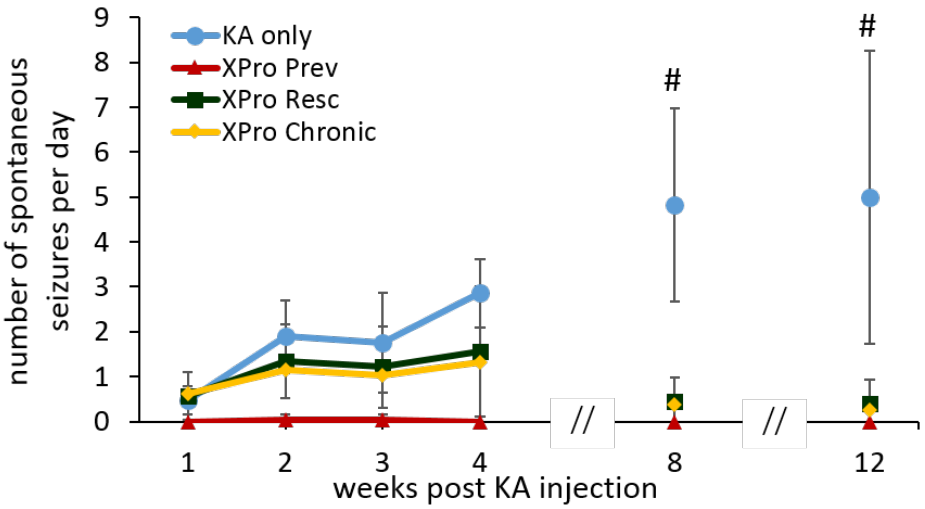

Figure 5.12 Seizure activity up to 3 months after epilepsy induction. Seizure activity was completely inhibited in XPro Prev animals, indicating that inactivation of solTNF-α prevented the development of seizure activity. Both XPro post-treatment conditions displayed a significant decrease in seizure frequency 8 and 12 weeks post SE, indicating that the application of XPro1595 significantly decreased seizure activity in the long-term. Diamonds point out significant difference from another treated group.

Table 5.6 Mean values of seizure activity in KA-only and XPro1595 treated animals

week	**KA-only**		**XPro Prev**		**XPro Resc**		**XPro Chronic**	
after SE	mean ± SD	n	mean ± SD	n	mean ± SD	n	mean ± SD	n
1	0.47 ± 0.31	4	0 ± 0	6	0.57 ± 0.53	14	0.61 ± 0.51	5
2	1.89 ± 0.80	4	0.05 ± 0.12	6	1.34 ± 0.82	14	1.16 ± 0.29	5
3	1.75 ± 1.11	4	0.05 ± 0.12	6	1.21 ± 0.91	14	1.04 ± 0.84	5
4	2.86 ± 0.76	3	0 ± 0	6	1.56 ± 1.45	14	1.32 ± 0.90	5
8	4.82 ± 2.15	6	0 ± 0	6	0.46 ± 0.51	5	0.37 ± 0.41	5
12	4.99 ± 3.26	6	0 ± 0	6	0.41 ± 0.53	4	0.25 ± 0.41	5

In conclusion, the treatment with XPro1595 reduced the seizure frequency in the long-term and suppressed the progression of epileptogenesis.

5.6.2 Morphological changes

Three months post SE induction HS was present in KA-only animals (chapter 5.1.2). In XPro treated animals some of the sclerosis characteristics are less promiment or even prevented. Fig. 5.16 shows an overview of sham, KA-only, XPro Prev, XPro Resc and XPro Chronic treated animals 3 months after SE induction.
Fig. 5.13 depicts the effect of XPro1595 treatment on GCD 3 months after SE. Whereas in KA-only animals the neurons on the ipsilateral side were significantly dispersed, the width of granule cell layer in all XPro1595 conditions showed no changes (table 5.7). Furthermore, no significant difference of GCD between the XPro1595 treatments were found (Prev vs. Resc p=0.44; Prev vs. Chronic p=0.899; Resc vs. Chronic p=0.141). That indicated that inhibiting solTNF-α prevented the development of GCD.

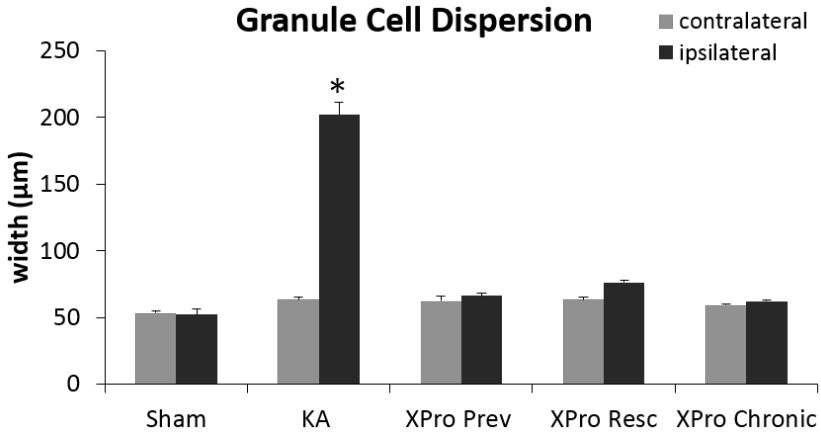

Figure 5.13 Effect of XPro1595 treatment on GCD 3 months after SE induction. GCD was most prominent in KA-only animals. In XPro1595 treated animals the granule cell layer was not significantly different between the contra- and ipsilateral hippocampus 3 months after SE, whereas KA-only animals showed significantly increased width of GCD on the ipsilateral side. These results demonstrate that XPro1595 inibits the development of GCD. Asterisk indicates significant difference from contralateral side.

Table 5.7 Granule cell dispersion 3 months after SE induction

hippocampal side	**sham** width in μm	**KA-only** width in μm	**XPro Prev** width in μm	**XPro Resc** width in μm	**XPro Chronic** width in μm
contralateral	53 ± 2	63 ± 2	62 ± 4	63 ± 2	59 ± 1
ipsilateral	52 ± 4	202 ± 9	66 ± 2	76 ± 2	62 ± 1
t-test	p=0.899	p=0.001*	p=0.899	p=0.167	p=0.899

Fig. 5.14 displays the number of pyramidal neurons in sham, KA-only and XPro1595 treated animals 3 months post Se induction. There was no significant difference between XPro1595 treatments comparing ipsilateral neuronal loss between each other (Prev vs. Resc p=0.607; Prev vs. Chronic p=0.178; Resc vs. Chronic p=0.899). However, neuronal loss in XPro Prev is not significantly altered compared with sham, indicating that XPro1595 application prior to KA-induced SE prevents the death of pyramidal neurons in CA1.

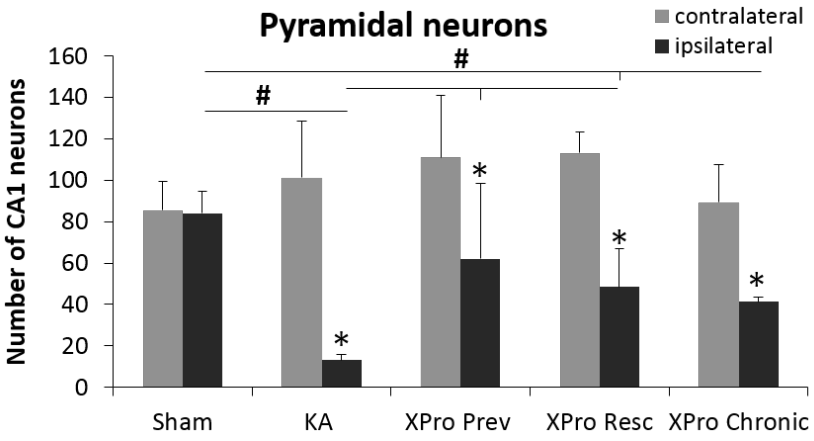

Figure 5.14 Effect of XPro1595 treatment on the number of pyramidal neurons 3 months after SE induction. KA-only treated animals showed almost complete loss of pyramidal neurons in the ipsilateral hippocampus. Ipsilateral neuronal numbers were also reduced in all XPro1595 conditions, but the extent of neurodegeneration is significantly less pronounced in XPro Prev and Resc animals than in KA-only animals. Asterisks indicate significant difference from contralateral hippocampus. Diamonds point out significant difference from another treated group.

Table 5.8 Pyramidal CA1 neurons 3 months after SE induction

hippocampal side	**sham** no. of neurons	**KA-only** no. of neurons	**XPro Prev** no. of neurons	**XPro Resc** no. of neurons	**XPro Chronic** no. of neurons
contralateral	85 ± 14	101 ± 27	111 ± 30	113 ± 10	89 ± 18
ipsilateral	84 ± 11	13 ± 3	62 ± 37	48 ± 18	41 ± 2
t-test	p=0.899	p=0.001*	p=0.002*	p=0.001*	p=0.002*

In Fig. 5.15 and table 5.9 the effect of XPro1595 treatment on the width of the *str. rad.* is shown in sham, KA-only and XPro1595 treated animals 3 months after SE induction. The ipsilateral side between XPro Prev and both XPro1595 post-treatments displayed a significant change (Prev vs. Resc/Chronic p=0.001#). However, no significant difference in the width of the *str. rad.* was observed between both XPro1595 post-treatments (p=0.899). These results indicate that pre-application of XPro1595 prevented a significant shrinkage of the *str. rad.* and that XPro1595 post-treatment attenuates further shrinkage after SE induction.

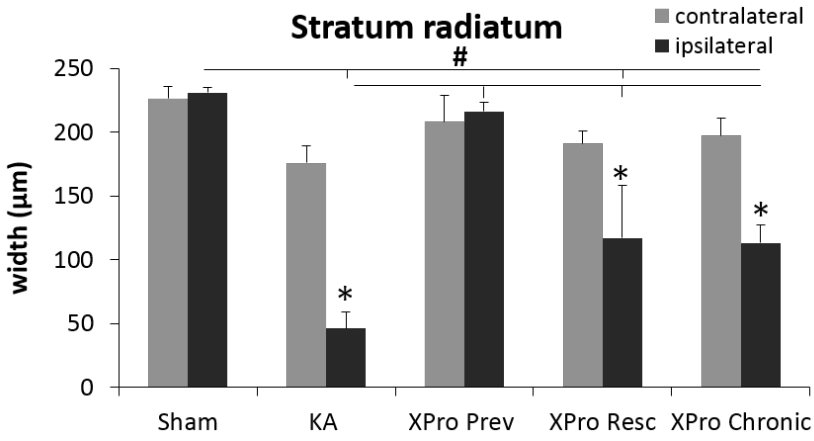

Figure 5.15 Effect of XPro1595 treatment on the *stratum radiatum* 3 months after SE induction. The thickness of the *str. rad.* is maintained in the XPro Prev condition. XPro1595 given after SE induction is attenuating the shrinkage and efficiently peters out the progression. Asterisks indicate significant difference from contralateral hippocampus. Diamonds point out significant difference from another treated group.

Table 5.9 Stratum radiatum 3 months after SE induction

hippocampal side	**sham** width in μm	**KA-only** width in μm	**XPro Prev** width in μm	**XPro Resc** width in μm	**XPro Chronic** width in μm
contralateral	226 ± 10	176 ± 13	208 ± 21	191 ± 10	197 ± 14
ipsilateral	213 ± 4	46 ± 13	216 ± 7	117 ± 41	113 ± 14
t-test	p=0.899	p=0.001*	p=0.889	p=0.001*	p=0.001*

In conclusion, the administration of XPro1595 before SE induction prevented the hippocampal sclerosis in the KA-induced mouse model of TLE. Notably, administering XPro1595 after SE induction also attenuated the hippocampal sclerosis.

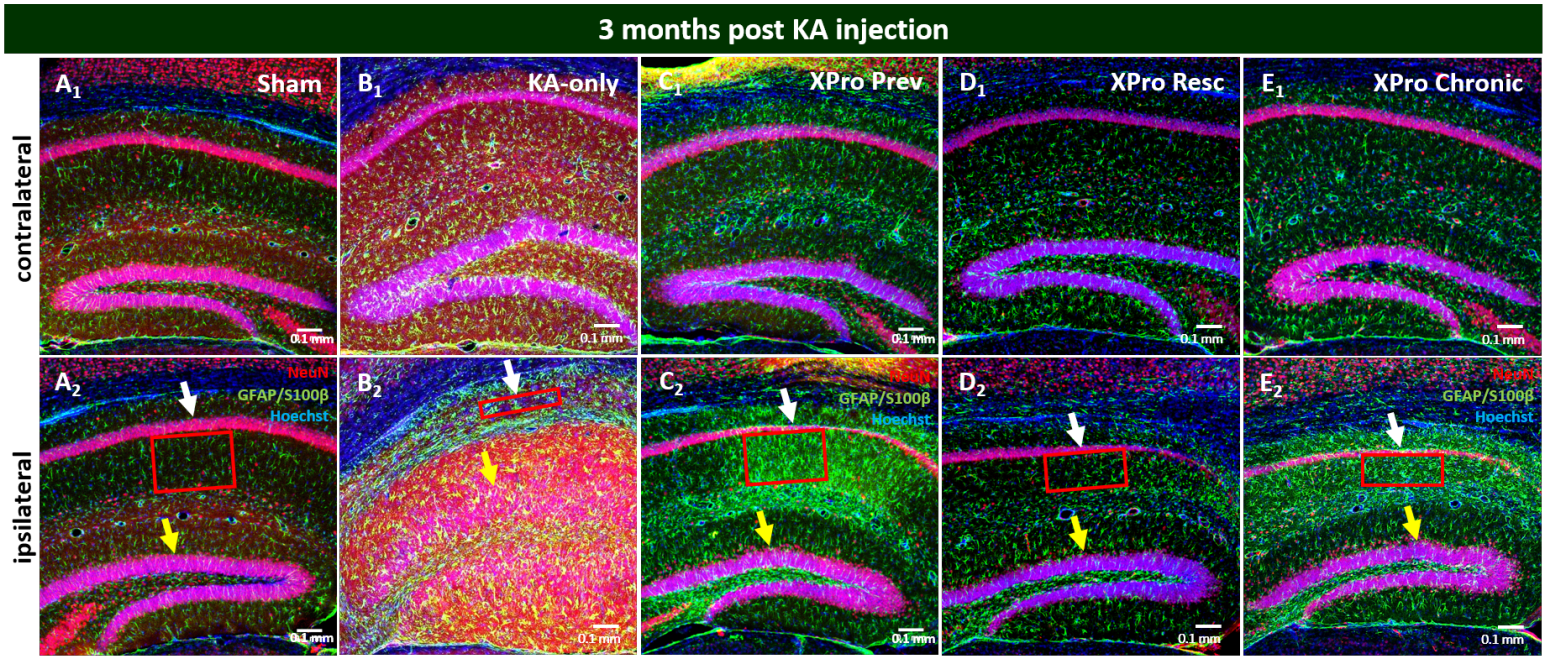

Figure 5.16 Effect of XPro1595 treatment on SE-induced hippocampal alterations. Immunhistochemical stainings in the hippocampus in sham, KA-only, XPro Prev, XPro Resc and XPro Chronic animals 3 months after SE induction. **KA-only (B_2)**: Hippocampal sclerosis is very prominent in the chronic phase, characterised by pyramidal neuronal loss in the CA1 region (white arrow), a shrinkage of the *str. rad.* (red box), and heavily dispersed granule cell layer (yellow arrow). **XPro Prev (C_2)**: Animals showed no significant loss of pyramidal neurons in the CA1 (white arrow). Furthermore, neither the width of the *str. rad.* was altered (red box) nor the granule cell layer was dispersed (yellow arrow), indicating that XPro1595 pre-treatment prevented the development of hippocampal sclerosis completely. **XPro Resc (D_2)**: Animals showed significantly less loss of pyramidal neurons in the CA1 (white arrow) compared with KA-only animals. Neither the *str. rad.* was altered (red box) nor the granule cell layer was dispersed (yellow arrow), indicating that XPro1595 treatment after SE rescued the development of hippocampal sclerosis. **XPro Chronic (E_2)**: Animals showed significant loss of pyramidal neurons in the CA1 (white arrow). The *str. rad.* was significantly less shrunken (red box) compared with KA-only animals and the granule cell layer was not dispersed (yellow arrow), indicating that XPro1595 therapeutical treatment salvages the development of hippocampal sclerosis. Scale bar = 0.1 mm

5.6.3 Astrocytic coupling is preserved by XPro1595

Astrocytic coupling is maintaining the homoeostasis of metabolites and ions in the brain. The loss of GJC between astrocytes also plays an important role in the development of epilepsy. An impairment of the astrocytic coupling strength by a reduction, contributes to the development and progression of TLE as recently reported (Bedner et al., 2015). Therefore, we studied the extent of coupling in animals treated with XPro1595 and KA-only.

To compare the loss of astrocytic GJC on the ipsilateral hippocampus between KA-only injected, XPro Prev and XPro Resc condition, three time points were chosen: 4 hrs after KA injection representing the GJC at the beginning of the SE, 3 days after KA injection representing the latent phase and 3 months after KA injection were chosen to represent the GJC in the chronic phase of TLE. In Fig. 5.17 only the ipsilateral astrocytic coupling strength is depicted (contralateral is shown as dashed line). At 4 hrs after SE induction no significant difference between the number of biocytin positive astrocytes of KA-only compared with XPro Prev is observed on the ipsilateral hippocampus (p=0.1). In the latent phase 3 days after SE, both XPro conditions were signficantly altered compared with KA-only ipsilateral side (KA-only vs. Prev p=0.007#, KA-only vs. Resc p=0.017#). The same revealed for the chronic phase (KA-only vs. both XPro conditions p=0.001#).

In summary, XPro1595 treatment before and after SE induction was able to prevent or restore the gap junction coupling.

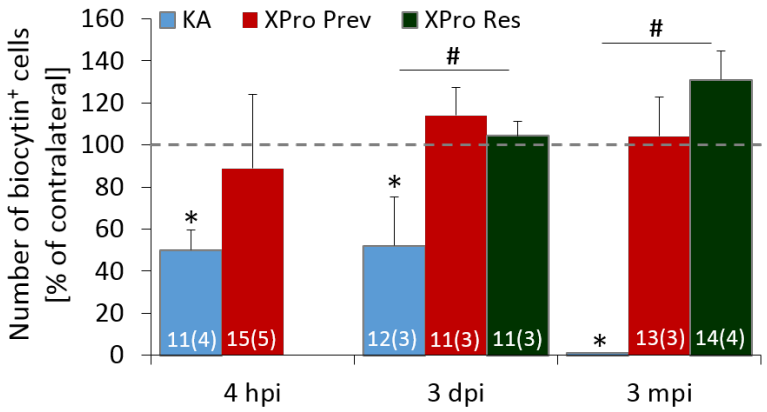

Figure 5.17 The effect of XPro1595 treatment on the SE-induced astrocytic uncoupling. Summary of mean values of astrocytic GJC in dorsal slices of the ipsilateral hippocampus, expressed as percentage of the number on the contralateral side. Contra- and ipsilateral measurements were always conducted in the same slice. Coupling analysis was investigated at the time points 4 hpi, 3 dpi and 3 mpi in KA-only, XPro Prev and XPro Resc injected animals (contralateral vs. ipsilateral). Number in bars indicate the number of slices and in brackets the number of investigated animals is displayed. Asterisks indicate significant difference from contralateral hippocampus. Diamonds point out significant difference from another treated group.

5.7 Mechanistic effect of XPro1595

5.7.1 Incubation of hippocampal slices from wildtype mice with TNF-α

To clarify the impact of TNF-α on astrocytic gap junction coupling we incubated acute brain slices *in situ* from WT animals with TNF-α [10 ng/ml]. After 1 hr incubation time patch-clamp recordings were started and after 5 hrs incubation time measurements were terminated. Potential time dependent changes in the GJC were statistically tested by grouping the slices into time frames; group I incubation time from 1-2 hrs, group II incubation time 2-3 hrs, group III incubation time 3-4 hrs and group IV incubation time 4-5 hrs incubation time. No significant alterations were detected (p-values between 0.81-0.89). We found no significant difference between the contralateral and ipsilateral side (220 $\pm$ 54.4 vs. 253 $\pm$ 63.8 biocytin positive cells, p=0.537, n=11 slices from 3 animals).
In conclusion, these data show that solTNF-α alone is not able to cause a reduction in astrocytic coupling strength, whereas a co-incubation with IL-1β does. Alternatively, a secondary unknown released molecule might be needed to induce astrocytic uncoupling.

5.7.2 TNFR1 KO in KA-only induced TLE

EEG recording

All TNFR1 KO animals injected with KA-only developed SE. The SE started immediately after KA injection and was followed by the latent phase of 10.5 $\pm$ 3.3 days with no seizure activity. The latent period was significantly longer in TNFR1 KO mice than in KA-only animals (p=0.011*). For seizure activity monitoring, we recorded 4 animals up to 3 months post SE induction. TNFR1 KO animals displayed significant less secondary generalised spontaneous seizures compared with KA-only animals, 1 month (p=0.004*) until 3 months (p=0.019*) after SE induction. The seizure activity is shown in table 5.10 and in Fig. 5.18b. Video-monitoring analysis showed that spontaneous electrographic seizures were always accompanied by behavioural tonic-clonic convulsions.

Unchanged astrocytic coupling strength

To examine, which influence the TNFR1 signalling cascade has on the astrocytic GJC we injected KA intracortically in TNFR1 KO animals. Four hours later the biocytin tracer spread assay was performed to access coupling efficiency in the dorsal hippocampus. We found no significant difference between the contralateral and ipsilateral side (171 $\pm$ 23.5 vs. 167 $\pm$ 22.5 biocytin positive cells, p=0.822, n=11 slices from 3 animals) (Fig. 5.18a).
These data indicate that the changes in astrocytic GJC are related to the TNFR1 signalling cascade.

Table 5.10 Mean values of seizure activity in KA-only and TNFR1 KO animals

week after SE	**KA-only** mean ± SD	n	**TNFR1 KO** mean ± SD	n	**statistical** t-test
1	0.47 ± 0.31	4	0.14 ± 0.29	4	p=0.166
2	1.89 ± 0.80	4	0.36 ± 0.38	4	p=0.013*
3	1.75 ± 1.11	4	0.71 ± 0.81	4	p=0.181
4	2.86 ± 0.76	3	0.43 ± 0.55	4	p=0.004*
8	4.82 ± 2.15	6	0.18 ± 0.36	4	p=0.003*
12	4.99 ± 3.26	6	0.14 ± 0.29	4	p=0.019*

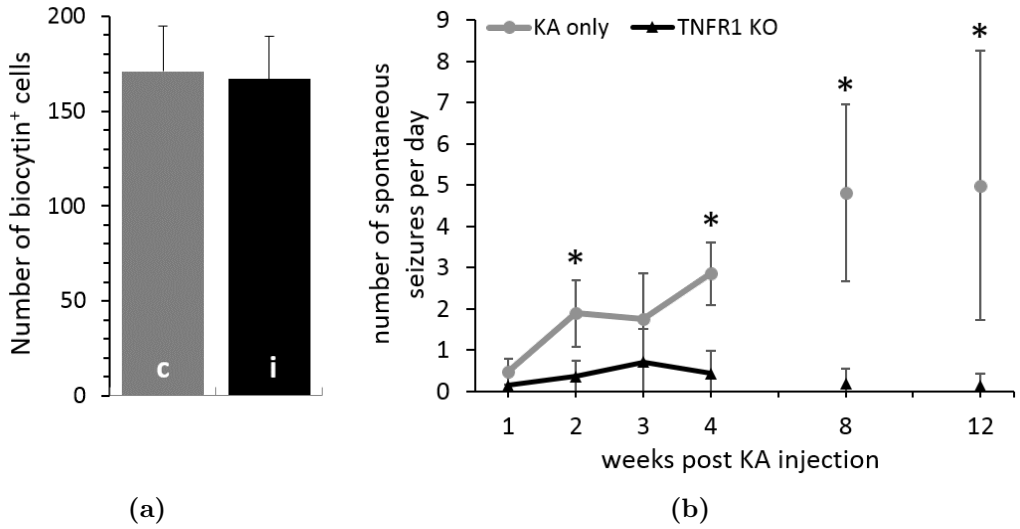

(a) **(b)**

Figure 5.18 TNFR1 KO mice in experimentally induced TLE. (a) In TNFR1 KO animals no reduction of astrocytic coupling occurs 4 hrs after KA injection (c=contralateral, i=ipsilateral). **(b)** Animals lacking the TNFR1 show almost complete lack of secondary generalised spontaneous seizure compared with KA-only animals in the chronic phase of epilepsy. Asterisks indicate significant difference from another treated group.

6 Discussion

Proinflammatory cytokines, such as TNF-α and IL-1β play an important role in neurodegenerative diseases. In epilepsy they activate glial cells, which boost the cytokine production. Cytokine release by glial cells contributes to the development and progression of epileptogenesis and the long-term manifestation of the disorder. Therefore, the use of antiinflammatory drugs might be helpful to attenuate the development of epileptogenesis.
As several studies found increased levels of IL-1β in epilepsy (Rizzi et al., 2003; Vezzani et al., 2002; Balosso et al., 2008) the drug Anakinra, an IL-1R1 antagonist, was tested for its anticonvulsant effect *in vivo* (Vezzani et al., 2000). The authors suggested that an imbalance between IL-1β and its naturally occurring receptor antagonist IL-1Ra contributes to seizure generalisation. If IL-1β is more present than IL-1Ra, IL-1β enhances NMDAR function by activating the Src tyrosine kinase, which phosphorylates the NR2A/B subunit leading to subsequent increased Ca^{2+} influx and may contribute glutamate-mediated neurodegeneration (Viviani et al., 2003). That is why VX-765, a selective inhibitor of interleukin-1 converting enzyme (ICE), which cleaves IL-1β into its active mature form, was shown to possess anticonvulsive effects in experimental animal models of epilepsy (Maroso et al., 2011; Ravizza et al., 2006). Moreover, a clinical research was investigated by the company Vertex Pharmaceuticals Incorporated, which was however stopped at clinical phase 2b, the dose finding phase (Vertex Pharmaceuticals Incorporated, 2011). No reason for this early termination is officially available by the manufacturer, but as it was stopped in the dose-finding phase, one can assume that the inhibition of IL-1β production had too little effect on the outcome in epileptic patients. The reason might be that still several other cytokines are able to induce seizure generalisation. Especially, TNF-α has been shown to promote epileptogenesis, as it shares common downstream signalling pathways with IL-1β, like the NFκB cascade, and is able to induce its own expression (Chu, 2013; Philip and Epstein, 1986; O'Neill and Bowie, 2007; Smolen and Steiner, 2003). Additionally, several studies have reported a proconvulsive role of the solTNF-α/TNFR1 signalling (Balosso et al., 2005; Weinberg et al., 2013) whereas drugs like etanercept and lenercept (binding both TNF-α ligand forms) showed no improvement or even caused severe side effects, such as sepsis, early septic shock, RA and MS (Kontermann et al., 2009; Sicotte and Voskuhl, 2001; Slifman et al., 2003; Shakoor et al., 2002). Therefore, inhibiting only the solTNF-α form seems to be a promising target for the treatment of epilepsy.

6.1 XPro1595 prevents the development of experimental TLE

In our animal model for MTLE-HS we could show that the application of solTNF-α inhibitor XPro1595 prevented or even restored the astrocytic GJC. Thus, we could reduce significantly seizure activity, which is a clinical parameter and read out for the efficiency of a therapeutical drug. Additionally, we could show that XPro1595 administration attenuated the development of HS in the TLE model. These results highlight the importance of astrocytic GJC on the initiation and development of MTLE: if coupling remains functionally, the seizure activity and HS are significantly reduced.
The biggest effect was obtained when XPro1595 was given before the induction of SE (XPro Prev), indicating that the inhibition of solTNF-α significantly prevented the loss of astrocytic GJC and consequently the development of seizures and MTLE-HS. We assume that XPro1595 administration prior to SE-induced epilepsy, immediately binds the microglial released solTNF-α, which is induced by KA injection (see Fig. 6.1b). Therefore, XPro1595 prevents solTNF-α to bind its astrocytic TNFR1, which is expressed during SE. Since no solTNF-α/TNFR1 signalling occurs, we suggest that the phosphorylation-induced astrocytic uncoupling is prevented. Moreover, since the solTNF-α/TNFR1 complex is not internalised, further gene expression and production of TNF-α via NFκB pathway does not occur. This prevents a second wave of TNF-α release from astrocytes. Since XPro1595 has no effect on the release of microglial IL-1β, which is also released after the KA injection, IL-1β might bind to astrocytic and neuronal IL-1R1. As Ravizza et al. (2008) found increased IL-1R1 expression after KA-induced SE on astrocytes, it might be possible that increased IL-1R1 expression via intracellular signalling cascades, such as NFκB pathway, could also activate nuclear gene expression and subsequently cause *de novo* synthesis of TNF-α. Since the astrocytic *de novo* synthesised and released TNF-α is depleted by XPro1595, activation of solTNF-α/TNFR1 signalling cascade-induced astrocytic uncoupling or release of secondary cytokine waves are consequently prevented. In the XPro Prev condition, only a slightly decreased number of pyramidal neurons on the ipsilateral hippocampus was obtained, compared with the contralateral side. This might be a direct effect of injected KA, which is well known to induce neuronal death within the first 24 hrs after injection (Doble, 1999). Notably, less neuronal cell death was also observed in the XPro Resc treatment compared with KA-only animals, when we applied XPro1595 4 hrs, 3 and 6 days after SE. In contrast, when XPro1595 was given after the first spontaneous generalised seizure (XPro Chronic), it had no effect on the extent of neurodegeneration of pyramidal neurons in the CA1 region.
Four hours after SE induction, we found a significant loss of astrocytic GJC in KA-only animals and from ELISA we know that TNF-α was significantly elevated at this time point. One day after SE induction TNF-α was decreased, but still significantly expressed above basal level on the ipsilateral hippocampus and GJC was also impaired. As we also

could show that TNF-α levels are more strongly upregulated than IL-1β in our animal model, these results indicate that the solTNF-α is mainly responsible for the loss of astrocytic GJC. It was shown by Bedner et al. (2015) that the loss of astrocytic GJC was already present 4 hrs after SE induction, whereas neuronal death started 6 hrs after SE. This result clearly demonstrated that impairment of astrocytic GJC is a causal event, while neuronal death and generalised spontaneous seizures are merely consequences. An unpublished study from our group by Deshpande et al. (2018) found that XPro1595 prevented the cytokine-induced phosphorylation of the Cx43 C-terminus at S262 and the consequential loss of coupling *in situ* 4 hrs after SE induction. They concluded that "TNF-α and/or IL-1β induced phosphorylation of S262 causes or critically contributes to astrocytic uncoupling" in the MTLE model. We could demonstrate in our XPro Prev animals, that even a massive TNF-α release 4 hrs after SE induction did not impair GJC due to the inhibition of solTNF-α by XPro1595. That demonstrates, that XPro1595 administration prevented the loss of astrocytic GJC *in vivo*. Moreover, XPro Prev animals showed no loss of astrocytic GJC in the latent and chronic phase, consequentially no generalised spontaneous seizures developed and almost no HS was found 3 months after SE induction (Fig. 6.1b). This provides further evidence that astrocytic GJC has an initiating role in the development and progression of TLE.
The administration of XPro1595 *in vivo* after SE was able to rescue and restore astrocytic GJC in the latent and chronic phase. We believe that this findings result from the fact that XPro1595 binds the second wave of TNF-α release by astrocytes, thereby inhibiting TNFR1-induced astrocytic uncoupling. Consequently, the functional astrocytic GJC allows an equal distribution of K^+ and glutamate via the astrocytic syncytium, which reduces neuronal hyperexcitability and decreases seizure activity, as we have also observed it 2-3 months after SE induction. Furthermore, the development of HS was attenuated in the long-term (Fig. 6.1c). All results from this study are depicted in a summarising figure, including our suggested mechanism of action of XPro1595 (Fig. 6.1b,c).
In conclusion, the inhibition of solTNF-α restored the astrocytic GJC in TLE and attentuated the clinical progression/manifestation of the disorder. Therefore, testing compounds that improve Cx43 gap junction-mediated coupling between astrocytes in the brain would be the next promising step in the development of new AEDs (see chapter 8).

6.2 Glial cells release cytokines in two waves

It is still unclear whether astrocytes or rather microglial cells are the major solTNF-α releasing cells.
As microglial cells, which belong to the innate immune system, are thought to act first by releasing cytokines, it might be that a "1st wave" of microglial TNF-α binds to neighbouring cells like neurons and astrocyte (Vezzani et al., 2002; Wang et al., 2015). When

we give XPro1595 before the SE induction, this first wave of TNF-α is inhibited and only IL-1β from microglia might be able to bind astrocytic and neuronal IL-1R1. The IL-1R1 signalling involves the activation of NFκB, which triggers the transcription of TNF-α and IL-1β in neurons and astrocytes. The production and release of a "2nd wave" of both cytokines from astrocytes might act as a positive feedback loop, strengthening the inflammatory processes (Novrup et al., 2014). As under our experimental conditions the released TNF-α is immediately bound by XPro1595, only IL-1β persists and binds to its receptor on astrocytes again (Fig. 6.1b). Astrocytes are thought to be the main cell influcencing the proinflammatory cytokine microenvironment at this phase (Vezzani and Baram, 2007). To understand which part and impact microglial cells and/or astrocytes have in the acute phase of epilepsy, studies investigating cell-specific knockout animals should be done to better understand how specifically they contribute to the neuroinflammatory signalling. Furthermore, studying other cytokine-producing cells, such as invading macrophages and T-cells, could help to understand better the activated pathways and contribution of the adaptive immune system leading to epileptogenesis.

6.3 Alterations in coupling are TNFR1-mediated

IL-1β was found to cause reduction in astrocytic GJC (Même et al., 2006; Bedner et al., 2015), which might explain the observed impaired coupling strength within the acute phase after SE induction. As the IL-1R1 expression was found to decrease in astrocytes after the acute phase of epileptogenesis (Vezzani et al., 2002; Balosso et al., 2008), the IL-1β/IL-1R1 feedback loop would stop by itself. Our results support this idea, as IL-1β levels were found to be significantly reduced in KA-only animals after the acute phase of SE induction and even the astrocytic GJC was found to be unaltered again in the latent phase at day 5 post KA injection. XPro Prev animals display unaltered astrocytic GJC 3 days after SE induction, whereas GJC is still impaired in KA-only animals at this time point. Hence, IL-1β alone cannot be the only reason for impaired coupling as we found no reduction in XPro Prev animals in the acute phase. This indicates that solTNF-α must also have an influence on the impairment of astrocytic GJC. Indeed, TNFR1 KO mice displayed no seizure-induced reduction in GJC, indicating that TNFR1 contributes to the uncoupling. These animals were less prone to generate secondary generalised spontaneous seizures, assuming that TNFR1 has a proconvulsive role in the development of TLE. This is in line with previously published studies from Balosso et al. (2005) and Weinberg et al. (2013), who also found a TNFR1-mediated proconvulsive effect. To directly assess the influence of increased TNF-α levels on the astrocytic coupling, we incubated acute brain slices from WT animals in ACSF solution containing high concentration of TNF-α (400-fold higher than the values observed by ELISA after SE induction) and found no impairment of astrocytic GJC. One explanation could be that high TNF-α concentration activate TNFR2-mediated anticonvulsive signalling cascade, due to its 30-fold higher dissociation rate of TNF/TNFR2 complex

(Grell et al., 1998). Additionally, our immunohistochemical analysis indicated TNFR1 expression only in astrocytes in the *str. rad.* on ipsilateral hippocampus of KA-injected mice 4 hrs after SE induction, but not in sham-injected animals (data not shown), indicating that seizure activity causes an upregulation of TNFR1. That KA indeed is able to induce receptor expression changes was already reported for TLR4 alterations in astrocytes by Maroso et al. (2010).
Obviously, in addition to TNF-α, a second mediator is needed for the reduction of GJC. This might be transiently present, such as IL-1β. There is some evidence that "TNF-α rarely induces apoptosis in the absence of a secondary signal" (Park and Bowers, 2010; Chao et al., 1995) or that "TNF-α and KA cooperate" to activate glial cells, which then produce and release more TNF-α and glutamate, "potentiated via a feedforward cascade, and thereby perpetuating the process" (Hermann et al., 2001). This may be another possible explanation for the lack of effect of TNF-α on GJC *in situ*, as KA seems to induce TNFR1 expression on astrocytes in our MTLE mouse model or that KA-induced hyperactivity is causing an TNFR1 upregulation.
Recently, our group Deshpande et al. (2018) incubated acute brain slices *in situ* with IL-1β and TNF-α and found unaltered protein expression levels of Cx43 and Cx30 4 hrs after SE, a finding that differs from previous studies in cortical astrocyte cultures (Même et al., 2006; Zhang et al., 2015). Desphande et al. (2018) found strong evidence that phosphorylation of S262 in the C-terminal tail of Cx43 accounts for an immediate loss of astrocytic GJC. S262 is phosphorylated by MAPKs, resulting in decreased open probability and a rapid internalisation of Cx43 GJ channels (Lampe et al., 1998; Thevenin et al., 2013). A loss of astrocytic GJC was prevented by XPro1595 co-incubation *in situ*. IL-1β and TNF-α can activate the MAPK pathway, which leads to the translocation of transcriptional factor AP-1 from the cytoplasm into the nucleus. In the nucleus AP-1 activates nuclear gene expression, which also includes the transcription of both inducer-cytokines (Smolen and Steiner, 2003; Takada and Aggarwal, 2004). In cultured astrocytes, cytokine-mediated uncoupling was prevented by application of a MAPK inhibitor, indicating that the loss of coupling was a consequence of MAPK activation (Retamal et al., 2007).
From our results, we know that TNF-α via TNFR1 signalling is able to cause astrocytic uncoupling, but we also found that TNF-α release only is not sufficient enough to cause a loss of astrocytic GJC. We suggest, that together with TNF-α another mediator is needed and both molecules induce long-term activation of glial cells or neuronal cell death. Allan et al. (2005) showed that "a solo-application of IL-1β into the brain of WT animals failed to cause detectable neuronal injury, suggesting that co-administration with other cytokines or molecules leads to greater impact of neurotoxicity".
Taken together, TNF-α rather initiates, enhances or prolongs the pathophysiological changes together with a secondary mediator, such as KA, IL-1β or a so far unknown molecule. Notably, TNF-α seems to be a key player in the development and progression/manifestation of TLE. Therefore, XPro1595 administration is effective in attenuating epileptogenesis in our model.

6.4 Effects of XPro1595 in neuroinflammation-induced diseases

We could show in our mouse model of MTLE-HS, that the preservation of astrocytic GJC due to XPro1595 administration significantly reduced generalised spontaneous seizures and attenuated HS in the long-term. We suggest, that beside its impact on preserving astrocytic GJC, XPro1595 might secondaryly decrease the inflammation response by glial cells, which might contribute by cytokine production and release to neuronal hyperactivity and/or morphological alterations, like HS in TLE.
As TNF-α plays an important role in several other neuroinflammation-induced diseases, XPro1595 has been shown to have secondaryly beneficial effects in experimental models of spinal cord injury (Novrup et al., 2014), multiple sclerosis (Karamita et al., 2017), Alzheimer's disease (MacPherson et al., 2017; Cavanagh et al., 2016), Parkinson's disease (Barnum et al., 2014), Huntington's disease (Hsiao et al., 2014) and limbic epilepsy (Patel et al., 2017).
XPro1595 was shown to prevent the induction of phenotypical transformation of microglial cells into an activated state (Karamita et al., 2017; Novrup et al., 2014) by local inhibition of solTNF-α and to reduce the immune response by blocking the invasion of early innate immune cells, such as infiltrating macrophages, monocytes and the adaptive immune response by reducing the number of activated $CD4^+$ T-cells and a $CD11^+$ immune cell population (Novrup et al., 2014; MacPherson et al., 2017). These results suggest that XPro1595 might be able to hinder immune cells crossing the BBB and the consequential upregulation of inflammation and neuronal damage in the brain tissue (Rezai-Zadeh et al., 2009; MacPherson et al., 2017). That XPro1595 reduces neuronal damage or even prevented the loss of dopaminergic neurons in the substantia nigra was shown in experimental models of SCI (Novrup et al., 2014), PD (Barnum et al., 2014) and HD (Hsiao et al., 2014). Also our data show a significant attenuation of neuronal loss in the hippocampus after XPro1595 administration in experimental TLE. This finding suggests that the inhibition of solTNF-α prevents secondarily cytokine-induced neuronal death by functional astroyctic GJC, which maintains the homoeostasis of metabolites and ions during seizure activity. Another possibility might be that XPro1595 inhibits astrocytic TNF-α glutamate release causing a spillover, which contributes to neuronal hyperexcitability and might lead to the trafficking of neuronal NMDAR/AMPARs. That XPro1595 is able to rescue hyperexcitability of glutamatergic synapses was demonstrateted in two transgenic mouse models for AD (Cavanagh et al., 2016; MacPherson et al., 2017). In a mouse model of SCI Novrup et al. (2014) found that XPro1595 even improved functional recovery, such as remyelination, and showed an upregulation of TLR4 protein levels, which promotes the remyelination by proliferating oligodendrocytes (Schonberg et al., 2007). It is well known, that TLR4 is activated by damage associated molecular pattern molecules, such as HMGB1, in the presence of TNF-α and IL-1β, which contributes to seizure generation (Vezzani et al., 2008;

Maroso et al., 2010). Therefore, it would be interesting to investigate the effect of XPro1595 on the HMGB1-TLR4 mediated activation of astrocytes. As our group has previously shown that TLR4 KO mice showed no loss of astrocytic GJC 1 day after SE induction (Bedner et al., 2015), it would be interesting to investigate seizure activity in these animals in the acute phase in our TLE model.
An increasing number of recent studies show that distinguishing between the two TNF-α forms and their induced receptor signalling pathways, is essential for the therapeutic outcome. The study by Novrup et al. (2014) even showed that the inhibition of both TNF-α forms by etanercept in a model of SCI had no effect, whereas the administration of XPro1595 had a protective effect with regard to pathophysiological changes. They observed a transient upregulation of TNFR2 protein levels after XPro1595 administration, suggesting that XPro1595 also promotes the signalling via TNFR2 pathway, which is well known for its function in neuroprotection and remyelination (Taoufik et al., 2011). Enhanced TNFR2 signalling was shown to have anticonvulsant effect in epileptic animals (Balosso et al., 2013; Patel et al., 2017). We found in our KA model of TLE that TNFR1 immunofluorescence is increased only in astrocytes in the acute phase. Other studies report a downregulation of TNFR2 in neurons and absence in astrocytes (Balosso et al., 2013; Weinberg et al., 2013). XPro1595 might also promote an upregulation of TNFR2 expression in TLE, thus inhibiting the hyperexcitability. It would be interesting to see, how the ratio of TNFR1 and TNFR2 changes under XPro1595 administration in experimental TLE.
Interestingly, a recent study in a limbic epilepsy model by Patel et al. (2017) reported that XPro1595 was ineffective in preventing seizures. These authors used an infection-induced mouse model, in which mice were infected with the theiler's murine encephalomyelitis virus (TMEV) through intracortical injection into the right hemisphere. The animals showed seizures 3-8 days after infection and developed chronic spontaneous seizures. The hippocampus displayed morphological changes, such as reactive glia cells, loss of pyramidal neurons in CA1 and increased cytokine expression, especially of proinflammatory cytokines IL-1β, TNF-α, interferon-γ (IFNγ) and of anti-inflammatory cytokine IL-10. Beside that, the model displayed oxidative stress markers and infiltrating macrophages in the first week after infection, which is thought to contribute to the initiation and/or propagation of acute seizures in TMEV-induced limbic epilepsy. Furthermore, they concluded from their data that the solTNF-α/TNFR1 signalling decreases the seizure threshold in limbic epilepsy by TNF-α-mediated AMPAR trafficking. Suprisingly, they detected no significant differences in the GluA1 and GluA2 subunits of AMPARs between WT and TNFR2 KO animals, suggesting that the hyperexcitability is not only based on AMPAR or depends on the regional variances of TNF-α and TNFR1 expression.
The TMEV-induced limbic seizure mouse model shows many similarities of pathophysiological changes compared with our KA model. Both display the development of HS and seizure activity. However, the cytokine profile of the two animal models is very different. Using the same ELISA kit as Patel et al. (2017), we found a significant increase in

TNF-α levels compared with the non-injected control side, whereas Patel et al. (2017) observed no significant increase in TNF-α compared with PBS-injected control mice 24 hrs after SE induction. As cytokine release is known to occur very early after the insult, we measured cytokine levels within the first 24 hrs after SE induction and found the highest levels of TNF-α and IL-1β after 4 hrs of SE induction. Both cytokines were significantly reduced after 24 hrs in our mouse model. However, Patel et al. (2017) found no significant changes of IL-1β, TNF-α, IFNγ, IL-10, IL-2 and IL-5 24 hrs after SE induction, but a significant increase 5 days after TMEV-infection in their model. Comparing the absolute levels of TNF-α between the models, they already display differences of cytokine expression 1 day after induction: Patel et al. (2017) measured 12-fold higher basal TNF-α in PBS-injected control mice than we did. The TMEV-infected animals showed 6-fold more TNF-α compared with our results from KA-injected animals.
Patel et al. (2017) injected XPro1595 (10 mg/kg s.c.) similarly to our treatment protocols. They tried several XPro1595 administration schemes: local administration into the ventricles, XPro1595 injection before TMEV-infection (which is similar to our XPro Prev condition) and they gave the first XPro1595 injection 2 hrs after TMEV-induced SE followed by two additional injections at 3-days interval (which is similar to our XPro Resc treatment). Despite that, Patel et al. (2017) never saw a beneficial effect on the number of seizure activity 3-8 days after induction. In our model XPro1595 administration before SE induction (XPro Prev) almost completely inhibited seizure activity 1 week after SE induction. The post-treatment condition XPro Resc received the first injection 4 hrs after SE induction and XPro Chronic animals received the first XPro1595 injection after the first generalised spontaneous seizure, which is even much later compared to the application scheme used by Patel et al. (2017) and, notably, we detected a significant decrease in seizure activity in both post-treated conditions 2 and 3 months after SE induction. Like Patel, we also measured increased TNF-α levels within the first 24 hrs after SE induction and did not see any significant reduction in seizure activity in the first week after SE induction. Seizure activity was only significantly reduced in the long-term. Thus, the seizure activity may not have been measured long enough to see significant differences in the study by Patel et al. (2017). Therefore, it would be very interesting to know whether in the TMEV-induced limbic epilepsy model the seizure activity would be reduced in the long-term as well and whether HS would be also less prominent, as it is the case in our study. These findings could help us to understand the relationship between inflammation-induced mechanisms and the progression of epilepsy, especially with regard to the loss of astrocytic GJC, reactive gliosis and neuronal cell death.
Another interesting result from Patel et al. (2017) is the finding of significantly upregulated cytokines IL-2, IL-5 and IL-10 within the first week after induction. This result indicates that the innate and adaptive immune system are closely linked in TLE. The invasion of cells of the adaptive immune system into the brain plays an important role in epileptogenesis. IL-2 activates T helper cells, which can recruit further cells of the adaptive immune response, such as B lymphocytes, and induce IL-5 production (Malek

and Castro, 2010). IL-5 enhances the immune response by stimulating B cells to produce antibodies (Takatsu, 2011). To avoid an overshoot of inflammation, T helper and T regulatory cells (T_{regs}) produce IL-10, which acts as an antiinflammatory mediator (Chaudhry et al., 2011; Ng et al., 2013). It would be interesting to see whether XPro1595 could prevent the response of the adaptive immune system by reducing or blocking the innate immune response and therefore might be also able to prevent an infiltration of immune cells into brain or the breakdown of BBB in epilepsy.
The elevation of proinflammatory cytokines, such as TNF-α and IL-1β, mainly influence the development and progression of TLE. Especially a selective inhibition of solTNF-α/TNFR1 signalling has the potential to modulate the immune response in the diseased brain, as it attenuates neuroinflammation and prevents or dampens the progression of the disease.
The development of selective inhibitors for the solTNF-α/TNFR1 cascade opens up new possibilities in the field of antiinflammation. It gives us the possibility to investigate TNF function and novel strategies in clinical approaches. Beside the dominant-negative TNF mutants that exclusively bind to the ligand solTNF-α, inhibitors that selectively bind to a TNFR1-domain, e.g. R1antTNF, DMS5540, TROS, ATROSAB, were developed (Kontermann et al., 2009; Fischer et al., 2015). The decision of using either solTNF-α or TNFR1-domain inhibitors in diseases with pronounced elevated TNF-α levels depends on the context. Arguments in favour of applying solTNF-α inhibitors are that the local cross-signalling of the tmTNF-α form via TNFR1 has a protective effect in the immune response. It was shown that treated animals were protected against viral and microbial infections and that the tmTNF-α/TNFR1 signalling promoted neuronal survival (Zalevsky et al., 2007; Taoufik et al., 2008). Therefore, using TNFR1-domain antagonists would inhibit these effects. An argument against the application of solTNF-α inhibitors is that solTNF-α is not able anymore to induce TNFR2 signalling in cells displaying high TNFR2 expression, such as T_{regs} cells, thus compromising the adaptive immune modulatory response via TNFR2 (Chen and Oppenheim, 2011). An advantage of TNFR1-domain antagonists is that the proinflammatory lymphotoxin-α (formerly known as TNF-β) cannot bind to its receptor, contributing to inflammatory diseases, like experimental allergic encephalomyelitis and RA (Suen et al., 1997; Calmon-Hamaty et al., 2011).
For future clinial approaches, one can only speculate which antagonist application is more beneficial or rather harmful. This aspect depends on the type of disease and its inflammatory progression. Another recently published stragtegy is to artifically enhance the protective function of the tmTNF/TNFR2 signalling pathway by using single chain TNF ligands (Fischer et al., 2017).
Beside preserving astrocytic GJC via inhibiting solTNF-α, XPro1595 might secondaryly modulate the expression and function of TNF-induced alterations of receptors, through phosphorylation at the membrane (Viviani et al., 2007). In a study with TNF-deficient astrocytes Santello et al. demonstrated that the administration of low picomolar amounts of solTNF-α was sufficient to restore astrocytic gliotransmission in the DG (Santello et

al., 2011). Under physiological conditions, local production of solTNF-α seems to rapidly regulate the strength of synaptic connectivity and thereby influencing the neuronal network (Probert, 2015). Elevated levels of proinflammatory cytokines in neurodegenerative diseases, might further induce a loss of GABAergic neurons in the hippocampus, thereby decreasing the seizure threshold (Samland et al., 2003). Beside a reduction in synaptic inhibition, TNF-α enhances neuronal excitability by modulating NMDAR and AMPAR (Balosso et al., 2009; Seifert et al., 2010). In limbic epilepsy the seizure threshold was found to be reduced by solTNF-α/TNFR1-mediated alterations in AMPAR trafficking (Patel et al., 2017). Hence, it would be interesting to see whether these mechanisms also contribute to the observed XPro-induced reduction in seizure frequency in our model of TLE. Nevertheless, XPro1595 preserves astrocytic GJC, and this seems to be the primary reason why the seizure activity in our model is decreasing. That the administration of XPro1595 also attenuated the HS is a secondary finding, which could be due to the effect that XPro1595 preserved the astrocytic GJC. Additionally, XPro1595 might have an influence on subordinate mechanisms of other cell types.

6.5 Antiinflammatory substances with potential clinical relevance in TLE

Inflammation is an attractive target for treating epilepsy. On the one hand, that gives various possibilities for the development of new drugs, targeting different mechanisms and approaching different cell signalling pathways. On the other hand, it displays exactly the difficulties, which arise when confronted with a great diversity. If an initial insult activates the innate immune system, blocking the inflammatory cascade, such as NFκB- and MAPK pathways could be beneficial. However, as signalling cross-talk occurs new drugs need to be carefully designed with the following characteristics: i) specific inhibition of proinflammatory cascades, while sparing antiinflammatory signalling, which contributes to cell protection or repair of neuronal circuits (Dedeurwaerdere et al., 2012), ii) avoidance of cascade cross-talk and iii) drug accessibility. The drugs should be designed with appropriate brain penetration properties if it should be used for future clinical approaches with systemic administration. Furthermore, the time course of epileptogenesis displays different immune responses. If a drug is intended to be administered in the acute phase, rather innate immune signalling should be targeted, whereas in the latent or chronic phase the adaptive immune response is probably a more relevant target.

The treatment with minocycline, an antibiotics, which has been shown to have neuronal protection, could prevent microglial activation after KA-induced SE (Abraham et al., 2012). In a viral-like CNS inflammation model, minocycline suppressed the increased seizure susceptibility or reduced the number of seizures in mice probably by lowering

the IL-1β levels by inhibiting the IL-1β converting enzyme (ICE) (Galic et al., 2009; Libbey et al., 2011). Targeting the IL-1β system by inhibiting ICE with the component VX-765 showed strong anticonvulsant effects in KA models of epilepsy and seemed to be a promising target, but clinical trials were terminated in phase 2b (Ravizza and Vezzani, 2006; Maroso et al., 2011; Vertex Pharmaceuticals Incorporated, 2011). Another study showed that the combination of Anakinra and VX-765 in two rat models of TLE was ineffective in neuroprotection and did not prevent the development of spontaneous seizures (Noe et al., 2013). Targeting other proinflammatory cytokines, such as TNF-α signalling by administering specific inhibitors of solTNF-α or blockers selectively binding to a TNFR1-domain, has shown to be more promising in animal models. The small molecule Minozac, a selective inhibitor of proinflammatory cytokine production prevented reactive gliosis and the increase of proinflammatory cytokines, like IL-1β, IL-6 and TNF-α in the hippocampus (Somera-Molina et al., 2007; Chrzaszcz et al., 2010). The advantage of Minozac is that it was shown to penetrate the BBB (Hu et al., 2007; Lloyd et al., 2008).

Leukocyte migration modifies the permeability of BBB in inflammatory disorders and BBB failure has been shown to contribute to the onset of epilepsy (Marchi et al., 2007; Larochelle et al., 2011). Conversely, epileptic seizures were shown to further destroy the BBB and a disrupted BBB allows further massive leukocytes infiltration into the brain (Marchi et al., 2007; Daneman and Prat, 2015). Beside leukocyte invasion also an influx of ions, serum proteins and other adaptive immune cells occur, which may enhance seizure activity. Blocking the leukocyte-endothelial interaction via antibodies, which inhibit the vascular cell adhesion protein1 or endothelial ligand intercellular adhesion molecule1, has been shown to reduce the seizure frequency in a pilocarpine-induced mouse model of epilepsy and in MS patients with epilepsy (Fabene et al., 2008; Sotgiu et al., 2010). Therefore, preventing leukocyte penetration into the brain might be a useful therapeutical target.

Another therapeutical target is the cyclooxygenase (COX) inhibition. COX-2 is primarily activated by inflammation. Administration of a selective COX-2 inhibitor (Celecoxib) or selective inhibitor for COX-1 (SC-560) as well as the application of non selective COX inhibitors (Aspirin, Indomethacine) have been reported to reduce the seizure frequency in pilocarpine-induced rat model of TLE (Jung et al., 2006; Tanaka et al., 2009) and even to attenuate the hippocampal neuronal loss, GCD and mossy fiber sprouting (Ma et al., 2012). Those studies assume that cyclooxygenase enzymes, derived from neurons and microglial cells, might also affect the development of seizures beside proinflammatory cytokines (Mirrione and Tsirka, 2011).

As mentioned above, several studies have reported that various ways of antiinflammatory treatment improve epileptogenesis in different animal models of epilepsy. That emphasises the importance of blocking inflammatory signalling as a treatment for epilepsy. Various signalling casacades are activated in the development of epilepsy, leading to an up- and/or downregulation of protein levels, receptor expression changes, molecule- and ions alterations influencing the homoeostasis in a bunch of cell-cell interactions and

their networks. Therefore, it is highly important that newly developed antiinflammatory drugs are tested in an animal model that closely mimicks functional and structural changes of human MTLE-HS. The intracortical KA model displays similar characteristics in the chronic phase like observed in hippocampal tissue resected from epileptic patients (Bedner et al., 2015). Thus, this model seems to be suitable for clarifying the underlying mechanisms initiating the human disease and might serve as a model of pharmacoresistance at the late stage. We could show that XPro1595 was able to attenuate the hallmarks of sclerosis and to reduce the seizure frequency in our model, even when the first administration occured after the first spontaneous generalised seizure. Our results indicate that XPro1595 *in vivo* is successfully dampening the progression of epileptogenesis by restoring functionality of astrocytic GJC, thus i) further proconvulsive effects were prevented and seizure activity was significantly reduced and ii) morphological changes like HS were attenuated. Importantly, XPro1595 has been shown to cross the BBB and to have no severe side effects in animals models of neurodegenerative diseases.

In conclusion, XPro1595 is a highly potent drug for clinical approaches as it dampens the neuroinflammational processes in the development of epilepsy and is easily administered systemically. In further clinical trials especially the dose-finding phase will be important, in which the optimum dose at which the drug shows biological activity with minimal side-effects, is studied.

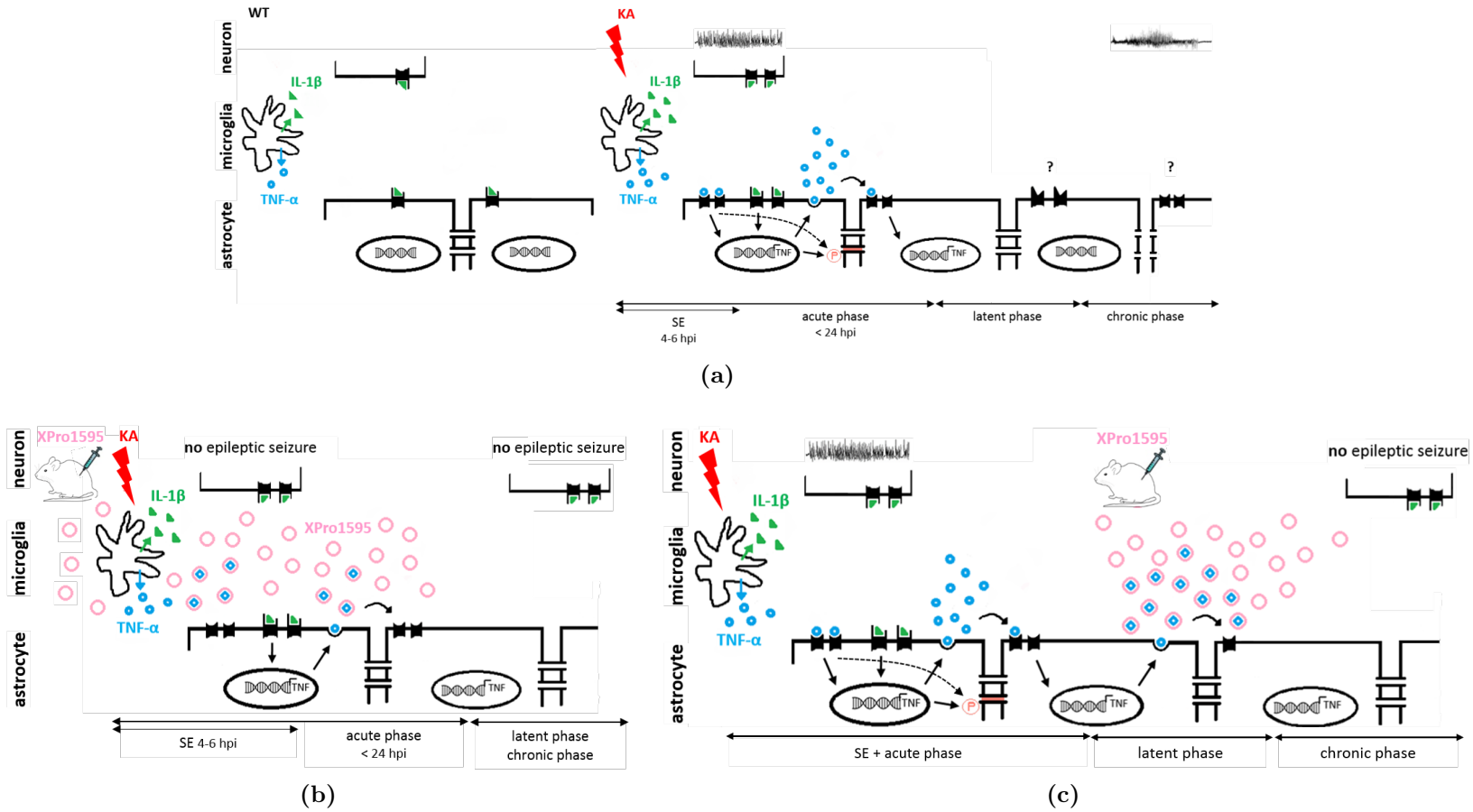

Figure 6.1 Potential mechanism of XPro1595: **(a)** In WT animals basal concentration of cytokines are expressed mainly by microglial cells. After KA-injection, SE-induced cytokine levels increase (primary TNF-α), TNFR1 is present on astrocytes and GJC is impaired. In the acute phase astrocytes produce and release TNF-α (2nd cytokine wave), followed by the latent phase. A loss of GJC is observed in the chronic phase and generalised spontaneous seizures occur. **(b)** XPro1595 administration before SE-induced epilepsy binds immediately microglial released TNF-α after KA injection. No TNF/TNFR1 signalling casacade is activated and astrocytic GJC preserved. No generalised spontaneous seizures occur. **(c)** XPro1595 administration after SE-induced epilepsy reduces further TNF-α production and release by astrocytes, thus TNFR1-mediated uncoupling is inhibited. Restoring astrocytic GJC reduces significantly seizure activity and attenuates HS in TLE in the long-term.

7 Summary

Antiepileptic therapies are mainly based on drugs which target neuronal function. One third of epileptic patients do not respond adequately to these treatments and, importantly, all available drugs merely suppress seizures without curing the underlying disorder. Consequentially, new strategies for the development of antiepileptogenic drugs are urgently needed.
Brain inflammation contributes to a loss of gap junction-mediated coupling between astrocytes, which is a causal event in the development of temporal lobe epilepsy (TLE). In a first step we assessed the effect of XPro1595 (a selective inhibitor of soluble TNF-α) and Anakinra (IL-1R antagonist) *in situ* in acute brain slices from epileptic mice and found that astrocytic coupling was restored. To investigate this in more detail, we checked the cytokine levels in the intracortical kainate (KA) model using ELISA. The results show elevated TNF-α levels immediately after KA-induced status epilepticus (SE), whereas IL-1β was less prominent. This finding prompted us to assess the effect of solTNF-α/TNFR1 signalling cascade on astrocytic coupling. Hence, we investigated the effect of XPro1595 i.p. injection on astrocytic coupling and the development of TLE. The results show that XPro1595 given *in vivo* prior to KA injection prevented the loss of astrocytic gap junction coupling and thus the development of generalised spontaneous seizures and hippocampal sclerosis (HS) were prevented.
Treatment with XPro1595 *in vivo* after KA injection rescued astrocytic coupling, significantly decreased chronic seizure frequency in the long-term and attenuated HS-specific morphological alterations.
To confirm the effect of solTNF-α/TNFR1 signalling cascade on astrocytic coupling, we used transgenic TNFR1 KO animals in our epilepsy model. We could show that TNFR1 KO astrocytic coupling was unaltered after SE-induction, indicating that TNFR1 activation regulates astrocytic coupling strength. Furthermore, these animals showed significantly less seizure activity, demonstrating the importance of astrocytic coupling on the progression of TLE. However, incubation of acute brain slices from wildtype mice with TNF-α *in situ* revealed no impaired astrocytic coupling. Therefore, we suggest that a second mediator, like IL-1β or a yet unknown molecule, might be needed to induce astrocytic uncoupling.
In conclusion, this study demonstrates that solTNF-α/TNFR1 mediates astrocytic uncoupling and plays a key role in the development of TLE-HS. Rescuing astrocytic coupling might represent a new strategy to develop antiepileptogenic therapies. The present project elucidated the therapeutic potential of targeting astrocytic proteins in epilepsy and also shed further light on the mechanisms underlying the disorder.

8 Perspective

In the present study, the most exciting discovery is that the preservation of astrocytic GJC (by inhibiting soluble TNF-α) even after the first generalised spontaneous seizure, is able to decrease epileptic seizures and to attenuate the hallmarks of sclerosis.
Therefore, the development of Cx43 gap junction activators or enhancers should be considered as potential new antiepileptic drugs. Such compounds would represent a proof-of-concept in terms of their antiepileptogenic potential as Cx43 enhancers. Activators for Cx43 gap junctions have already been developed for the treatment of reperfusion injury after acute myocardial infarction. Danegaptide (ZP1609, from Zealand Pharma) is a dipeptide that increases gap junction conductance in the heart by modulating Cx43 phosphorylation. In an animal model, Danegaptide was able to prevent atrial fibrillation and was tested in the clinical phase 2 for its treatment of reperfusion injury after myocardial infarction. The study was terminated prematurely as there was no significant effect. The advantage of Danegaptide, compared to other Cx43 activators such as Rotigaptide or PQ7, is its oral bioavailability and its ability to penetrate into the mouse brain (Wang et al., 2018; Shishido et al., 2013). However, Danegaptide and other Cx43 enhancers are still far from being used as an ideal drug for preserving astrocytic gap junctional coupling in the epileptic brain. For the use of Cx43 activators, with regard to their antiepileptogenic potential, the compounds would have to be further developed. To avoid undesirable side effects, Cx43 activators should exclusively address Cx43 GJ-mediated coupling between astrocytes in the brain. In addition, such compounds must be able to penetrate the BBB in order to maintain or improve GJC. To determine whether the identified Cx43 activators act through proinflammatory cytokines and their signalling pathways, acute brain slices could be incubated with proinflammatory molecules such as IL-1β and TNF-α in the presence and absence of the Cx43 activators and the consequences on astrocytic GJC assessed. Therefore, testing Cx43 astrocytic GJC enhancers for their antiepileptogenic potential and the mechanism of action in our KA model of TLE, as well as in acute hippocampal specimen, surgically resected from intractable MTLE patients, would be the next promising step towards a new strategy for the development of new AEDs.
Furthermore, to gain a better understanding on the role of XPro1595 and its protecting/ rescuing effect on astrocytic coupling, it would be worthwhile to investigate next whether XPro1595 exerts its antiepileptogenic effect exclusively by preserving the coupling. To answer this question, transgenic mice devoid of astrocytic GJC ($Cx30^{-/-}$; $Cx43^{fl/fl}$ hGFAP-Cre mice) could be subjected to the KA model of TLE. If astrocytic coupling is the target of XPro1595 action, the substance should be ineffective in these

transgenic animals.
Seizures disrupt the BBB and cause albumin leakage into the brain parenchyma (Ivens et al., 2007; Van Vliet et al., 2012). Extravascular albumin decreases the gap junctional coupling in astrocytes (Braganza et al., 2012). The astrocytic coupling experiments performed under XPro1595 administration in the present study never showed altered GJC. It might be interesting to analyse the influence of XPro1595 on BBB disruption in the hippocampus. Albumin-bound Evans blue enters the CNS when the BBB is compromised. Thus, no extravasation of Evans blue or immunohistochemically detected albumin should be detectable if XPro1595 prevents the BBB breakdown. In addition, it might be useful to characterise the infiltration of adaptive immune cells, such as lymphocytes, and their contribution to the cytokine levels in the brain.
Since solTNF-α can also affect neuronal and microglial functions, it would be worthwhile to investigate the contribution of microglial cells in the development and progression of TLE. Studies with Plexxikon-feeded animals may help to elucidate this question. Plexxikon transiently depletes exclusively microglial cells and spares macrophages, after its oral administration. Plexxikon has been shown to maintain BBB integrity, thus lowering infiltrating immune cells, decreasing neuroinflammation (Szalay et al., 2016) and possibly reducing seizure activity.
One hour after SE induction, TNF-α and IL-1β were expressed as in sham-injected control animals, and yet we found a significant reduction in astrocytic coupling at this time (Henning et al., unpublished). These results raise the question of the underlying molecular mechanism, since both cytokine levels are not significantly elevated and therefore have hardly any influence on astrocytic uncoupling. A possible explanation is that cytoskeletal pathology causes retraction of astrocyte processes, even before activation of the innate immune system occurs. This retraction may lead to the observed reduction in coupling. Therefore, studying the astrocytic coupling with substances that prevent cytoskeletal changes, could be a further step in understanding the mechanisms of impaired astrocytic GJC at a very early stage after SE.
In our study we could show that the selective inhibition of solTNF-α has a very strong influence on the progression of TLE. The impact of solTNF-α on the development of TLE was extensively characterised in an experimental mouse model of TLE. The administration of XPro1595 *in vivo* provided new insights into the mechanisms of the solTNF-α/TNFR1 signalling pathway underlying the progression of TLE.
Inhibition of TNFR1 signalling cascade has been shown to have anticonvulsant effects (Balosso et al., 2005; Weinberg et al., 2013). To improve our understanding of the involvement of the tmTNF ligand and its TNFR2 signalling, it might be useful to specifically activate TNFR2 by using novel mimetic single-chain TNF trimer ligands. A combination of solTNF-α inhibition and TNFR2 activation might even slow down the progression of epilepsy much faster than using only one approach.
Further experiments investigating the role of astrocytic coupling and underlying functional mechanism of XPro1595, will help us to understand the complex progression of TLE.

Bibliography

Abbott NJ (2002) Astrocyte-endothelial interactions and blood-brain barrier permeability. *Journal of Anatomy* 200:629–638.

Abraham J, Fox PD, Condello C, Bartolini A, Koh S (2012) Minocycline attenuates microglia activation and blocks the long-term epileptogenic effects of early-life seizures. *Neurobiology of Disease* 46:425–430.

Allan SM, Tyrrell PJ, Rothwell NJ (2005) Interleukin-1 and neuronal injury. *Nature Reviews Immunology* 5:629–640.

Allen NJ, Barres BA (2009) Neuroscience: Glia - more than just brain glue. *Nature* 457:675–677.

Araki T, Simon RP, Taki W, Lan JQ, Henshall DC (2002) Characterization of neuronal death induced by focally evoked limbic seizures in the C57BL/6 mouse. *Journal of Neuroscience Research* 69:614–621.

Araque A, Carmignoto G, Haydon PG, Oliet SHR, Robitaille R, Volterra A (2014) Gliotransmitters travel in time and space. *Neuron* 81:728–739.

Aronica E, Gorter Ja, Jansen GH, Leenstra S, Yankaya B, Troost D (2001) Expression of connexin 43 and connexin 32 gap-junction proteins in epilepsy-associated brain tumors and in the perilesional epileptic cortex. *Acta neuropathologica* 101:449–459.

Aronica E, Bauer S, Bozzi Y, Caleo M, Dingledine R, Gorter JA, Henshall DC, Kaufer D, Koh S, Löscher W, Louboutin JP, Mishto M, Norwood BA, Palma E, Poulter MO, Terrone G, Vezzani A, Kaminski RM (2017) Neuroinflammatory targets and treatments for epilepsy validated in experimental models. *Epilepsia* 58:27–38.

Ashhab MU, Omran A, Kong H, Gan N, He F, Peng J, Yin F (2013) Expressions of tumor necrosis factor alpha and MicroRNA-155 in immature rat model of status epilepticus and children with mesial temporal lobe epilepsy. *Journal of Molecular Neuroscience* 51:950–958.

Balosso S, Ravizza T, Pierucci M, Calcagno E, Invernizzi R, Di Giovanni G, Esposito E, Vezzani A (2009) Molecular and functional interactions between tumor necrosis factor-alpha receptors and the glutamatergic system in the mouse hippocampus: Implications for seizure susceptibility. *Neuroscience* 161:293–300.

Balosso S, Maroso M, Sanchez-Alavez M, Ravizza T, Frasca A, Bartfai T, Vezzani A (2008) A novel non-transcriptional pathway mediates the proconvulsive effects of interleukin-1β. *Brain* 131:3256–3265.

Balosso S, Ravizza T, Aronica E, Vezzani A (2013) The dual role of TNF-α and its receptors in seizures. *Experimental Neurology* 247:267–271.

Balosso S, Ravizza T, Perego C, Peschon J, Campbell IL, De Simoni MG, Vezzani A (2005) Tumor necrosis factor-alpha inhibits seizures in mice via p75 receptors. *Annals of Neurology* 57:804–812.

Barnum CJ, Chen X, Chung J, Chang J, Williams M, Grigoryan N, Tesi RJ, Tansey MG (2014) Peripheral administration of the selective inhibitor of soluble tumor necrosis factor (TNF) XPro1595 attenuates nigral cell loss and glial activation in 6-OHDA hemiparkinsonian rats. *Journal of Parkinson's disease* 4:349–360.

Barres BA (2008) The Mystery and Magic of Glia: A Perspective on Their Roles in Health and Disease. *Neuron* 60:430–440.

Beach T, Woodhurst W, MacDonald D, Jones M (1995) Reactive microglia in hippocampal sclerosis associated with human temporal lobe epilepsy. *Neuroscience Letters* 191:27–30.

Beattie EC, Stellwagen D, Morishita W, Bresnahan JC, Ha BK, Zastrow MV, Beattie MS, Malenka RC, Von Zastrow M, Beattie MS, Malenka RC (2002) Control of Synaptic Strength by Glial TNFα. *Science* 295:2282–2285.

Bedner P, Dupper A, Hüttmann K, Müller J, Herde MK, Dublin P, Deshpande T, Schramm J, Häussler U, Haas CA, Henneberger C, Theis M, Steinhäuser C (2015) Astrocyte uncoupling as a cause of human temporal lobe epilepsy. *Brain* 138:1208–1222.

Bedner P, Niessen H, Odermatt B, Kretz M, Willecke K, Harz H (2006) Selective permeability of different connexin channels to the second messenger cyclic AMP. *Journal of Biological Chemistry* 281:6673–6681.

Berg AT, Berkovic SF, Brodie MJ, Buchhalter J, Cross JH, Van Emde Boas W, Engel J, French J, Glauser TA, Mathern GW, Moshé SL, Nordli D, Plouin P, Scheffer IE (2010) Revised terminology and concepts for organization of seizures and epilepsies: Report of the ILAE Commission on Classification and Terminology, 2005-2009. *Epilepsia* 51:676–685.

Bernardinelli Y, Muller D, Nikonenko I (2014) Astrocyte-synapse structural plasticity. *Neural Plasticity* 2014.

Bezzi P, Domercq M, Brambilla L, Galli R, Schols D, De Clercq E, Vescovi A, Bagetta G, Kollias G, Meldolesi J, Volterra A (2001) CXCR4-activated astrocyte glutamate release via TNFa: Amplification by microglia triggers neurotoxicity. *Nature Neuroscience* 4:702–710.

Binder DK, Steinhäuser C (2006) Functional changes in astroglial cells in epilepsy. *Glia* 54:358–368.

Black RA, Rauch CT, Kozlosky CJ, Peschon JJ, Slack JL, Wolfson MF, Castner BJ, Stocking KL, Reddy P, Srinivasan S, Nelson N, Boiani N, Schooley KA, Gerhart M, Davis R, Fitzner JN, Johnson RS, Paxton RJ, March CJ, Cerretti DP (1997) A metalloproteinase disintegrin that releases tumour-necrosis factor- from cells. *Nature* 385:729–733.

Bliss TV, Gardner-Medwin aR (1973) Long-lasting potentiation of synaptic transmission in the dentate area of the unanaestetized rabbit following stimulation of the perforant path. *The Journal of Physiology* 232:357–374.

Blümcke I, Beck H, Lie AA, Wiestler OD (1999) Molecular neuropathology of human mesial temporal lobe epilepsy. *Epilepsy Research* 36:205–223.

Blümcke I, Kistner I, Clusmann H, Schramm J, Becker AJ, Elger CE, Bien CG, Merschhemke M, Meencke HJ, Lehmann T, Buchfelder M, Weigel D, Buslei R, Stefan H, Pauli E, Hildebrandt M (2009) Towards a clinico-pathological classification of granule cell dispersion in human mesial temporal lobe epilepsies. *Acta Neuropathologica* 117:535–544.

Boche D, Perry VH, Nicoll JAR (2013) Review: Activation patterns of microglia and their identification in the human brain. *Neuropathology and Applied Neurobiology* 39:3–18.

Bordey A, Sontheimer H (1998) Properties of human glial cells associated with epileptic seizure foci. *Epilepsy Research* 32:286–303.

Borges K, McDermott D, Irier H, Smith Y, Dingledine R (2006) Degeneration and proliferation of astrocytes in the mouse dentate gyrus after pilocarpine-induced status epilepticus. *Experimental Neurology* 201:416–427.

Bouilleret V, Ridoux V, Depaulis A, Marescaux C, Nehlig A, Le Gal La Salle G (1999) Recurrent seizures and hippocampal sclerosis following intrahippocampal kainate injection in adult mice: Electroencephalography, histopathology and synaptic reorganization similar to mesial temporal lobe epilepsy. *Neuroscience* 89:717–729.

Boutin H, Kimber I, Rothwell NJ, Pinteaux E (2003) The Expanding Interleukin-1 Family and Its Receptors: Do Alternative IL-1 Receptor/Signaling Pathways Exist in the Brain? *Molecular Neurobiology* 27:239–248.

Bowser DN, Khakh BS (2007) Vesicular ATP Is the Predominant Cause of Intercellular Calcium Waves in Astrocytes. *The Journal of General Physiology* 129:485–491.

Braganza O, Bedner P, Hüttmann K, Von Staden E, Friedman A, Seifert G, Steinhäuser C (2012) Albumin is taken up by hippocampal NG2 cells and astrocytes and decreases gap junction coupling. *Epilepsia* 53:1898–1906.

Bruce AJ, Boling W, Kindy MS, Peschon J, Kraemer PJ, Carpenter MK, Holtsberg FW, Mattson MP (1996) Altered neuronal and microglial responses to excitotoxic and ischemic brain injury in mice lacking TNF receptors. *Nature Medicine* 2:788–794.

Buckmaster PS, Zhang GF, Yamawaki R (2002) Axon sprouting in a model of temporal lobe epilepsy creates a predominantly excitatory feedback circuit. *The Journal of Neuroscience* 22:6650–6658.

Buras JA, Holzmann B, Sitkovsky M (2005) Model organisms: Animal models of sepsis: Setting the stage. *Nature Reviews Drug Discovery* 4:854–865.

Bushong EA, Martone ME, Jones YZ, Ellisman MH (2002) Protoplasmic astrocytes in CA1 stratum radiatum occupy separate anatomical domains. *The Journal of Neuroscience* 22:183–192.

Calmon-Hamaty F, Combe B, Hahne M, Morel J (2011) Lymphotoxin α revisited: General features and implications in rheumatoid arthritis. *Arthritis Research and Therapy* 13:4.

Cavanagh C, Tse YC, Nguyen HB, Krantic S, Breitner JC, Quirion R, Wong TP (2016) Inhibiting tumor necrosis factor-α before amyloidosis prevents synaptic deficits in an Alzheimer's disease model. *Neurobiology of Aging* 47:41–49.

Chao CC, Hu S, Ehrlich L, Peterson PK (1995) Interleukin-1 and tumor necrosis factor-alpha synergistically mediate neurotoxicity: involvement of nitric oxide and of N-methyl-D-aspartate receptors. *Brain, Behavior and Immunity* 9:355–65.

Chapman AG (1998) Glutamate receptors in epilepsy. *Progress in Brain Research* 116:371–83.

Chaudhry A, Samstein RM, Treuting P, Liang Y, Pils MC, Heinrich JM, Jack RS, Wunderlich FT, Brüning JC, Müller W, Rudensky AY (2011) Interleukin-10 Signaling in Regulatory T Cells Is Required for Suppression of Th17 Cell-Mediated Inflammation. *Immunity* 34:566–578.

Chaudhry FA, Lehre KP, van Lookeren Campagne M, Ottersen OP, Danbolt NC, Storm-Mathisen J (1995) Glutamate transporters in glial plasma membranes: Highly differentiated localizations revealed by quantitative ultrastructural immunocytochemistry. *Neuron* 15:711–720.

Chen X, Oppenheim JJ (2011) Contrasting effects of TNF and anti-TNF on the activation of effector T cells and regulatory T cells in autoimmunity. *FEBS Letters* 585:3611–3618.

Ching S, He L, Lai W, Quan N (2005) IL-1 type I receptor plays a key role in mediating the recruitment of leukocytes into the central nervous system. *Brain, Behavior and Immunity* 19:127–137.

Cho IH, Hong J, Suh EC, Kim JH, Lee H, Lee JE, Lee S, Kim CH, Kim DW, Jo EK, Lee KE, Karin M, Lee SJ (2008) Role of microglial IKKbeta in kainic acid-induced hippocampal neuronal cell death. *Brain* 131:3019–3033.

Choy M, Dubé CM, Ehrengruber M, Baram TZ (2014) Inflammatory processes, febrile seizures, and subsequent epileptogenesis. *Epilepsy Currents* 14:15–22.

Chrzaszcz M, Venkatesan C, Dragisic T, Watterson DM, Wainwright MS (2010) Minozac Treatment Prevents Increased Seizure Susceptibility in a Mouse Two-Hit Model of Closed Skull Traumatic Brain Injury and Electroconvulsive Shock-Induced Seizures. *Journal of Neurotrauma* 27:1283–1295.

Chu WM (2013) Tumor necrosis factor. *Cancer Letters* 328:222–225.

Clark IA, Alleva LM, Vissel B (2010) The roles of TNF in brain dysfunction and disease. *Pharmacology and Therapeutics* 128:519–548.

Collignon F, Wetjen NM, Cohen-Gadol AA, Cascino GD, Parisi J, Meyer FB, Marsh WR, Roche P, Weigand SD (2006) Altered expression of connexin subtypes in mesial temporal lobe epilepsy in humans. *Journal of Neurosurgery* 105:77–87.

Colonna M, Butovsky O (2017) Microglia Function in the Central Nervous System During Health and Neurodegeneration. *Annual Review of Immunology* 35:441–468.

Coras R, Siebzehnrubl FA, Pauli E, Huttner HB, Njunting M, Kobow K, Villmann C, Hahnen E, Neuhuber W, Weigel D, Buchfelder M, Stefan H, Beck H, Steindler DA, Blümcke I (2010) Low proliferation and differentiation capacities of adult hippocampal stem cells correlate with memory dysfunction in humans. *Brain* 133:3359–3372.

Coulter D, Steinhauser C (2015) Role of Astrocytes in Epilpesy. *Cold Spring Harbor Perspectives in Medicine* 5:1–13.

Crespel A, Coubes P, Rousset MC, Brana C, Rougier A, Rondouin G, Bockaert J, Baldy-Moulinier M, Lerner-Natoli M (2002) Inflammatory reactions in human medial temporal lobe epilepsy with hippocampal sclerosis. *Brain Research* 952:159–169.

D'Ambrosio R, Wenzel J, Schwartzkroin Pa, McKhann GM, Janigro D (1998) Functional specialization and topographic segregation of hippocampal astrocytes. *Journal of Neuroscience* 18:4425–4438.

D'Ambrosio R, Gordon DS, Winn HR (2002) Differential role of KIR channel and Na(+)/K(+)-pump in the regulation of extracellular K(+) in rat hippocampus. *Journal of Neurophysiology* 87:87–102.

Daneman R, Prat A (2015) The bloodbrain barrier. *Cold Spring Harbor Perspectives in Biology* 7:1.

Das A, Wallace GC, Holmes C, McDowell ML, Smith JA, Marshall JD, Bonilha L, Edwards JC, Glazier SS, Ray SK, Banik NL (2012) Hippocampal tissue of patients with refractory temporal lobe epilepsy is associated with astrocyte activation, inflammation, and altered expression of channels and receptors. *Neuroscience* 220:237–246.

De Lanerolle NC, Kim JH, Williamson A, Spencer SS, Zaveri HP, Eid T, Spencer DD (2003) A retrospective analysis of hippocampal pathology in human temporal lobe epilepsy: Evidence for distinctive patient subcategories. *Epilepsia* 44:677–687.

Dedeurwaerdere S, Friedman A, Fabene PF, Mazarati A, Murashima YL, Vezzani A, Baram TZ (2012) Finding a better drug for epilepsy: Antiinflammatory targets. *Epilepsia* 53:1113–1118.

Deng W, Aimone JB, Gage FH (2010) New neurons and new memories: How does adult hippocampal neurogenesis affect learning and memory? *Nature Reviews Neuroscience* 11:339–350.

Dericioglu N, Soylemezoglu F, Gursoy-Ozdemir Y, Akalan N, Saygi S, Dalkara T (2013) Cell death and survival mechanisms are concomitantly active in the hippocampus of patients with mesial temporal sclerosis. *Neuroscience* 237:56–65.

Deshpande T, Sylvester M, Dupper A, Bedner P, Gieselmann V, Steinhäuser C (2018) Phosphorylation at position S262 of connexin 43 protein impairs astrocyte coupling and initiates epileptogenesis. *submitted* .

Deshpande T, Li T, Herde MK, Becker A, Vatter H, Schwarz MK, Henneberger C, Steinhäuser C, Bedner P (2017) Subcellular reorganization and altered phosphorylation of the astrocytic gap junction protein connexin43 in human and experimental temporal lobe epilepsy. *Glia* 65:1809–1820.

Ding S, Fellin T, Zhu Y, Lee SY, Auberson YP, Meaney DF, Coulter DA, Carmignoto G, Haydon PG (2007) Enhanced Astrocytic Ca2+ Signals Contribute to Neuronal Excitotoxicity after Status Epilepticus. *Journal of Neuroscience* 27:10674–10684.

Doble A (1999) The role of excitotoxicity in neurodegenerative disease: Implications for therapy. *Pharmacology and Therapeutics* 81:163–221.

Drage MG, Holmes GL, Seyfried TN (2002) Hippocampal neurons and glia in epileptic EL mice. *Journal of Neurocytology* 31:681–692.

Dupper A (2014) Entkopplung von Astrozyten als Ursache von Temporallappenepilepsie Ph.D. diss., Rheinische Friedrich-Wilhelms-Universität Bonn.

Edwards JR, Gibson WG (2010) A model for Ca2+ waves in networks of glial cells incorporating both intercellular and extracellular communication pathways. *Journal of Theoretical Biology* 263:45–58.

Elisevich K, Rempel SA, Smith B, Hirst K (1998) Temporal profile of connexin 43 mRNA expression in a tetanus toxin-induced seizure disorder. *Molecular and Chemical Neuropathology* 35:23–37.

Elisevich K, Rempel SA, Smith BJ, Edvardsen K (1997) Hippocampal connexin 43 expression in human complex partial seizure disorder. *Experimental Neurology* 145:154–164.

Engel T, Schindler CK, Sanz-Rodriguez A, Conroy RM, Meller R, Simon RP, Henshall DC (2011) Expression of neurogenesis genes in human temporal lobe epilepsy with hippocampal sclerosis. *International Journal of Physiology, Pathophysiology and Pharmacology* 3:38–47.

Fabene PF, Mora GN, Martinello M, Rossi B, Merigo F, Ottoboni L, Bach S, Angiari S, Benati D, Chakir A, Zanetti L, Schio F, Osculati A, Marzola P, Nicolato E, Homeister JW, Xia L, Lowe JB, McEver RP, Osculati F, Sbarbati A, Butcher EC, Constantin G (2008) A role for leukocyte-endothelial adhesion mechanisms in epilepsy. *Nature Medicine* 14:1377–1383.

Fahrner A, Kann G, Flubacher A, Heinrich C, Freiman TM, Zentner J, Frotscher M, Haas CA (2007) Granule cell dispersion is not accompanied by enhanced neurogenesis in temporal lobe epilepsy patients. *Experimental Neurology* 203:320–332.

Fetler L, Amigorena S (2005) Brain under surveillance: The microglia patrol. *Science* 309:392–393.

Figiel I (2008) Pro-inflammatory cytokine TNF-alpha as a neuroprotective agent in the brain. *Acta Neurobiologiae Experimentalis* 68:526–534.

Fink MP (2014) Animal models of sepsis. *Virulence* 5:143–153.

Fischer R, Kontermann R, Maier O (2015) Targeting sTNF/TNFR1 Signaling as a New Therapeutic Strategy. *Antibodies* 4:48–70.

Fischer R, Marsal J, Guttà C, Eisler SA, Peters N, Bethea JR, Pfizenmaier K, Kontermann RE (2017) Novel strategies to mimic transmembrane tumor necrosis factor-dependent activation of tumor necrosis factor receptor 2. *Scientific Reports* 7:6607.

Fisher RS, Cross JH, French JA, Higurashi N, Hirsch E, Jansen FE, Lagae L, Moshé SL, Peltola J, Roulet Perez E, Scheffer IE, Zuberi SM (2017) Operational classification of seizure types by the International League Against Epilepsy: Position Paper of the ILAE Commission for Classification and Terminology. *Epilepsia* 58:522–530.

Fisher RS, Van Emde Boas W, Blume W, Elger C, Genton P, Lee P, Engel J (2005) Epileptic seizures and epilepsy: Definitions proposed by the International League Against Epilepsy (ILAE) and the International Bureau for Epilepsy (IBE). *Epilepsia* 46:470–472.

Fleischmann R, Tesser J, Schiff MH, Schechtman J, Burmester GR, Bennett R, Modafferi D, Zhou L, Bell D, Appleton B (2006) Safety of extended treatment with anakinra in patients with rheumatoid arthritis. *Annals of the Rheumatic Diseases* 65:1006–1012.

Fonseca CG, Green CR, Nicholson LFB (2002) Upregulation in astrocytic connexin 43 gap junction levels may exacerbate generalized seizures in mesial temporal lobe epilepsy. *Brain Research* 929:105–116.

Freiman TM, Eismann-Schweimler J, Frotscher M (2011) Granule cell dispersion in temporal lobe epilepsy is associated with changes in dendritic orientation and spine distribution. *Experimental Neurology* 229:332–338.

French JA, Williamson PD, Thadani VM, Darcey TM, Mattson RH, Spencer SS, Spencer DD (1993) Characteristics of medial temporal lobe epilepsy: I. Results of history and physical examination. *Annals of Neurology* 34:774–780.

Galic MA, Riazi K, Henderson AK, Tsutsui S, Pittman QJ (2009) Viral-like brain inflammation during development causes increased seizure susceptibility in adult rats. *Neurobiology of Disease* 36:343–351.

Garden GA, Möller T (2006) Microglia biology in health and disease. *Journal of Neuroimmune Pharmacology* 1:127–137.

Georgiadis I, Kapsalaki EZ, Fountas KN (2013) Temporal Lobe Resective Surgery for Medically Intractable Epilepsy: A Review of Complications and Side Effects. *Epilepsy Research and Treatment* 2013:1–12.

Giaume C, Koulakoff A, Roux L, Holcman D, Rouach N (2010) Astroglial networks: A step further in neuroglial and gliovascular interactions. *Nature Reviews Neuroscience* 11:87–99.

Giaume C, Venance L (1998) Intercellular calcium signaling and gap junctional communication in astrocytes. *Glia* 24:50–64.

Goldberg EM, Coulter DA (2013) Mechanisms of epileptogenesis: A convergence on neural circuit dysfunction. *Nature Reviews Neuroscience* 14:337–349.

Gonzalez-Perez O, Lopez-Virgen V, Quiñones-Hinojosa A (2015) Astrocytes: everything but the glue. *Neuroimmunology and Neuroinflammation* 2:115.

Gosejacob D, Dublin P, Bedner P, Hüttmann K, Zhang J, Tress O, Willecke K, Pfrieger F, Steinhäuser C, Theis M (2011) Role of astroglial connexin30 in hippocampal gap junction coupling. *Glia* 59:511–519.

Grell M, Wajant H, Zimmermann G, Scheurich P (1998) The type 1 receptor (CD120a) is the high-affinity receptor for soluble tumor necrosis factor. *Proceedings of the National Academy of Sciences of the United States of America* 95:570–575.

Grell M, Douni E, Wajant H, Löhden M, Clauss M, Maxeiner B, Georgopoulos S, Lesslauer W, Kollias G, Pfizenmaier K, Scheurich P (1995) The transmembrane form of tumor necrosis factor is the prime activating ligand of the 80 kDa tumor necrosis factor receptor. *Cell* 83:793–802.

Griemsmann S, Höft SP, Bedner P, Zhang J, Von Staden E, Beinhauer A, Degen J, Dublin P, Cope DW, Richter N, Crunelli V, Jabs R, Willecke K, Theis M, Seifert G, Kettenmann H, Steinhäuser C (2015) Characterization of panglial gap junction networks in the thalamus, neocortex, and hippocampus reveals a unique population of glial cells. *Cerebral Cortex* 25:3420–3433.

Gröticke I, Hoffmann K, Löscher W (2008) Behavioral alterations in a mouse model of temporal lobe epilepsy induced by intrahippocampal injection of kainate. *Experimental Neurology* 213:71–83.

Halassa MM, Fellin T, Takano H, Dong JH, Haydon PG (2007) Synaptic Islands Defined by the Territory of a Single Astrocyte. *Journal of Neuroscience* 27:6473–6477.

Hanahan D, Weinberg RA (2000) The hallmarks of cancer. *Cell* 100:57–70.

Hanisch UK (2002) Microglia as a source and target of cytokines. *Glia* 40:140–155.

Hatton GI, Parpura V, editors (2004) *Glial Neuronal Signaling* Springer US.

Haydon PG, Carmignoto G (2006) Astrocyte Control of Synaptic Transmission and Neurovascular Coupling. *Physiological Reviews* 86:1009–1031.

Hebb DO (1949) *The Organization of Behaviour* Taylor & Francis Inc.

Heneka MT, Petzold GC, Kummer MP, Brosseron F, Latz E, Heneka MT, Carson MJ, El Khoury J, Landreth GE, Brosseron F, Feinstein DL, Jacobs AH, Wyss-Coray T, Vitorica J, Ransohoff RM, Herrup K, Frautschy SA, Finsen B, Brown GC, Verkhratsky A, Yamanaka K, Koistinaho J, Latz E, Halle A, Petzold GC, Town T, Morgan D, Shinohara ML, Hugh Perry V, Holmes C, Bazan NG, Brooks DJ, Hunot S, Joseph B, Deigendesch N, Garaschuk O, Boddeke E, Dinarello CA, Breitner JC, Cole GM, Golenbock DT, Kummer MP (2015) Neuroinflammation in Alzheimer's disease. *Neurology Review Lancet Neurology* 14:388–405.

Henshall D (2007) Apoptosis signalling pathways in seizure-induced neuronal death and epilepsy. *Biochemical Society Transactions* 35:421–423.

Hermann GE, Rogers RC, Bresnahan JC, Beattie MS (2001) Tumor necrosis factor-alpha induces cFOS and strongly potentiates glutamate-mediated cell death in the rat spinal cord. *Neurobiology of Disease* 8:590–9.

Hinterkeuser S, Schröder W, Hager G, Seifert G, Blümcke I, Elger CE, Schramm J, Steinhäuser C (2000) Astrocytes in the hippocampus of patients with temporal lobe epilepsy display changes in potassium conductances. *European Journal of Neuroscience* 12:2087–2096.

Howarth C (2014) The contribution of astrocytes to the regulation of cerebral blood flow. *Frontiers in Neuroscience* 8:103.

Hsiao HY, Chiu FL, Chen CM, Wu YR, Chen HM, Chen YC, Kuo HC, Chern Y (2014) Inhibition of soluble tumor necrosis factor is therapeutic in Huntington's disease. *Human Molecular Genetics* 23:4328–4344.

Hu S, Sheng WS, Ehrlich LC, Peterson PK, Chao CC (2000) Cytokine effects on glutamate uptake by human astrocytes. *Neuroimmunomodulation* 7:153–159.

Hu W, Ralay Ranaivo H, Roy SM, Behanna HA, Wing LK, Munoz L, Guo L, Van Eldik LJ, Watterson DM (2007) Development of a novel therapeutic suppressor of brain proinflammatory cytokine up-regulation that attenuates synaptic dysfunction and behavioral deficits. *Bioorganic and Medicinal Chemistry Letters* 17:414–418.

Hubbard JA, Binder DK (2016) *Astrocytes and Epilepsy* Elsevier.

Hufnagel A, Weber J, Marks S, Ludwig T, De Greiff A, Leonhardt G, Widmann G, Stolke D, Forsting M (2003) Brain diffusion after single seizures. *Epilepsia* 44:54–63.

Hwang EM, Kim E, Yarishkin O, Woo DH, Han KS, Park N, Bae Y, Woo J, Kim D, Park M, Lee CJ, Park JY (2014) A disulphide-linked heterodimer of TWIK-1 and TREK-1 mediates passive conductance in astrocytes. *Nature Communications* 5:3227.

Ivens S, Kaufer D, Flores LP, Bechmann I, Zumsteg D, Tomkins O, Seiffert E, Heinemann U, Friedman A (2007) TGF-β receptor-mediated albumin uptake into astrocytes is involved in neocortical epileptogenesis. *Brain* 130:535–547.

Jäkel S, Dimou L (2017) Glial Cells and Their Function in the Adult Brain: A Journey through the History of Their Ablation. *Frontiers in Cellular Neuroscience* 11:24.

Jefferys J, Steinhäuser C, Bedner P (2016) Chemically-induced TLE models: Topical application. *Journal of Neuroscience Methods* 260:53–61.

Jung KH, Chu K, Lee ST, Kim J, Sinn DI, Kim JM, Park DK, Lee JJ, Kim SU, Kim M, Lee SK, Roh JK (2006) Cyclooxygenase-2 inhibitor, celecoxib, inhibits the altered hippocampal neurogenesis with attenuation of spontaneous recurrent seizures following pilocarpine-induced status epilepticus. *Neurobiology of Disease* 23:237–246.

Kandratavicius L, Alves Balista P, Lopes-Aguiar C, Ruggiero RN, Umeoka EH, Garcia-Cairasco N, Bueno-Junior LS, Leite JP (2014) Animal models of epilepsy: Use and limitations. *Neuropsychiatric Disease and Treatment* 10:1693–1705.

Karádi K, Janszky J, Gyimesi C, Horváth Z, Lucza T, Dóczi T, Kállai J, Ábrahám H (2012) Correlation between calbindin expression in granule cells of the resected hippocampal dentate gyrus and verbal memory in temporal lobe epilepsy. *Epilepsy and Behavior* 25:110–119.

Karamita M, Barnum C, Möbius W, Tansey MG, Szymkowski DE, Lassmann H, Probert L (2017) Therapeutic inhibition of soluble brain TNF promotes remyelination by increasing myelin phagocytosis by microglia. *Journal of Clinical Investigation Insight* 2:8.

Kettenmann H, Kirchhoff F, Verkhratsky A (2013) Microglia: New Roles for the Synaptic Stripper. *Neuron* 77:10–18.

Kettenmann H, Ransom BR (2013) The Concept of Neuroglia: A Historical Perspective In *Neuroglia*. Oxford University Press.

Khan D, Dupper A, Deshpande T, Graan PNED, Steinhäuser C, Bedner P (2016) Experimental febrile seizures impair interastrocytic gap junction coupling in juvenile mice. *Journal of Neuroscience Research* 94:804–813.

Khurgel M, Ivy GO (1996) Astrocytes in kindling: Relevance to epileptogenesis. *Epilepsy Research* 26:163–175.

Kofuji P, Newman EA (2010) Potassium Homeostasis in Glia In *Encyclopedia of Neuroscience*, pp. 867–872. Elsevier Ltd.

Kontermann RE, Scheurich P, Pfizenmaier K (2009) Antagonists of TNF action: Clinical experience and new developments. *Expert Opinion on Drug Discovery* 4:279–292.

Kreutzberg GW (1996) Microglia: A sensor for pathological events in the CNS. *Trends in Neurosciences* 19:312–318.

Kriegler M, Perez C, DeFay K, Albert I, Lu SD (1988) A novel form of TNF/cachectin is a cell surface cytotoxic transmembrane protein: Ramifications for the complex physiology of TNF. *Cell* 53:45–53.

Lampe PD, Kurata WE, Warn-Cramer BJ, Lau AF (1998) Formation of a distinct connexin43 phosphoisoform in mitotic cells is dependent upon p34cdc2 kinase. *Journal of Cell Science* 111 (Pt 6:833–841.

Larochelle C, Alvarez JI, Prat A (2011) How do immune cells overcome the blood-brain barrier in multiple sclerosis? *FEBS Letters* 585:3770–3780.

Lévesque M, Avoli M (2013) The kainic acid model of temporal lobe epilepsy. *Neuroscience and Biobehavioral Reviews* 37:2887–2899.

Li D, Ropert N, Koulakoff A, Giaume C, Oheim M (2008) Lysosomes Are the Major Vesicular Compartment Undergoing Ca2+-Regulated Exocytosis from Cortical Astrocytes. *Journal of Neuroscience* 28:7648–7658.

Li T, Lytle N, Lan JQ, Sandau US, Boison D (2012) Local disruption of glial adenosine homeostasis in mice associates with focal electrographic seizures: A first step in epileptogenesis? *Glia* 60:83–95.

Li T, Ren G, Lusardi T, Wilz A, Lan JQ, Iwasato T, Itohara S, Simon RP, Boison D (2008) Adenosine kinase is a target for the prediction and prevention of epileptogenesis in mice. *Journal of Clinical Investigation* 118:571–582.

Libbey JE, Kennett NJ, Wilcox KS, White HS, Fujinami RS (2011) Once initiated, viral encephalitis-induced seizures are consistent no matter the Treatment or lack of interleukin-6. *Journal of NeuroVirology* 17:496–499.

Liddelow SA, Barres BA (2017) Reactive Astrocytes: Production, Function, and Therapeutic Potential. *Immunity* 46:957–967.

Liddelow SA, Guttenplan KA, Clarke LE, Bennett FC, Bohlen CJ, Schirmer L, Bennett ML, Münch AE, Chung WS, Peterson TC, Wilton DK, Frouin A, Napier BA, Panicker N, Kumar M, Buckwalter MS, Rowitch DH, Dawson VL, Dawson TM, Stevens B, Barres BA (2017) Neurotoxic reactive astrocytes are induced by activated microglia. *Nature* 541:481–487.

Lieberman AP, Pitha PM, Shin HS, Shin ML (1989) Production of tumor necrosis factor and other cytokines by astrocytes stimulated with lipopolysaccharide or a neurotropic virus. *Proceedings of the National Academy of Sciences* 86:6348–6352.

Lloyd E, Somera-Molina K, Van Eldik LJ, Watterson DM, Wainwright MS (2008) Suppression of acute proinflammatory cytokine and chemokine upregulation by post-injury administration of a novel small molecule improves long-term neurologic outcome in a mouse model of traumatic brain injury. *Journal of Neuroinflammation* 5:28.

Löscher W, Brandt C (2010) Prevention or Modification of Epileptogenesis after Brain Insults: Experimental Approaches and Translational Research. *Pharmacological Reviews* 62:668–700.

Löscher W (2011) Critical review of current animal models of seizures and epilepsy used in the discovery and development of new antiepileptic drugs. *Seizure* 20:359–368.

Lowenstein DH, Bleck T, Macdonald RL (1999) It's time to revise the definition of status epilepticus. *Epilepsia* 40:120–122.

Lu MO, Zhang XM, Mix E, Quezada HC, Jin T, Zhu J, Adem A (2008) TNF-α receptor 1 deficiency enhances kainic acid-induced hippocampal injury in mice. *Journal of Neuroscience Research* 86:1608–1614.

Lund S, Christensen KV, Hedtjärn M, Mortensen AL, Hagberg H, Falsig J, Hasseldam H, Schrattenholz A, Pörzgen P, Leist M (2006) The dynamics of the LPS triggered inflammatory response of murine microglia under different culture and in vivo conditions. *Journal of Neuroimmunology* 180:71–87.

Ma L, Cui XL, Wang Y, Li XW, Yang F, Wei D, Jiang W (2012) Aspirin attenuates spontaneous recurrent seizures and inhibits hippocampal neuronal loss, mossy fiber sprouting and aberrant neurogenesis following pilocarpine-induced status epilepticus in rats. *Brain Research* 1469:103–113.

MacPherson KP, Sompol P, Kannarkat GT, Chang J, Sniffen L, Wildner ME, Norris CM, Tansey MG (2017) Peripheral administration of the soluble TNF inhibitor XPro1595 modifies brain immune cell profiles, decreases beta-amyloid plaque load, and rescues impaired long-term potentiation in 5xFAD mice. *Neurobiology of Disease* 102:81–95.

Malarkey EB, Parpura V (2008) Mechanisms of glutamate release from astrocytes. *Neurochemistry International* 52:142–154.

Malek TR, Castro I (2010) Interleukin-2 Receptor Signaling: At the Interface between Tolerance and Immunity. *Immunity* 33:153–165.

Marchetti L, Klein M, Schlett K, Pfizenmaier K, Eisel ULM (2004) Tumor Necrosis Factor (TNF)-mediated Neuroprotection against Glutamate-induced Excitotoxicity Is Enhanced by N -Methyl-D-aspartate Receptor Activation. *Journal of Biological Chemistry* 279:32869–32881.

Marchi N, Angelov L, Masaryk T, Fazio V, Granata T, Hernandez N, Hallene K, Diglaw T, Franic L, Najm I, Janigro D (2007) Seizure-promoting effect of blood-brain barrier disruption. *Epilepsia* 48:732–742.

Maroso M, Balosso S, Ravizza T, Liu J, Bianchi ME, Vezzani A (2011) Interleukin-1 type 1 receptor/Toll-like receptor signalling in epilepsy: The importance of IL-1beta and high-mobility group box 1. *Journal of Internal Medicine* 270:319–326.

Maroso M, Balosso S, Ravizza T, Liu J, Aronica E, Iyer AM, Rossetti C, Molteni M, Casalgrandi M, Manfredi AA, Bianchi ME, Vezzani A (2010) Toll-like receptor 4 and high-mobility group box-1 are involved in ictogenesis and can be targeted to reduce seizures. *Nature Medicine* 16:413–419.

McCoy MK, Tansey MG (2008) TNF signaling inhibition in the CNS: implications for normal brain function and neurodegenerative disease. *Journal of Neuroinflammation* 5:45.

McKhann GM, Schoenfeld-McNeill J, Born DE, Haglund MM, Ojemann GA (2000) Intraoperative hippocampal electrocorticography to predict the extent of hippocampal resection in temporal lobe epilepsy surgery. *Journal of Neurosurgery* 93:44–52.

Meldrum BS (1994) The role of glutamate in epilepsy and other CNS disorders. *Neurology* 44:S14–23.

Même W, Calvo CF, Froger N, Ezan P, Amigou E, Koulakoff A, Giaume C (2006) Proinflammatory cytokines released from microglia inhibit gap junctions in astrocytes: potentiation by beta-amyloid. *The FASEB Journal* 20:494–496.

Mirrione M, Tsirka S (2011) A Functional Role for Microglia in Epilepsy In *Clinical and Genetic Aspects of Epilepsy*. IntechOpen.

Mirrione MM, Schiffer WK, Fowler JS, Alexoff DL, Dewey SL, Tsirka SE (2007) A novel approach for imaging brain-behavior relationships in mice reveals unexpected metabolic patterns during seizures in the absence of tissue plasminogen activator. *NeuroImage* 38:34–42.

Mishima T, Hirase H (2010) In Vivo Intracellular Recording Suggests That Gray Matter Astrocytes in Mature Cerebral Cortex and Hippocampus Are Electrophysiologically Homogeneous. *Journal of Neuroscience* 30:3093–3100.

Mouri G, Jimenez-Mateos E, Engel T, Dunleavy M, Hatazaki S, Paucard A, Matsushima S, Taki W, Henshall DC (2008) Unilateral hippocampal CA3-predominant damage and short latency epileptogenesis after intra-amygdala microinjection of kainic acid in mice. *Brain Research* 1213:140–151.

Murphy BL, Danzer SC (2011) Somatic Translocation: A Novel Mechanism of Granule Cell Dendritic Dysmorphogenesis and Dispersion. *Journal of Neuroscience* 31:2959–2964.

Nakajima K, Tohyama Y, Kohsaka S, Kurihara T (2001) Ability of rat microglia to uptake extracellular glutamate. *Neuroscience Letters* 307:171–174.

Nakase T, Fushiki S, Söhl G, Theis M, Willecke K (2003) Neuroprotective role of astrocytic gap junctions in ischemic stroke. *Cell Communication and Adhesion* 10:413–7.

Naus CCG, Bechberger JF, Paul DL (1991) Gap junction gene expression in human seizure disorder. *Experimental Neurology* 111:198–203.

Neher E, Sakmann B (1976) Single-channel currents recorded from membrane of denervated frog muscle fibres. *Nature* 260:799–802.

Newman EA (2003) New roles for astrocytes: Regulation of synaptic transmission. *Trends in Neurosciences* 26:536–542.

Ng THS, Britton GJ, Hill EV, Verhagen J, Burton BR, Wraith DC (2013) Regulation of adaptive immunity; the role of interleukin-10. *Frontiers in Immunology* 4:129.

Niermann H, Amiry-Moghaddam M, Holthoff K, Witte OW, Ottersen OP (2001) A novel role of vasopressin in the brain: modulation of activity-dependent water flux in the neocortex. *The Journal of Neuroscience* 21:3045–51.

Nimmerjahn A, Kirchhoff F, Helmchen F (2005) Neuroscience: Resting microglial cells are highly dynamic surveillants of brain parenchyma in vivo. *Science* 308:1314–1318.

Noe FM, Polascheck N, Frigerio F, Bankstahl M, Ravizza T, Marchini S, Beltrame L, Banderó CR, Löscher W, Vezzani A (2013) Pharmacological blockade of IL-1β/IL-1 receptor type 1 axis during epileptogenesis provides neuroprotection in two rat models of temporal lobe epilepsy. *Neurobiology of Disease* 59:183–193.

Nolte C, Matyash M, Pivneva T, Schipke CG, Ohlemeyer C, Hanisch UK, Kirchhoff F, Kettenmann H (2001) GFAP promoter-controlled EGFP-expressing transgenic mice: a tool to visualize astrocytes and astrogliosis in living brain tissue. *Glia* 33:72–86.

Novrup HG, Bracchi-Ricard V, Ellman DG, Ricard J, Jain A, Runko E, Lyck L, Yli-Karjanmaa M, Szymkowski DE, Pearse DD, Lambertsen KL, Bethea JR (2014) Central but not systemic administration of XPro1595 is therapeutic following moderate spinal cord injury in mice. *Journal of Neuroinflammation* 11:159.

O'Neill LAJ, Bowie AG (2007) The family of five: TIR-domain-containing adaptors in Toll-like receptor signalling. *Nature Reviews Immunology* 7:353–364.

Orkand RK (1986) General Discussion on GlialInterstitial Fluid Exchange. *Annals of the New York Academy of Sciences* 481:354–354.

Palladino MA, Bahjat FR, Theodorakis EA, Moldawer LL (2003) Anti-TNF-α therapies: the next generation. *Nature Reviews Drug Discovery* 2:736–746.

Panayiotopoulos CP (2012) The new ILAE report on terminology and concepts for the organization of epilepsies: Critical review and contribution. *Epilepsia* 53:399–404.

Pannasch U, Vargova L, Reingruber J, Ezan P, Holcman D, Giaume C, Sykova E, Rouach N (2011) Astroglial networks scale synaptic activity and plasticity. *Proceedings of the National Academy of Sciences* 108:8467–8472.

Park KM, Bowers WJ (2010) Tumor necrosis factor-alpha mediated signaling in neuronal homeostasis and dysfunction. *Cellular Signalling* 22:977–983.

Pascual O, Ben Achour S, Rostaing P, Triller A, Bessis A (2012) Microglia activation triggers astrocyte-mediated modulation of excitatory neurotransmission. *Proceedings of the National Academy of Sciences* 109:E197–E205.

Patel DC, Wallis G, Dahle EJ, McElroy PB, Thomson KE, Tesi RJ, Szymkowski DE, West PJ, Smeal RM, Patel M, Fujinami RS, White HS, Wilcox KS (2017) Hippocampal TNFα Signaling Contributes to Seizure Generation in an Infection-Induced Mouse Model of Limbic Epilepsy. *eNeuro* 4:2.

Pekny M, Nilsson M (2005) Astrocyte activation and reactive gliosis. *Glia* 50:427–434.

Pekny M, Wilhelmsson U, Pekna M (2014) The dual role of astrocyte activation and reactive gliosis. *Neuroscience Letters* 565:30–38.

Penkowa M, Florit S, Giralt M, Quintana A, Molinero A, Carrasco J, Hidalgo J (2005) Metallothionein reduces central nervous system inflammation, neurodegeneration, and cell death following kainic acid-induced epileptic seizures. *Journal of Neuroscience Research* 79:522–534.

Persson M, Sandberg M, Hansson E, Rönnbäck L (2006) Microglial glutamate uptake is coupled to glutathione synthesis and glutamate release. *European Journal of Neuroscience* 24:1063–1070.

Philip R, Epstein LB (1986) Tumour necrosis factor as immunomodulator and mediator of monocyte cytotoxicity induced by itself, gamma-interferon and interleukin-1. *Nature* 323:86–89.

Probert L (2015) TNF and its receptors in the CNS: The essential, the desirable and the deleterious effects. *Neuroscience* 302:2–22.

Probert L, Akassoglou K, Kassiotis G, Pasparakis M, Alexopoulou L, Kollias G (1997) TNF-α transgenic and knockout models of CNS inflammation and degeneration. *Journal of Neuroimmunology* 72:137–141.

Racine RJ (1972) Modification of seizure activity by electrical stimulation: II. Motor seizure. *Electroencephalography and Clinical Neurophysiology* 32:281–294.

Ramón y Cajal S (1909) *Histologie du Systeme Nerveux de l'Homme et des Vertebres. Maloine, Paris: 1911. chap. II*, Vol. v.1 Maloine.

Raol YH, Brooks-Kayal AR (2012) Experimental models of seizures and epilepsies. *Progress in Molecular Biology and Translational Science* 105:57–82.

Ravizza T, Vezzani A (2006) Status epilepticus induces time-dependent neuronal and astrocytic expression of interleukin-1 receptor type I in the rat limbic system. *Neuroscience* 137:301–308.

Ravizza T, Gagliardi B, Noé F, Boer K, Aronica E, Vezzani A (2008) Innate and adaptive immunity during epileptogenesis and spontaneous seizures: Evidence from experimental models and human temporal lobe epilepsy. *Neurobiology of Disease* 29:142–160.

Ravizza T, Lucas SM, Balosso S, Bernardino L, Ku G, Noé F, Malva J, Randle JC, Allan S, Vezzani A (2006) Inactivation of caspase-1 in rodent brain: A novel anticonvulsive strategy. *Epilepsia* 47:1160–1168.

Retamal MA, Froger N, Palacios-Prado N, Ezan P, Saez PJ, Saez JC, Giaume C (2007) Cx43 Hemichannels and Gap Junction Channels in Astrocytes Are Regulated Oppositely by Proinflammatory Cytokines Released from Activated Microglia. *Journal of Neuroscience* 27:13781–13792.

Rezai-Zadeh K, Gate D, Town T (2009) CNS infiltration of peripheral immune cells: D-Day for neurodegenerative disease? *Journal of Neuroimmune Pharmacology* 4:462–475.

Riban V, Bouilleret V, Pham-Lê BT, Fritschy JM, Marescaux C, Depaulis A (2002) Evolution of hippocampal epileptic activity during the development of hippocampal sclerosis in a mouse model of temporal lobe epilepsy. *Neuroscience* 112:101–111.

Rizzi M, Perego C, Aliprandi M, Richichi C, Ravizza T, Colella D, Velískvá J, Moshé SL, De Simoni MG, Vezzani A (2003) Glia activation and cytokine increase in rat hippocampus by kainic acid-induced status epilepticus during postnatal development. *Neurobiology of Disease* 14:494–503.

Rogawski MA, Löscher W (2004) The neurobiology of antiepileptic drugs. *Nature Reviews Neuroscience* 5:553–564.

Rouach N, Koulakoff A, Abudara V, Willecke K, Giaume C (2008) Astroglial metabolic networks sustain hippocampal synaptic transmission. *Science* 322:1551–1555.

Samland H, Huitron-Resendiz S, Masliah E, Criado J, Henriksen SJ, Campbell IL (2003) Profound increase in sensitivity to glutamatergic- but not cholinergic agonist-induced seizures in transgenic mice with astrocyte production of IL-6. *Journal of Neuroscience Research* 73:176–187.

Samoilova M, Li J, Pelletier MR, Wentlandt K, Adamchik Y, Naus CC, Carlen PL (2003) Epileptiform activity in hippocampal slice cultures exposed chronically to bicuculline: Increased gap junctional function and expression. *Journal of Neurochemistry* 86:687–699.

Santello M, Bezzi P, Volterra A (2011) TNFα Controls Glutamatergic Gliotransmission in the Hippocampal Dentate Gyrus. *Neuron* 69:988–1001.

Sasaki T, Ishikawa T, Abe R, Nakayama R, Asada A, Matsuki N, Ikegaya Y (2014) Astrocyte calcium signalling orchestrates neuronal synchronization in organotypic hippocampal slices. *Journal of Physiology* 592:2771–2783.

Schafer DP, Lehrman EK, Stevens B (2013) The "quad-partite" synapse: Microglia-synapse interactions in the developing and mature CNS. *Glia* 61:24–36.

Schmidt D, Löscher W (2005) Drug resistance in epilepsy: Putative neurobiologic and clinical mechanisms. *Epilepsia* 46:858–877.

Schnell C, Hagos Y, Hülsmann S (2012) Active Sulforhodamine 101 Uptake into Hippocampal Astrocytes. *PLoS ONE* 7:11.

Schonberg DL, Popovich PG, McTigue DM (2007) Oligodendrocyte generation is differentially influenced by toll-like receptor (TLR) 2 and TLR4-mediated intraspinal macrophage activation. *Journal of Neuropathology and Experimental Neurology* 66:1124–1135.

Sedger LM, McDermott MF (2014) TNF and TNF-receptors: From mediators of cell death and inflammation to therapeutic giants - past, present and future. *Cytokine and Growth Factor Reviews* 25:453–472.

Seifert G, Huttmann K, Binder DK, Hartmann C, Wyczynski A, Neusch C, Steinhauser C (2009) Analysis of Astroglial K+ Channel Expression in the Developing Hippocampus Reveals a Predominant Role of the Kir4.1 Subunit. *Journal of Neuroscience* 29:7474–7488.

Seifert G, Carmignoto G, Steinhäuser C (2010) Astrocyte dysfunction in epilepsy. *Brain Research Reviews* 63:212–221.

Seri B, García-Verdugo JM, McEwen BS, Alvarez-Buylla A (2001) Astrocytes give rise to new neurons in the adult mammalian hippocampus. *The Journal of Neuroscience* 21:7153–7160.

Shaked I, Tchoresh D, Gersner R, Meiri G, Mordechai S, Xiao X, Hart RP, Schwartz M (2005) Protective autoimmunity: Interferon-gamma enables microglia to remove glutamate without evoking inflammatory mediators. *Journal of Neurochemistry* 92:997–1009.

Shakoor N, Michalska M, Harris CA, Block JA (2002) Drug-induced systemic lupus erythematosus associated with etanercept therapy. *Lancet* 359:579–580.

Shishido SN, Prasain K, Beck A, Nguyen TDT, Hua DH, Nguyen TA (2013) Bioavailability and Efficacy of a Gap Junction Enhancer (PQ7) in a Mouse Mammary Tumor Model. *PLoS ONE* 8.

Shorvon SD (2011) The etiological classification of epilepsy. *Epilepsia* 6:1052–1057.

Siao CJ, Fernandez SR, Tsirka SE (2003) Cell type-specific roles for tissue plasminogen activator released by neurons or microglia after excitotoxic injury. *The Journal of neuroscience : the official journal of the Society for Neuroscience* 23:3234–3242.

Sicotte NL, Voskuhl RR (2001) Onset of multiple sclerosis associated with anti-TNF therapy. *Neurology* 57:1885–1888.

Slifman NR, Gershon SK, Lee JH, Edwards ET, Braun MM (2003) Listeria monocytogenes infection as a complication of treatment with tumor necrosis factor α-neutralizing agents. *Arthritis and Rheumatism* 48:319–324.

Smolen JS, Steiner G (2003) Therapeutic strategies for rheumatoid arthritis. *Nature Reviews Drug Discovery* 2:473–488.

Söhl G, Güldenagel M, Beck H, Teubner B, Traub O, Gutiérrez R, Heinemann U, Willecke K (2000) Expression of connexin genes in hippocampus of kainate-treated and kindled rats under conditions of experimental epilepsy. *Molecular Brain Research* 83:44–51.

Somera-Molina KC, Robin B, Somera CA, Anderson C, Stine C, Koh S, Behanna HA, Van Eldik LJ, Watterson DM, Wainwright MS (2007) Glial activation links early-life seizures and long-term neurologic dysfunction: Evidence using a small molecule inhibitor of proinflammatory cytokine upregulation. *Epilepsia* 48:1785–1800.

Sotgiu S, Murrighile MR, Constantin G (2010) Treatment of refractory epilepsy with natalizumab in a patient with multiple sclerosis. Case report. *BMC Neurology* 10.

Steed PM, Tansey MG, Zalevsky J, Zhukovsky EA, Desjarlais JR, Szymkowski DE, Abbott C, Carmichael D, Chan C, Cherry L, Cheung P, Chirino AJ, Chung HH, Doberstein SK, Eivazi A, Filikov AV, Gao SX, Hubert RS, Hwang M, Hyun L, Kashi S, Kim A, Kim E, Kung J, Martinez SP, Muchhal US, Nguyen DHT, O'Brien C, O'Keefe D, Singer K, Vafa O, Vielmetter J, Yoder SC, Dahiyat BI (2003) Inactivation of TNF signaling by rationally designed dominant-negative TNF variants. *Science* 301:1895–1898.

Steinhäuser C, Seifert G (2012) *Astrocyte dysfunction in epilepsy* National Center for Biotechnology Information (US).

Steinhäuser C, Seifert G, Bedner P (2012) Astrocyte dysfunction in temporal lobe epilepsy: K + channels and gap junction coupling. *Glia* 60:1192–1202.

Stellwagen D, Malenka RC (2006) Synaptic scaling mediated by glial TNF-α. *Nature* 440:1054–1059.

Suen WE, Bergman CM, Hjelmström P, Ruddle NH, Hjelmstrom P, Ruddle NH (1997) A critical role for lymphotoxin in experimental allergic encephalomyelitis. *The Journal of Experimental Medicine* 186:1233–1240.

Szalay G, Martinecz B, Lénárt N, Környei Z, Orsolits B, Judák L, Császár E, Fekete R, West BL, Katona G, Rózsa B, Dénes Á (2016) Microglia protect against brain injury and their selective elimination dysregulates neuronal network activity after stroke. *Nature Communications* 7.

Szente M, Gajda Z, Said Ali K, Hermesz E (2002) Involvement of electrical coupling in the in vivo ictal epileptiform activity induced by 4-aminopyridine in the neocortex. *Neuroscience* 115:1067–1078.

Takada Y, Aggarwal BB (2004) TNF Activates Syk Protein Tyrosine Kinase Leading to TNF-Induced MAPK Activation, NF-kappaB Activation, and Apoptosis. *The Journal of Immunology* 173:1066–1077.

Takahashi DK, Vargas JR, Wilcox KS (2010) Increased coupling and altered glutamate transport currents in astrocytes following kainic-acid-induced status epilepticus. *Neurobiology of Disease* 40:573–585.

Takatsu K (2011) Interleukin-5 and IL-5 receptor in health and diseases. *Proceedings of the Japan Academy* 87:463–485.

Tanaka S, Nakamura T, Sumitani K, Takahashi F, Konishi R, Itano T, Miyamoto O (2009) Stage- and region-specific cyclooxygenase expression and effects of a selective COX-1 inhibitor in the mouse amygdala kindling model. *Neuroscience Research* 65:79–87.

Taniwaki Y, Kato M, Araki T, Kobayashi T (1996) Microglial activation by epileptic activities through the propagation pathway of kainic acid-induced hippocampal seizures in the rat. *Neuroscience Letters* 217:29–32.

Tansey MG, Wyss-Coray T (2008) Cytokines in CNS inflammation and disease In *Central Nervous System Diseases and Inflammation*, pp. 59–106. Springer.

Taoufik E, Petit E, Divoux D, Tseveleki V, Mengozzi M, Roberts ML, Valable S, Ghezzi P, Quackenbush J, Brines M, Cerami A, Probert L (2008) TNF receptor I sensitizes neurons to erythropoietin- and VEGF-mediated neuroprotection after ischemic and excitotoxic injury. *Proceedings of the National Academy of Sciences* 105:6185–6190.

Taoufik E, Tseveleki V, Chu SY, Tselios T, Karin M, Lassmann H, Szymkowski DE, Probert L (2011) Transmembrane tumour necrosis factor is neuroprotective and regulates experimental autoimmune encephalomyelitis via neuronal nuclear factor-κB. *Brain* 134:2722–2735.

Thevenin AF, Kowal TJ, Fong JT, Kells RM, Fisher CG, Falk MM (2013) Proteins and Mechanisms Regulating Gap-Junction Assembly, Internalization, and Degradation. *Physiology* 28:93–116.

Thom M (2014) Review: Hippocampal sclerosis in epilepsy: A neuropathology review. *Neuropathology and Applied Neurobiology* 40:520–543.

Thornberry NA, Bull HG, Calaycay JR, Chapman KT, Howard AD, Kostura MJ, Miller DK, Molineaux SM, Weidner JR, Aunins J, Elliston KO, Ayala JM, Casano FJ, Chin J, Ding GJF, Egger LA, Gaffney EP, Limjuco G, Palyha OC, Raju SM, Rolando AM, Salley JP, Yamin TT, Lee TD, Shively JE, MacCross M, Mumford RA, Schmidt JA, Tocci MJ (1992) A novel heterodimeric cysteine protease is required for interleukin-1βprocessing in monocytes. *Nature* 356:768–774.

Tian GF, Takano T, Lin JH, Wang X, Bekar L, Nedergaard M (2006) Imaging of cortical astrocytes using 2-photon laser scanning microscopy in the intact mouse brain. *Advanced Drug Delivery Reviews* 58:773–787.

Tracey KJ, Cerami A (1994) TUMOR NECROSIS FACTOR: A Pleiotropic Cytokine and Therapuetic Target. *Annual Review of Medicine* 45:491–503.

Van Vliet EA, Forte G, Holtman L, Den Burger JCG, Sinjewel A, De Vries HE, Aronica E, Gorter JA (2012) Inhibition of mammalian target of rapamycin reduces epileptogenesis and blood-brain barrier leakage but not microglia activation. *Epilepsia* 53:1254–1263.

Vertex Pharmaceuticals Incorporated (2011) A Study to Evaluate the Efficacy and Safety of VX-765 in Subjects With Treatment-Resistant Partial Epilepsy.

Vezzani A, Conti M, De Luigi A, Ravizza T, Moneta D, Marchesi F, De Simoni M (1999) Interleukin-1beta immunoreactivity and microglia are enhanced in the rat hippocampus by focal kainate application: functional evidence for enhancement of electrographic seizures. *The Journal of Neuroscience* 19:5054–5065.

Vezzani A, Moneta D, Conti M, Richichi C, Ravizza T, De Luigi A, De Simoni MG, Sperk G, Andell-Jonsson S, Lundkvist J, Iverfeldt K, Bartfai T (2000) Powerful anticonvulsant action of IL-1 receptor antagonist on intracerebral injection and astrocytic overexpression in mice. *Proceedings of the National Academy of Sciences* 97:11534–11539.

Vezzani A, Balosso S, Ravizza T (2008) The role of cytokines in the pathophysiology of epilepsy. *Brain, Behavior and Immunity* 22:797–803.

Vezzani A, Baram TZ (2007) New Roles for Interleukin-1 Beta in the Mechanisms of Epilepsy. *Epilepsy Currents* 7:45–50.

Vezzani A, French J, Bartfai T, Baram TZ (2011) The role of inflammation in epilepsy. *Nature Reviews Neurology* 7:31–40.

Vezzani A, Moneta D, Richichi C, Aliprandi M, Burrows SJ, Ravizza T, Perego C, Grazia De Simoni M (2002) Functional role of inflammatory cytokines and antiinflammatory molecules in seizures and epileptogenesis. *Epilepsia* 43:30–35.

Vinet J, Vainchtein ID, Spano C, Giordano C, Bordini D, Curia G, Dominici M, Boddeke HW, Eggen BJ, Biagini G (2016) Microglia are less pro-inflammatory than myeloid infiltrates in the hippocampus of mice exposed to status epilepticus. *Glia* 64:1350–1362.

Viviani B, Bartesaghi S, Gardoni F, Vezzani A, Behrens MM, Bartfai T, Binaglia M, Corsini E, Di Luca M, Galli CL, Marinovich M (2003) Interleukin-1beta enhances NMDA receptor-mediated intracellular calcium increase through activation of the Src family of kinases. *The Journal of Neuroscience* 23:8692–700.

Viviani B, Gardoni F, Marinovich M (2007) Cytokines and Neuronal Ion Channels in Health and Disease. *International Review of Neurobiology* 82:247–263.

Wajant H, Pfizenmaier K, Scheurich P (2003) Tumor necrosis factor signaling. *Cell Death and Differentiation* 10:45–65.

Wajant H, Scheurich P (2011) TNFR1-induced activation of the classical NF-κB pathway. *FEBS Journal* 278:862–876.

Wallraff A (2006) The Impact of Astrocytic Gap Junctional Coupling on Potassium Buffering in the Hippocampus. *Journal of Neuroscience* 26:5438–5447.

Wallraff A, Odermatt B, Willecke K, Steinhäuser C (2004) Distinct types of astroglial cells in the hippocampus differ in gap junction coupling. *Glia* 48:36–43.

Wang DD, Bordey A (2008) The astrocyte odyssey. *Progress in Neurobiology* 86:342–367.

Wang JS, Freitas-Andrade M, Bechberger JF, Naus C, Yeung KKC, Whitehead SN (2018) MALDI IMS of Intraperitoneally Injected Danegaptide (ZP1609) for Treatment of Stroke-Reperfusion Injury in Mice. *Rapid Communications in Mass Spectrometry* .

Wang WY, Tan MS, Yu JT, Tan L (2015) Role of pro-inflammatory cytokines released from microglia in Alzheimer's disease. *Annals of Translational Medicine* 3:136.

Weinberg MS, Blake BL, McCown TJ (2013) Opposing actions of hippocampus TNFα receptors on limbic seizure susceptibility. *Experimental Neurology* 247:429–437.

White HS, Smith MD, Wilcox KS (2007) Mechanisms of Action of Antiepileptic Drugs. *International Review of Neurobiology* 81:85–110.

Wilhelmsson U (2004) Absence of Glial Fibrillary Acidic Protein and Vimentin Prevents Hypertrophy of Astrocytic Processes and Improves Post-Traumatic Regeneration. *Journal of Neuroscience* 24:5016–5021.

Wilhelmsson U, Bushong EA, Price DL, Smarr BL, Phung V, Terada M, Ellisman MH, Pekny M (2006) Redefining the concept of reactive astrocytes as cells that remain within their unique domains upon reaction to injury. *Proceedings of the National Academy of Sciences* 103:17513–17518.

Winokur RS, Kubal T, Liu D, Davis SF, Smith BN (2004) Recurrent excitation in the dentate gyrus of a murine model of temporal lobe epilepsy. *Epilepsy Research* 58:93–105.

Xu L, Zeng LH, Wong M (2009) Impaired astrocytic gap junction coupling and potassium buffering in a mouse model of tuberous sclerosis complex. *Neurobiology of Disease* 34:291–299.

Yamamoto A, Schindler CK, Murphy BM, Bellver-Estelles C, So NK, Taki W, Meller R, Simon RP, Henshall DC (2006) Evidence of tumor necrosis factor receptor 1 signaling in human temporal lobe epilepsy. *Experimental Neurology* 202:410–420.

Ye ZC, Sontheimer H (1996) Cytokine modulation of glial glutamate uptake: a possible involvement of nitric oxide. *Neuroreport* 7:2181–2185.

Zalevsky J, Secher T, Ezhevsky SA, Janot L, Steed PM, O'Brien C, Eivazi A, Kung J, Nguyen DHT, Doberstein SK, Erard F, Ryffel B, Szymkowski DE (2007) Dominant-Negative Inhibitors of Soluble TNF Attenuate Experimental Arthritis without Suppressing Innate Immunity to Infection. *The Journal of Immunology* 179:1872–1883.

Zattoni M, Mura ML, Deprez F, Schwendener RA, Engelhardt B, Frei K, Fritschy JM (2011) Brain Infiltration of Leukocytes Contributes to the Pathophysiology of Temporal Lobe Epilepsy. *Journal of Neuroscience* 31:4037–4050.

Zhang FF, Morioka N, Kitamura T, Hisaoka-Nakashima K, Nakata Y (2015) Proinflammatory cytokines downregulate connexin 43-gap junctions via the ubiquitin-proteasome system in rat spinal astrocytes. *Biochemical and Biophysical Research Communications* 464:1202–1208.

Zhang Z, Chen G, Zhou W, Song A, Xu T, Luo Q, Wang W, Gu XS, Duan S (2007) Regulated ATP release from astrocytes through lysosome exocytosis. *Nature Cell Biology* 9:945–953.

Zhao X, Liao Y, Morgan S, Mathur R, Feustel P, Mazurkiewicz J, Qian J, Chang J, Mathern GW, Adamo MA, Ritaccio AL, Gruenthal M, Zhu X, Huang Y (2018) Noninflammatory Changes of Microglia Are Sufficient to Cause Epilepsy. *Cell Reports* 22:2080–2093.

Zheng H, Zhu W, Zhao H, Wang X, Wang W, Li Z (2009) Kainic acid-activated microglia mediate increased excitability of rat hippocampal neurons in vitro and in vivo: Crucial role of interleukin-1beta. *NeuroImmunoModulation* 17:31–38.

Zhu W, Zheng H, Shao X, Wang W, Yao Q, Li Z (2010) Excitotoxicity of TNF alpha derived from KA activated microglia on hippocampal neurons in vitro and in vivo. *Journal of Neurochemistry* 114:386–396.

List of Figures

List of Tables

Erklärung

Hiermit versichere ich, dass diese Dissertation von mir selbst und ohne unerlaubte Hilfe angefertigt worden ist. Es wurden keine anderen als die angegebenen Hilfsmittel verwendet. Ferner erkläre ich, dass die vorliegende Arbeit an keiner anderen Hochschule als Dissertation eingereicht worden ist.

Bonn, den 03.05.2018

Julia Müller

Publication

PUBLICATION

Müller, J., Bedner, P., Brosseron, F., Heneka, M.T., Steinhäuser, C., (in preparation). **Rescue of Astrocytic Gap Junction Coupling as a New Strategy to Prevent Epileptogenesis.**

Müller, J., Timmermann, A., Seifert, G., Steinhäuser, C., Bedner, P. (in preparation). **GABA Accumulation in Astrocytes in an experimental model of Epilepsy.**

Bres E., Safina, D., Müller, J., Bedner, P., Yang, H., Helluy, X., Shchyglo, O., Jansen, S., Mark, M., Esser, A., Steinhäuser, C., Herlitze, S., Pietrzik, CU., Götz, M., Manahan-Vaughan, D., Faissner, A. (submitted). **Epileptic seizures in mice with lipoprotein receptor deficient neural radial glia stem cells.** *Nature Neuroscience*

Brawek, B., Chesters, R., Klement, D., Müller, J., Lerdkrai C., Hermes, M., Garaschuk, O., 2017. **A bell-shaped dependence between amyloidosis and GABA accumulation in astrocytes in a mouse model of Alzheimer's disease.** *Neurobiology Aging, 61: 187-197.*

Aberg, KC., Müller, J., Schwartz, S., 2017. **Trial-by-Trial Modulation of Associative Memory Formation by Reward Prediction Error and Reward Anticipation as Revealed by a Biologically Plausible Computational Model.** *Front. Hum. Neuroscience, 11:56.*

Salar, S., Lapilover, E., Müller, J., Hollnagel, JO., Lippmann, K., Friedman, A., Heinemann, U., 2016. **Synaptic plasticity in area CA1 of rat hippocampal slices following intraventricular application of albumin**. *Neurobiology of Disease,* 91, 155-165.

Bedner, P., Dupper, A., Hüttmann, K., Müller, J., Herde, M.K., Dublin, P., Deshpande, T., Schramm, J., Haussler, U., Haas, C.A., Henneberger, C., Theis, M., Steinhäuser, C., 2015. **Astrocyte uncoupling as a cause of human temporal lobe epilepsy**. *Brain 138*, 1208–1222.